Ageing and Lifetime of Medium Voltage ROV Umbilical Cables

Shibanni Shah

Master Thesis

July 8, 2023

Delft University of Technology

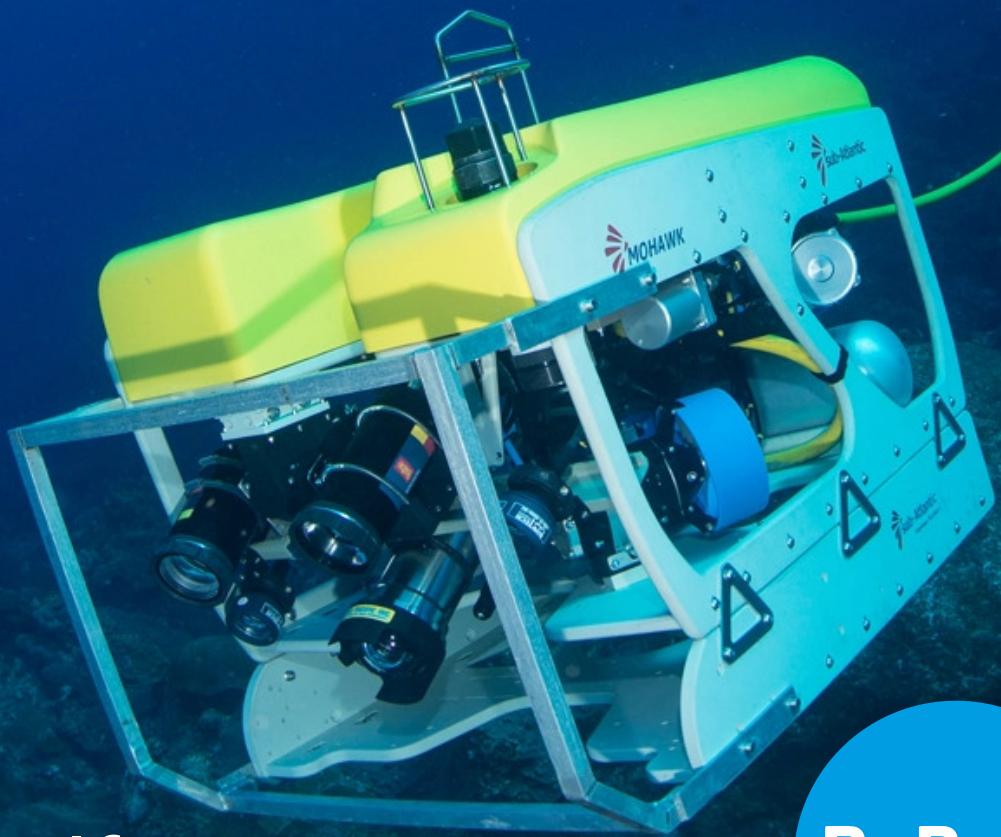

TU Delft

DeRegt

A SERCEL COMPANY

Ageing and Lifetime of Medium Voltage ROV Umbilical Cables

by

Shibanni Shah

to obtain the degree of Master of Science
at the Delft University of Technology.
to be defended publicly on Friday July 14, 2023 at 10:00AM.

Author:	Shibanni Shah	5445361
Project duration:	October 3, 2022 – July 14, 2023	
Supervisors:	Dr. M. Ghaffarian Niasar,	TU Delft
	ir. E. van Veldhuizen,	DeRegt Cables
	A. Sans, MSc.,	DeRegt Cables
Defense:	July 14, 2023 10:00 – 12:00	
Thesis committee:	Prof.ir. P. Vaessen,	TU Delft
	Dr. M. Ghaffarian Niasar,	TU Delft
	Dr.ir. A. Shekhar,	TU Delft
	ir. E. van Veldhuizen,	DeRegt Cables

This thesis is confidential and cannot be made public until July 14, 2025.

An electronic version of this thesis is available at http://repository.tudelft.nl/.

Cover image: The Mohawk ROV on its inaugural run at East Flower Garden Bank. Photo: FGBNMS/Schmahl. URL: https://flowergarden.noaa.gov/science/mohawkrov.html.

TU Delft HIGH VOLTAGE TECHNOLOGIES DeRegt

Abstract

Remotely operated vehicles (ROV) are used for the inspection, maintenance and repair of submarine and offshore cables, subsea exploration, and rescue operations. ROVs are powered by umbilical cables, which have to withstand electrical, mechanical, and thermal stresses. This thesis investigates the effect of repetitive bending on the insulation properties of ROV umbilical cables for medium voltage.

Umbilical cables with XLPE, polypropylene, and HDPE insulation were mechanically aged using a cyclic bend-over-sheave setup, after which the dielectric properties were analysed using electrical breakdown tests and several diagnostic tests, such as partial discharge analysis.

The cables with XLPE and HDPE insulation showed delamination of the conductor–insulation interface, which resulted in increased partial discharge activity, a reduced breakdown voltage, and a significantly decreased lifetime. For HDPE, the lifetime power law exponent n dropped from 18 to 9 after 23,000 cycles of mechanical ageing. Polypropylene, on the other hand, did not show delamination but an increase in dielectric-bounded cavities with mechanical ageing.

Keywords: Remotely operated vehicles, bending fatigue, XLPE, polypropylene, HDPE, partial discharges, electrical breakdown

Part of this thesis was presented as a paper at the Jicable'23 conference in Lyon, 2023. The paper was titled "The Effect of Bending Fatigue on the Breakdown Strength of Polymer-Insulated Conductors" [1] and was awarded as best paper in the Young Researcher Award.

Preface

This thesis was completed within nine months as part of the MSc Electrical Power Engineering program. The research topic is “Ageing and Lifetime of Medium Voltage ROV Umbilical Cables”. The project was a collaboration between the Delft University of Technology and DeRegt Cables for their medium voltage project.

These past two years have been a journey of professional and personal growth. Having completed my bachelor’s in 2018, it was a different experience to return to a university after such a long break. Perhaps this time I had more clarity on what I would want from a degree. I feel fortunate to have discovered my passion through the High Voltage specialisation, thanks to the valuable knowledge imparted by lecturers like Prof. Peter Vassen, Dr. Mohamad Ghaffarian Niasar, and Dr. Armando Rodrigo Mor.

I would like to thank my parents for investing in my education, fostering my independence, and always encouraging me to explore my interests. The older I get, the more I realise the positive virtues they imparted through their life experiences. To my friends back in India, who have been a constant source of support and with whom I could always connect despite the distance of thousands of kilometers. To my friends in Delft, with whom I could share university life experiences over dinner. To Gijs, whose support and presence in my life have made this journey all the more meaningful. And to his family, who provided me with a second home to enjoy the Dutch holidays.

To Dr. Mohamad Ghaffarian Niasar, who helped me shape this journey into the cable industry and guided me in many professional decisions. His curious energy to understand things and learn is an inspiration. His High Voltage Cable Systems course led me to pursue an internship and thesis in this field, making him an enduring and significant influence in my future professional endeavours. Also, I want to thank him for the extra late hours he spent in the lab so I could finish my tests. To High Voltage lab technicians who helped me with the testing setups. Especially Wim Termorshuizen, who supported me in implementing my ideas and always came early to the lab so that we could do our tests.

I am grateful to DeRegt for entrusting me with this project and allowing me to explore my interests. Their belief in me played a significant role in the success of this endeavour. To Cabri and Afum from Quality, who were essential in making this project a success. To Evert, who gave me many opportunities to showcase my work. To Auguste, with whom I could have technical discussions about the cable industry. To Phil and Sander, whose extensive expertise in their respective fields provided valuable insights which contributed to my research.

Shibanni Shah
Delft, July 2023

Contents

1 Introduction

Remotely operated vehicles (ROVs) are utilised for diverse underwater applications, including inspection, exploration, marine research, search and rescue operations, small-scale drilling, repairing and maintenance of offshore and subsea structures [2]. Hence they play a vital role in the energy transition. An ROV system typically comprises the following components: a support vessel, an umbilical cable, a tether management system (TMS), and an ROV equipped with specialised tools and sensors tailored to the specific mission. The support vessel functions as a launching and recovery base for the ROV. The ROV umbilical cable functions include power transmission and communication capabilities [3]. In addition, it must carry the weight of the ROV during launching and recovery. The ROV umbilical cables are thus a type of dynamic subsea cable, since it experiences various mechanical stresses during their operation underwater.

A cross-section of a simple three-phase umbilical cable is shown in Figure 1.1. The armour plays an important role as the cable must be able to carry the load of the ROV. Cables are typically designed with a helical structure to ensure that the armour carries most of the tensile load. A steel armoured cable is typically used to a length of less than 4 km.

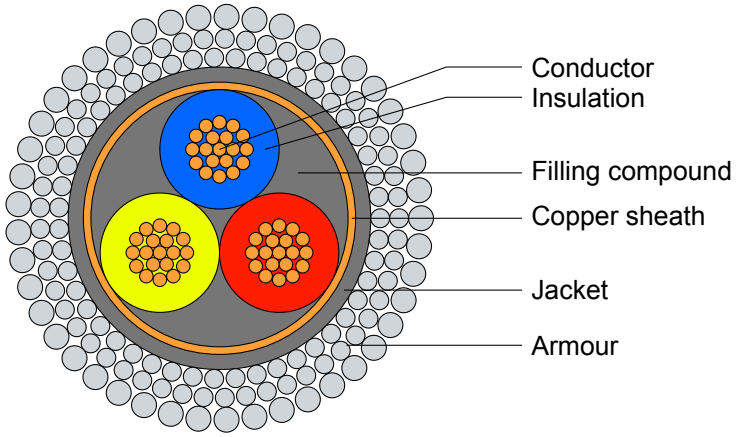

Figure 1.1: Cross-section of a generic three-phase umbilical cable showing the three insulated conductors with a shared copper shield. The three-layer steel armour takes most of the mechanical stress.

ROV umbilical cables are made for a short lifetime of 10,000 to 20,000 h due to mechanical limitations. For example, the armour, or the strength member, will experience mechanical fatigue and fail. This means that the IEC standard design recommendations for low- and medium-voltage cables, which aim for a lifetime of 30 yr or more, are too conservative and result in a large cable diameter. Since the cable and vehicle experience drag proportional to the cable diameter, the insulation should be designed as thin as possible. The ROV cable must handle electrical, mechanical, and thermal stress and be spooled in and out of the water over drums or sheaves [4].

Currently, no standards exist for the testing of umbilical cables. Only best practices such as DNV-GL-RP-F40 are available, and more research must be performed for such short-lifetime cables at high voltage ratings. The umbilical cable can be divided into two parts during operation: (i) the part of cable on the winch on the ship, and (ii) the part under water. These two parts undergo different mechanical and environmental stresses. The part under the water is mostly wet and undergoes tension forces and electrical stress. These mechanical forces are a combination of gravitational, vertical acceleration forces and drag force [5]. The part on the winch undergoes combined effects of electrical, mechanical and thermal stresses. It is mainly dry and thermally stressed up to the maximum conductor temperature due to the cable layers on the winch. This factor is absent for the cable under water.

Most of the studies focus on the cable under water. This part is insignificant for lifetime analysis as such parts undergo annual cutting: after an expedition, the part of the cable that was regularly used underwater is cut off and re-terminated. Very few electrical failures were reported, and most cable failures are caused by the failure of non-polymeric components [6]. Hence, the part on the winch is explored for lifetime and ageing analysis. A schematic presentation of the ROV system with the different kinds of stress is shown in Figure 1.2.

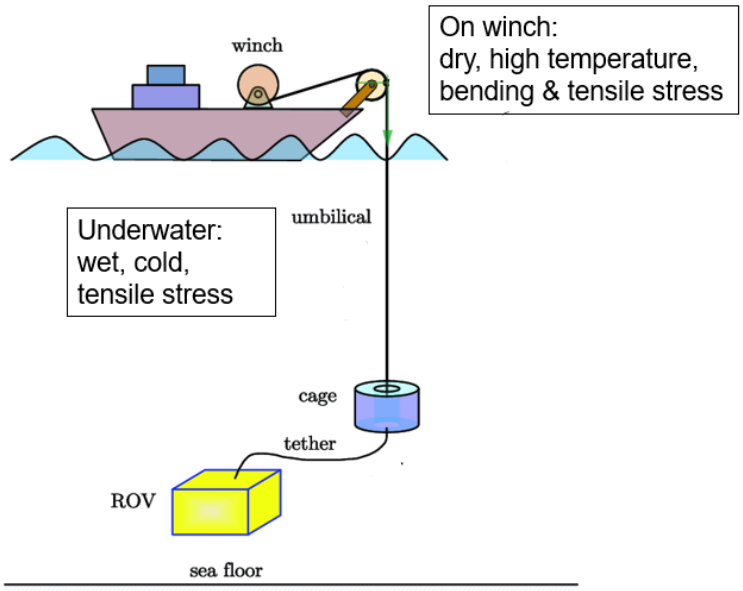

Figure 1.2: Schematic representation of the ROV system used for deep sea exploration (adapted from Quan et.al [7]).

1.1. Research Questions

DeRegt Cables uses conventional extruders to make their umbilical cables. The maximum line-to-line voltage of these cables is up to 4.5 kV. They are interested in understanding the limits of this production process in terms of electrical lifetime. Therefore, the following research questions were formulated.

- What are the factors influencing the ageing and lifetime of the cables?
- How can the cyclic bending fatigue that occurs during operation be accurately replicated in testing the cables?
- What methods can be used to electrically test the single conductors of a cable without the grounded sheath?
- How does cyclic bending stress affect the dielectric properties of the cable, and what is the extent of this effect?

1.2. Research Methodology

Research into the questions described above is performed through electrical tests on samples prepared in several ways:

1. Material samples: dielectric spectroscopy was performed on thin flat samples of XLPE, polypropylene, and HDPE prepared according to the procedure described in Chapter 3.
2. Single conductors: all cable tests are performed on single conductors, which form the fundamental building block of the cables under consideration. The cables are subjected to various degrees of mechanical ageing using a cyclic bend-over sheave (CBoS) test:
   - Single conductor ageing: a single conductor is mechanically aged without the presence of other polymer/non-polymer components
   - Triple ageing: three conductors with a shared copper sheath and jacket make a triple. Triples are subjected to mechanical ageing, after which the conductors are taken out for testing.
   - Full cable ageing: here, an umbilical cable consisting of power conductors, TMS power conductors, optic fibres, and armour is mechanically aged (bending and tensile stress). This is the most representative of real operating conditions.

XLPE- and polypropylene-insulated cables are used for the single and triple ageing, while for the full cable, HDPE-insulated cables were tested.

1.3. Outline

The document consists of the following chapters. Chapter 2 explains the manufacturing process of DeRegt's cables and reviews the ageing mechanisms encountered in static power cables and dynamic offshore wind cables. Chapter 3 describes the process of making thin samples followed by dielectric spectroscopy on the samples. Chapter 4 studies the effect of mechanical cyclic bending on single conductors. Chapter 5 investigates the effect of cabling the conductors into a triple. Chapter 6 deals with cyclic bend-over-sheave testing on a full ROV cable and studying its effect on the lifetime of the cable. Chapter 7 presents the main conclusions and recommendations for future work.

2

Manufacturing and Ageing of Cables

This chapter explains the manufacturing process of umbilical cables in DeRegt's factory. Starting with the extrusion processes for the three most common insulating materials (XLPE, polypropylene, and HDPE) and the potential effects on the insulation performance are discussed. Finally, the most commonly observed electrical, mechanical, and thermal ageing mechanisms are reviewed.

2.1. Insulation Material

Depending on the operating environment and current ratings, the insulation materials can be thermoset or thermoplastic [4]. In this research, three insulation materials are taken for study: cross-linked polyethylene (XLPE), polypropylene (PP), and high-density polyethylene (HDPE).

2.1.1. Cross-linked Polyethylene (XLPE)

Polyethylene is one of the most used plastic materials in the world, with a wide range of applications. However, it melts at relatively low temperatures, which is undesirable for cable insulation. It was found that cross-linking improves the material's characteristics, which are briefly summarised in Table 2.1 [8]. During the cross-linking process, the thermoplastic is converted to thermoset XLPE material. Four common types of cross-linking processes are: (i) peroxide method, (ii) silane moisture curing, (iii) azo method, and (iv) radiation method [8–11].

Table 2.1: Changes in the properties of PE after cross-linking [8].

Property of PE	Changes after cross-linking
Tensile strength	No change/slightly increased
Elongation at break	Decreased
Impact resistance	Significantly improved
Abrasion resistance	Greatly improved
Stress-crack resistance	Greatly improved
Elastic properties	Greatly improved
Environmental stress crack resistance	Increased
Resistance to slow crack growth	Increased
Temperature resistance	Greatly improved
Chemical resistance	Significantly increased

XLPE is the most used insulation in medium voltage AC, HVAC and HVDC cables due to all the properties mentioned in Table 2.1 [8, 12, 13]. Medium-density polyethylene pre-grafted base compound from POLIDAN was used in this research. This consists of a moisture-curable compound, and a catalyst is used to speed up the cross-linking in water. These are moisture-sensitive materials; care should be taken to prevent premature cross-linking. According to previous research, pre-crosslinking can create defects in the insulation [14].

2.1.2. Polypropylene (PP)

Polypropylene is becoming more popular because it does not require degassing and is more recyclable than other cable insulation materials. The most significant difference is that PP is a thermoplastic, while materials like XLPE are thermosetting. Polypropylene also has excellent electrical, thermal and high-temperature properties [14]. One of the most successful variants is high-performance thermoplastic elastomer (HPTE) by Prysmian [15]. Additionally, PP can be manufactured using a one-shot process where the insulation and sheath/jacket are extruded simultaneously [14, 15]. Hence any damage to the cable core during drum transportation can be avoided [15].

Polypropylene becomes brittle below 0 °C according to data sheet [16], which could be a risk in subsea applications. Hence it is essential to analyse the potential advantages and risks of the polypropylene material currently used for cable production.

2.1.3. High-Density Polyethylene (HDPE)

HDPE is also a thermoplastic with the same production advantages as polypropylene, including recyclability, a one-shot production line, and no cross-linking. Since there is no risk of premature cross-linking, finer melt filters may be used to achieve a higher material purity [17]. HDPE has a higher melting temperature compared to XLPE or PP. The extrusion process also requires a relatively low die-head pressure compared to other materials, according to datasheet [18]. However, it is brittle and may crack or fracture due to external impact [19]. HE3366 by Borealis is used for this research.

2.1.4. Summary Material Properties

Table 2.2 summarises the material properties from the datasheet.

Table 2.2: Datasheet properties of insulation materials.

Mechanical properties	XLPE [20]	PP [16]	HDPE [18]
Tensile strength	21.5 MPa	20 to 28 MPa	23 MPa
Modulus of elasticity	210 MPa	>800 MPa	
Elongation at break	420 %	>800 %	600 %

Main cable characteristics	XLPE	PP	HDPE
Breakdown strength	32 kV/mm	–	22 kV/mm
Thermal performance	Good	Excellent	Medium
Operating temperature	90 °C	100 °C	80 °C
Emergency temperature	105 °C	135 °C	120 °C
Dielectric constant	2.4	2.3	2.3
Dielectric loss [10^{-4}]	5	5	0.6

2.2. Cable Manufacturing Process

The cable manufacturing process for umbilical cables can be divided into the following sections: extrusion, cabling, jacketing, and armouring.

2.2.1. Extrusion

Figure 2.1 shows an overview of the extrusion process. The insulation is coloured by incorporating masterbatches, which consist of a blend of organic and inorganic pigments within a suitable polymer carrier [21]. This colour is introduced into the insulation during the extrusion process. After extrusion, the conductor continues into a cooling line (extruder tank) with varying temperature zones, which is not shown in the figure. The cooling line contains three zones with the following temperatures:

- Zone 1: 70 ± 10 °C
- Zone 2: 50 ± 10 °C
- Zone 3: 30 ± 10 °C

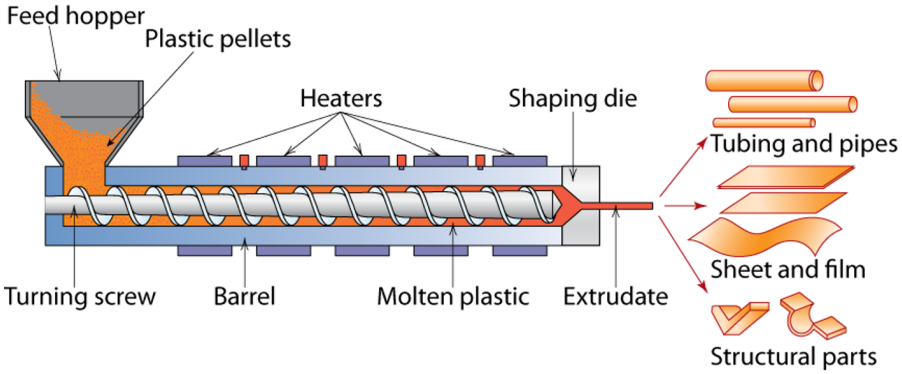

Figure 2.1: Schematic of a plastic extrusion machine [22].

XLPE Cable Extrusion & Curing The XLPE under study is cross-linked using silane-curing, which will be discussed further to evaluate its impact on the cable's electrical properties. This method is used in low voltage (LV) cables and, more recently, medium voltage (MV) cables up to 30 kV [9, 23].

Silane cross-linking is performed in a warm-water bath, following the Sioplas technology. This technology was developed by Dow Corning using conventional cross-linking process [8, 24]. Since this cross-linking requires immersion in water, it is most probable that the polymer contains moisture. The silane compound is grafted into the polyethylene (containing Si-OR groups) and fed into the extruder hoppers with a catalyst and additives in the appropriate ratio as discussed in Section 2.1.1. This mixture can then be extruded using a conventional extruder.

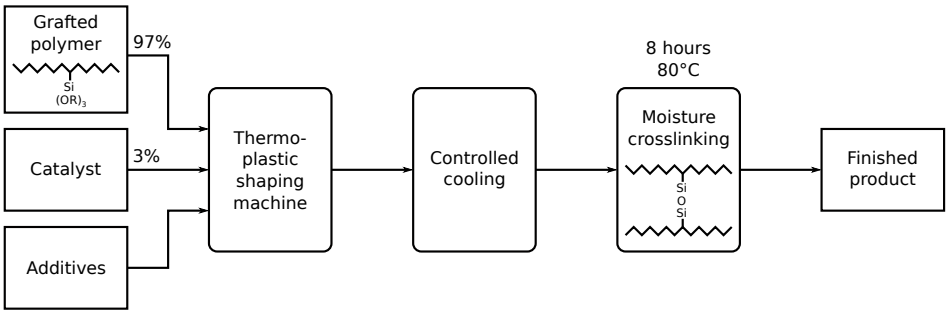

Figure 2.2: Schematic of the Sioplas shaping and cross-linking process (adapted from Narkis, et al. [24]).

After extrusion, the cable is cooled down in a controlled manner by a cooling line with different temperature zones. Curing takes place in a solid state by putting the extruded cable on a reel in a water tank at 80 °C for 8 h. The Si-OR groups hydrolyse, condense, and cross-link PE chains through Si-O-Si cross-links. The moisture curing time for medium-voltage cables depends on the insulation thickness. During this process, the silane groups require a large amount of water for cross-linking, which is extracted from the polymer. Therefore, the finished XLPE cable is expected to have low moisture content [9]. The properties of the Sioplas method are summarised in Table 2.3.

Table 2.3: Advantages and disadvantages of Sioplas (adapted from [8]).

Advantages	Disadvantages
Fast curing when compared to other moisture curing technologies	Two step process
Low capital cost	Limited shelf life; when opened the bag must be used within 4 h
No special equipment required	High raw material cost
Low scrap rates	Risk of pre-cross-linking on the surface of pellets during storage

The amounts of residual/scrap products are much smaller than the peroxide-curing processes described above. The most important residual products are methanol, cumyl alcohol and acetophenone. These products diffuse out of the insulation throughout the curing process [24, 25]. These byproducts proved to be detrimental to the treeing resistance of XLPE. Their removal is an essential step in assuring the quality of the insulation [26].

From experiments conducted by Bulinski et al., immersion without voltage application on unaged cables does not affect the AC breakdown voltage [27]. Even temperature changes during the immersion have no effect, as shown in Figure 2.3. Hence, the moisture curing of silane cross-linking does not compromise the short-term AC breakdown strength. Thus, the cross-linking process with warm water does not affect the quality of XLPE.

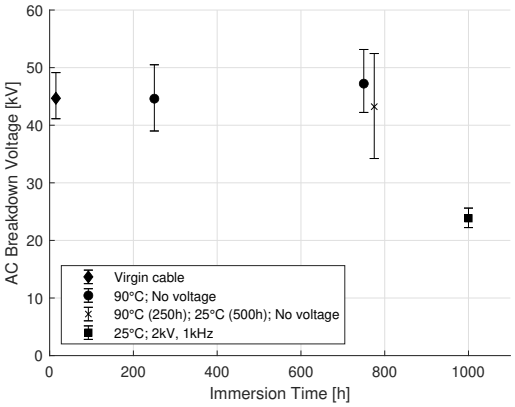

Figure 2.3: Breakdown voltage vs immersion time (reproduced from Bulinski et al. [27]).

PP Cable Extrusion Unlike XLPE, polypropylene is extruded without an extra curing process. Hence, this process takes less production time. Since no additives (except masterbatch) or co-polymers are used, this insulation material is expected to degrade quicker (due to its brittle nature) in terms of mechanical and thermal properties under dynamic mechanical stress. Elastomer fillers could be added to the raw polypropylene to improve these properties. The following chapters will explore the properties of polypropylene and its degradation under dynamic stress.

HDPE Cable Extrusion The HDPE used also has no additives except masterbatch added during extrusion. HDPE insulation does not need any additives since it relies on high crystallinity (high purity) to achieve good insulating performance. Like polypropylene, the production process will take less time than XLPE since no cross-linking is required.

2.2.2. Cabling

ROV power, signal and optic fibre cables are wrapped around in a helical structure along with copper metallic tapes during the cabling stage. The helical structure gives more flexibility, compactness and protection from mechanical stress.

In the cabling process, cable reels containing the different types of cables are loaded into a cabling machine. The cabling machine then wraps the cables around a central core, often with the addition of copper metallic tapes. A helical structure is formed as the cables are wound around the core, creating a helix pattern.

2.2.3. Jacketing

The jacket is the outermost layer of a cable that provides overall protection. It is designed to resist snags and cuts and helps prevent the interior bundle from becoming twisted or tangled. The commonly used materials for extrusion include polyurethane, thermoplastic elastomers, and polyolefins [4].

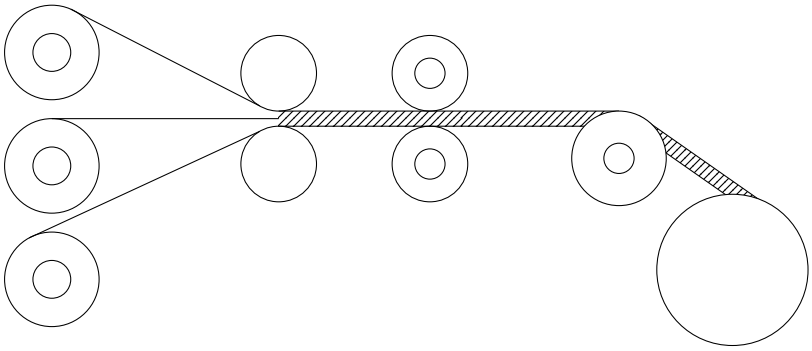

Figure 2.4: Schematic of the cabling process.

2.2.4. Armouring

Armouring is a technique used to increase the mechanical strength and provide tension stability of umbilical cables [28]. A helical geometry is also chosen for the armour to ensure it takes most of the tensile and bending stresses [29]. Even though the steel armour wires are typically galvanised, this may not provide enough protection against corrosion, given that umbilical cables are submerged in seawater. Hence it is a common practice in the industry to coat the armour wires with bitumen. Bitumen has been proven highly effective in protecting armour wires from corrosion [30].

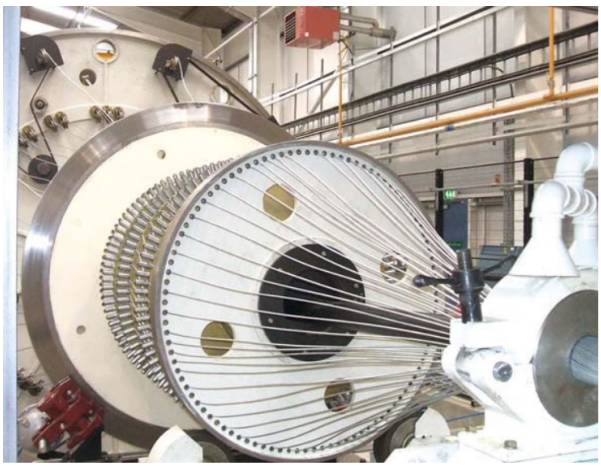

Figure 2.5: Armouring machine using galvanised steel wires.

2.3. Ageing Mechanisms in Cables

Cables do not fail only because of their age, but rather as a function of their age, loading and quality [23]. In solid materials, the breakdown of insulation is caused by electrical breakdown. However, electrical stress alone is not the primary factor contributing to ageing under normal operating conditions. The degradation occurs due to various stresses, most significantly thermal and mechanical stresses [31]. The main ageing mechanisms due to ageing factors in cables are shown in Table 2.4.

Table 2.4: Ageing mechanisms in plastic cables (adapted from Densley [32]).

Electrical	Mechanical	Thermal	Environmental
Electrical treeing	Bending	High temperature	Radiation
Water treeing	Tensile stress	Low temperature	Water/humidity
Partial discharges	Compressive stress	Thermal cycling	Corrosive chemicals
	Vibration		

2.4. Electrical Ageing

This section describes the dominant electrical ageing mechanisms in subsea and dynamic cables. The degradation is most commonly due to electrical or water treeing, which are investigated here. Electrical ageing finally leads to the electrical breakdown of the insulation.

2.4.1. Electrical Treeing

A failure mechanism known as electrical treeing can occur in cables exposed to high electric field stresses. Trees are initiated at locations where the field is distorted due to voids, contaminants, etc. [13]. According to the literature, the main ageing factor in XLPE insulated cables is water tree initiation and growth when exposed to humidity. Electrical trees can eventually be initiated at the tip of a water tree [12]. Electrical trees can initiate from eroded surfaces in a void, water trees, and locations of field enhancement without voids. For the latter, these are two phases of electrical treeing:

- Initiation phase: the movement of charges during each half-cycle of the applied voltage gradually degrades the polymer, forming a small void.
- Growth phase: the initial void is extended to form a tree-like network of branches due to partial discharge activity.

The PD characteristics can help identify electrical trees. However, PD characteristics and the tree-growth rate depend upon the electrical stress applied, temperature, mechanical, and environmental stress.

2.4.2. Water Treeing

Water treeing is the most common cause of ageing in cables with a wet design or high-humidity operating conditions. Over the years, much research has been performed on the initiation and growth of water trees in XLPE-insulated cables [12, 25, 32], as well as its effect on the lifetime of the cable [33]. The initiation and growth of water trees mainly depend on impurity content, moisture content, and micro-voids inside the insulation.

Two types of water trees are found in the cable insulation:

- *Bow-tie trees* [12, 25, 32] grow from water-soluble contaminants or water-filled voids (range of tens of µm) [25, 32]. They propagate perpendicular to the electric field [12, 25].

  The size of the contamination limits the length of the bow-tie tree. The trees formed due to voids grow more rapidly under high temperatures due to the increased moisture diffusion rate. Trees from soluble contaminants grow with time when under electrical stress and are not affected much by temperature or mechanical stress.

  The residual moisture from the cross-linking process can result in small bow-tie trees. However, these trees do not degrade on the breakdown strength as they do not grow to a critical length [25].

- *Vented trees* [12, 32] are initiated at the interfaces due to protrusions or contaminations. When originating from soluble contaminants, they grow with time under electrical and mechanical stress and are not affected much by temperature. Vented trees are dangerous because they can grow through the entire insulation and cause breakdown.

Steennis concludes that the length of bow-tie trees did not increase after 3000 h, while the length of vented trees kept increasing when XLPE cable samples were submerged in a water tank with tap water at 30 °C [25].

Water trees can cause local field enhancements that can become initiation sites for electrical trees (50 Hz or transient overvoltages). At high temperatures, oxidation reactions lead to increased absorption of water. At lower temperatures, water trees take longer to oxidise or become electrical trees, which can cause failure.

Detection of Water Treeing The presence of water trees results in non-linear conduction currents with AC voltages in the range 0.001 to 60 Hz in small samples or short lengths of cables. Measurements at 60 Hz have shown that the capacitance and dissipation factor increase with increasing voltage for

treed-insulation but remain constant for healthy insulation. The drawback of these techniques is that they are only useful when there are many water trees in the insulation.

Withstand tests at 0.1 Hz are used to detect imperfections in aged cables. The density of trees can be derived from visual inspection of small sections of cable insulation, which also provides information on the state of the cable.

Effect on $\tan\delta$ and Capacitance Water treeing or moisture in insulation leads to an increase in $\tan\delta$. $\mathrm{Tan}\,\delta$ and capacitance are measured as an indication of the dielectric quality in the case of underground cables. Measurements are performed at ambient temperature and 50 Hz. The higher the value of $\tan\delta$, the higher the chance of breakdown of the cable insulation.

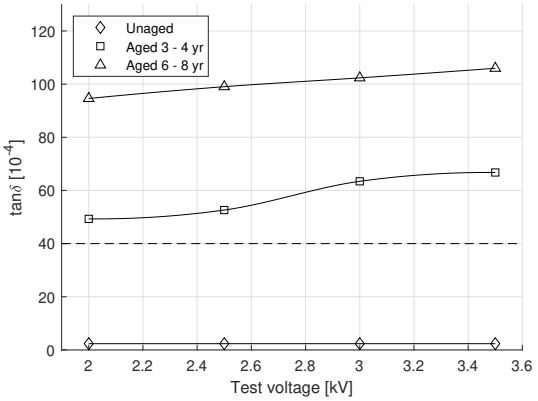

Figure 2.6: Influence of wet ageing on $\tan\delta$ vs voltage (reproduced from Ponniran et al. [34]).

Figure 2.6 shows the change in $\tan\delta$ with the voltage for unaged and aged samples. According to IEC standard 60502 [35], the $\tan\delta$ must be <40 × 10^{-4} at U_0 and the maximum normal operating temperature. Before testing, the aged samples were kept in an open environment for moisture absorption. It is shown that the environmental conditions, mechanical and electrical stress and temperature also significantly influence the $\tan\delta$ values.

Ideally, the capacitance should be constant over the range of test voltages. If not, it may indicate voids, contaminants, or protrusions in the dielectric. These are defects that affect the insulation properties [34].

Water Treeing in Dynamic Cables Dynamic stress (such as bending) increases the growth rate of water- and electrical trees. Tensile and compressive stress (i.e., in the lengthwise direction) respectively increase and decrease the growth of trees. In the experiment by Hellesø et al., the number of bow tie trees after dynamic stress was twice the number observed in the static cable in both tensile and compressive regions. However, the lengths were approximately the same.

However, vented trees were not found during the experiment as their initiation requires a longer time. The main reason was that electrical ageing was only carried out for 3 months at 50 Hz, while the mechanical ageing reached 800,000 cycles (corresponding to many years of ageing in the field) [12].

Summary of water tree initiation and growth factors Table 2.5 summarises the factors influencing the initiation and growth of water trees.

Table 2.5: Initiation and growth factors of water treeing (reproduced from Abideen et al. [36]).

Factor	Pre-requisites	Consequences
Water ingress	Sufficient solubility, diffusion and supersaturation (temperature cycling)	Condensation of water and the build-up of hydrostatic pressure that can result in the growth of water trees
Hydrostatic pressure	Water ingress in the polymer and supersaturation (temperature cycling)	Condensation of water within micro-voids and the initiation or expansion of water trees
Mechanical stress	Sufficient tensile stresses on crazes tip	Formation of microcracks which can initiate trees or influence the growth of existing trees
Stress-induced electrochemical degradation (SIED)	Aluminium conductors and water ingress to the conductor initiating corrosion	SIED structures on the semicon and vented water trees can grow from the conductor screen
Static strain	Sufficient tensile stresses	Formation of microcracks which can initiate trees or influence the growth of existing trees
Dynamic strain	Above 1 % dynamic strain	Formation of microcracks which can initiate trees or influence the growth of existing trees
Voltage/field	Microvoids and sufficient water diffusion into the polymer	Sufficient Maxwell stresses at the crazes tip that can induce further growth of water trees
Frequency	Sufficient resulting mechanical stresses	Accelerating the ageing process of the polymer causing the initiation and growth of water trees
Ionic contamination	Ions diffusion	Accelerated chemical degradation, which can lead to the growth of longer trees
Morphology	Significant amorphous regions	Lowering the mechanical resistance, which can yield the presence of more water trees

Influence of Moisture on XLPE Electrical Properties Moisture leads to a decrease in AC breakdown strength and increased dielectric losses. Polyethylene (PE) cables are prone to water treeing under the combined influence of AC electric stress and humidity [37].

Moisture effect on insulation lifetime The worst case for cables in subsea applications is the insulation getting saturated by water. In the research done by Bulinski et al., the effect of moisture on the XLPE cable is studied [27]. Conductors with 0.75 mm insulation thickness are studied, similar to the thicknesses in this research. The cables were pre-immersed at 90 °C for 250 h, which is presumed enough for the entire insulation to be saturated with water.

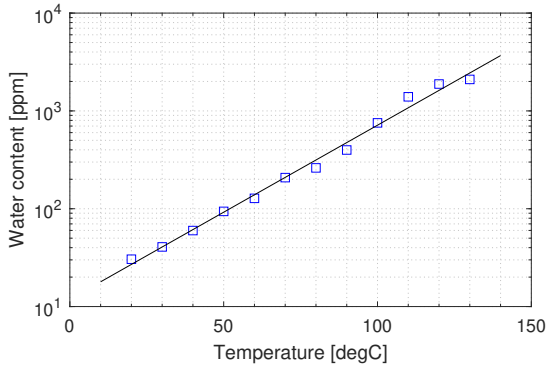

Figure 2.7: Saturated water content of XLPE vs temperature (adapted from Steennis [25]).

Figure 2.8 presents the voltage lifetime curves for several conditions (unaged and pre-immersed as described above). The power law exponent n could be derived using this data, which is a critical parameter in determining cable lifetime. The value is $n = 10.8$ for the cable unsaturated by water, representing the dry conditions. In contrast, the cable saturated with water shows $n = 5.6$. This also seems to be in the range used by Mellinger et al. [38], where $n = 6$ was used for wet-aged cables to calculate the lifetime. Saturation with water will result in a significant reduction in lifetime.

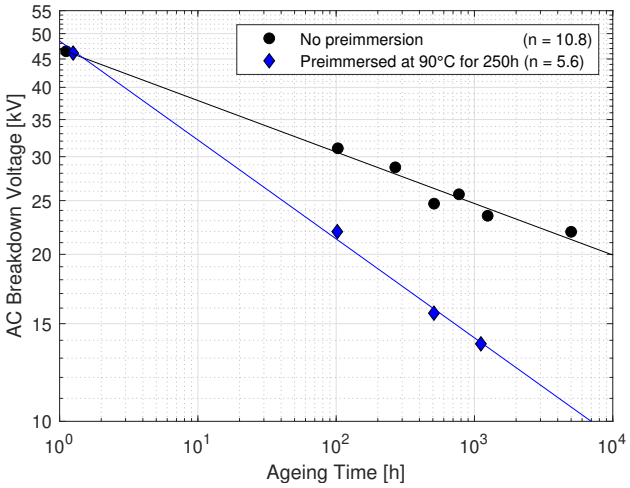

Figure 2.8: Effect of ageing and preconditioning on AC breakdown voltage (adapted from Bulinski et al. [27]).

2.4.3. Partial Discharges (PD)

A partial discharge is a local electrical breakdown event that only partially bridges the insulation system between conductors. The primary factors contributing to partial discharge are cavities within solid dielectrics [39]. Partial discharge can cause deterioration of the insulation material due to the high-energy electrons produced during the discharge. This can lead to chemical decomposition in the insulation material, which could result in complete insulation breakdown. Therefore, it is crucial to monitor partial discharges as an indication of the health of the insulation system [40].

PD can occur due to several reasons like electrical treeing, voids, cuts, cracks, fillers, contaminants with poor adhesion to the polymer, and delaminations at interfaces. The initiation of PD in voids requires a specific level of electrical stress, and the characteristics of PD, including its magnitude and repetition rate, depend on several factors. These factors include the void's size, shape, location, type of gas, and pressure. PD activity in voids can increase the conductivity of the void walls, resulting in PD extinction. Alternatively, it causes erosion, pitting of surfaces, and eventually concentrates in the pits to form electrical trees [32].

2.5. Mechanical Ageing

Mechanical ageing is one of the critical ageing mechanisms in dynamic subsea cables. The life expectancy of dynamic umbilical cables is predominantly analysed for mechanical fatigue. Little consideration is given to the effect of mechanical stress on the dielectric under the assumption that the non-polymeric components will fail (for, e.g., the armour) before the polymeric components [5]. However, in this section, the effect of mechanical stress on the insulation is also covered.

In service, the XLPE insulation is subjected to various stresses due to temperature variations, humidity, pollution, mechanical forces, electrical stress, and irradiation due to sunlight. These can lead to the formation of cracks and breakdown of insulation [26]. Concerning polypropylene, it is already known that its high stiffness and brittleness are restricting factors for dynamic cables [41].

2.5.1. Fractures in Polymers

Stress cracking or brittle cracking has also been identified as a cause of dielectric degradation in polymers. Stress cracking or low mechanical stress leads to the formation of small cracks known as crazes. These are localised deformed regions consisting of voids or fibrils. They propagate perpendicular to the local stress.

Stress cracking occurs at low temperatures when insulation is brittle and subjected to AC stress for an extended period of time [25, 42]. This means polypropylene insulation might be more prone to stress cracking due to its brittleness at low temperatures.

2.5.2. Mechanically-Induced Electrical Breakdown

Mechanical stress and strain significantly influence the electrical performance of insulation materials. These stresses can also initiate electrical treeing. The ageing process of XLPE cables under AC stress can be accelerated by mechanical stress on air-filled cavities. Experiments also found that the degassed and relaxed XLPE samples showed high values of electrical tree inception time [26].

However, according to Spencer et al. [6], there was an increase in electric field enhancement of 12 % or more in the deformed cable, depending on the load. This enhancement may lead to insulation breakdown before the actual mechanical failure. COMSOL simulations demonstrated this phenomenon in regions subjected to the minimum bending radius. In ROV cables, this cannot be fully controlled when underwater. Therefore the usual approach is to cut off the part of the cable that experienced a mechanically-induced electrical breakdown.

2.5.3. Effect of Conductor Cross-section

Currently, non-compressed stranded conductors are used for the cables under study. However, research on marine cables by Yan et al. [43] found that compressed stranded conductors were most resistant to bending fatigue since they had the largest energy dissipation. However, the cross-section also plays an important role. For larger cross-sections, slippage during bending may result in the deformation of the conductor. As a result, the compressed round conductor is the best choice for this application.

2.6. Thermal Ageing

The mechanical behaviour of a material is affected by temperature, and the stress exerted on the material is further increased by temperature gradients [44]. From the literature, heating XLPE samples after mechanical ageing can lead to relaxation and an increase in AC breakdown voltage [26]. It was also found that when silane cross-linked XLPE sheets were put at 80 °C for 90 days, the tensile stress and breakdown voltage decreased while the leakage current increased. This rise in leakage current and fall in breakdown voltage can lead to dielectric failure. This would limit the use of silane cross-linked XLPE in hot environments [45].

2.7. Diagnostic Tests for Extruded Cables

Various diagnostic tests are presently utilised for extruded insulating materials and cable systems. Most of these tests are conducted in laboratory settings to assess the properties of the materials. They can be employed alongside cable tests to evaluate the overall “condition” of the cable system. However, it is essential to establish specific criteria for the “condition” assessment in relation to various cable tests.

Table 2.6 briefly summarises these tests.

Table 2.6: Diagnostic tests on extruded cables (adapted from Densley [32]).

Destructive	Frequency Range	Critical Value
AC breakdown	50 Hz	–
Impulse breakdown	–	–

Non-Destructive	IEC 60326	Comment
AC withstand	0.1 Hz	2.5 to 3U_0 for 15 min
Capacitance & $\tan\delta$	0.1 Hz, 50 Hz	Versus U; Test $\leq U_0$
Dielectric spectroscopy	0.001 to 1000 Hz	Versus f; Test $\leq U_0$
Partial discharges	0.1 Hz, 50 Hz	

2.8. Conclusion

The chapter explored the insulation materials used in umbilical cables, namely XLPE, PP, and HDPE. XLPE was noted for its excellent properties after cross-linking and wide usage in medium voltage AC, HVAC, and HVDC cables. PP and HDPE were recognised for their cost efficiency and reduced environmental impact. However, it is important to note that PP can become brittle in low temperatures, and HDPE is susceptible to cracking from external impact.

The main ageing mechanisms of static and dynamic power cables were discussed, highlighting electrical and water treeing as the main degradation factors. Electrical treeing occurs under high electric field stresses, forming tree-like structures within the insulation. In contrast, water treeing is the common cause of ageing in cables operating in wet or high-humidity conditions. Furthermore, the growth of water and electrical trees can be influenced by mechanical stresses in dynamic cables, such as bending, tensile, and compressive stress. Dynamic stress, in particular, accelerates the growth rate of water and electrical trees.

Moisture was recognised as a significant factor impacting the electrical properties and lifetime of cables. Saturation of insulation with water can decrease AC breakdown strength and increase dielectric losses, resulting in reduced cable lifetime compared to dry cables. The following chapters investigate the effect of bending stress and moisture on the insulation properties of umbilical cables.

3

Material Testing

In this chapter, the focus will be on material testing. Non-destructive diagnostic test, like dielectric spectroscopy (DS), is performed to study the insulation material and its dielectric properties at different temperatures.

3.1. Flat Sample Preparation

Thin, uniform, flat samples are required for most material-level tests (such as breakdown tests, dielectric spectroscopy, etc.). A mechanical press and a custom-made mould were used to manufacture these samples. The necessary steps to obtain thin samples involve determining an appropriate temperature-pressure profile and designing a mould with a smooth surface.

3.1.1. Press Profiles

The mechanical press and mould were preheated to 180 °C for 30 min. The melt from the extruder was then subjected to a pressure of 100 MPa for 15 min. Afterwards, the pressure is removed, and the sample is cooled to room temperature before removing it from the mould.

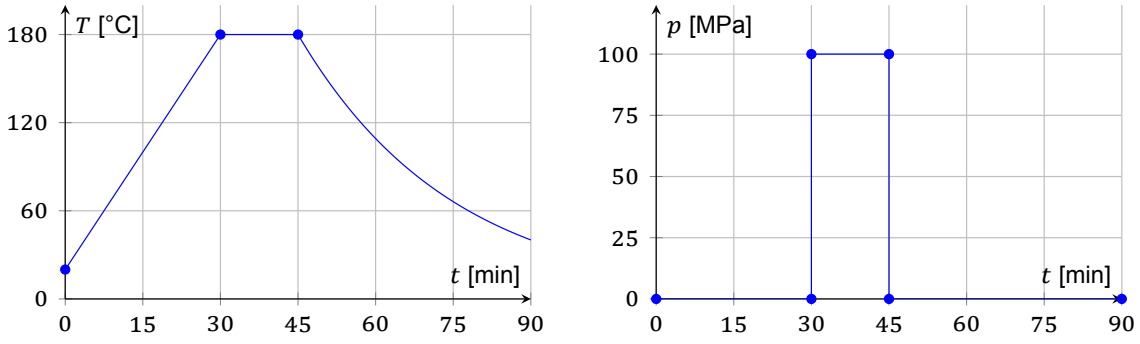

(a) Temperature profile

(b) Pressure profile

Figure 3.1: Temperature and pressure profiles for flat sample manufacturing.

Several iterations were required to obtain the final mould design, which could ensure the desired properties. For this, the mould needed constant thickness and very flat surfaces. Furthermore, it had to be made of a material that could handle the required heat and pressure without deforming. Finally, the samples should release from the mould without sticking to it or deforming. The trials using XLPE leading to this mould are briefly described below.

3.1.2. Trial 1

This initial attempt aimed to determine if flat samples could be made from the melt of the extrusion machine. Melt was collected just before the extrusion head, and two flat aluminium plates were used

to shape the sample in the press. Even though the samples became relatively flat, the thickness was quite variable (0.1 to 0.8 mm). This variation in thickness is undesirable for material testing as it can lead to bad contact with the electrodes and deviations in the measured material properties.

A Teflon sheet was placed between the metal plates and the sample to prevent the XLPE from getting stuck or damaged during the removal of the sample.

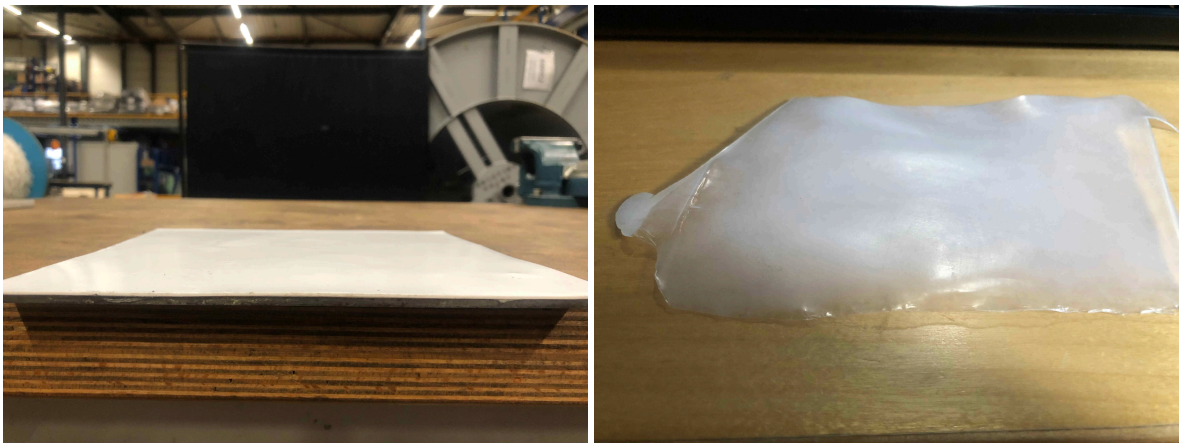

(a) Mould with Teflon sheet (b) Flat XLPE sample with varying thickness

Figure 3.2: Flat sample trial 1.

3.1.3. Trial 2

During this trial, a stainless steel mould with a slot thickness 1.25 ± 0.10 mm was made. This slot thickness was chosen to obtain 250 µm thick samples, taking into account the thickness of the Teflon sheet (1 mm). The Teflon sheets were observed to deform under high pressure. This led to indentations on the Teflon and varying thicknesses of the samples.

Therefore, the Teflon sheets were removed, and silicone grease was sprayed on the mould as releasing agent. This allowed for the fabrication of samples with a uniform thickness of 1.25 ± 0.10 mm.

(a) Mould with 1.25 mm slot thickness (b) Flat XLPE with 1.25 ± 0.10 mm thickness

Figure 3.3: Flat sample trial 2.

3.1.4. Trial 3

The previously accumulated experience resulted in a final stainless steel mould. This mould was circular with a slot thickness of 225 ± 25 µm and diameter of 14 cm. With this mould, samples of the desired size, shape, and constant thickness could be produced reliably.

(a) Mould with 0.25 mm slot thickness.

(b) Flat PP with 152 ± 22 µm thickness.

Figure 3.4: Flat sample trial 3.

3.1.5. Conclusion

The iterations described above are summarised in Table 3.1. After successful mould design iterations, flat thin samples of XLPE, polypropylene, and HDPE material were made using mould number 3.

Table 3.1: Summary of flat sample trials.

Trials	Conclusions
Trial 1	Non-uniform thickness due to insufficient flatness of brass mould plates
Trial 2	Teflon deformed under high pressure. Varying thickness of samples and unwanted indentations. Use a releasing agent like silicone grease instead.
Trial 3	Samples of uniform thickness. Can be used for testing.

3.2. Dielectric Spectroscopy

Dielectric spectroscopy is a technique used to study the dielectric properties of materials. It measures the complex permittivity $\dot{\varepsilon}$ of a material as a function of frequency [46].

$$\dot{\varepsilon}(\omega) = \varepsilon'(\omega) - j\varepsilon''(\omega) = \varepsilon_0\varepsilon_r'(\omega)(1 - j\tan\delta(\omega)), \tag{3.1}$$

where the real part shows the energy-storing capability (capacitance) while the imaginary part represents the losses in the dielectric. The loss factor $\tan\delta$ will increase with the increase in impurities or defects as the resistive current component increases [47].

3.2.1. Novocontrol Alpha

The Novocontrol Alpha is a dielectric spectrometer used to measure the electrical properties of materials as a function of frequency and temperature. It is capable of performing broadband measurements (30 µHz to 40 MHz) of the complex permittivity and conductivity of materials. Experiments were conducted in the frequency range of 10 mHz to 1 MHz. The samples were subjected to frequency sweeps at temperatures from −30 to 90 °C in steps of 20 °C. The thin samples were sandwiched between electrodes of 4 cm diameter as shown in Figure 3.5b.

3.2.2. XLPE

Samples from the manufacturer (Padanplast) are compared with the samples made by the silane cross-linking process. The manufacturer samples were cross-linked in a climatic cell for 12 h at 60 °C with a relative humidity of 90 %. The samples made from the melt by extrusion were cross-linked in a warm

(a) Novocontrol Alpha with the liquid nitrogen tank.

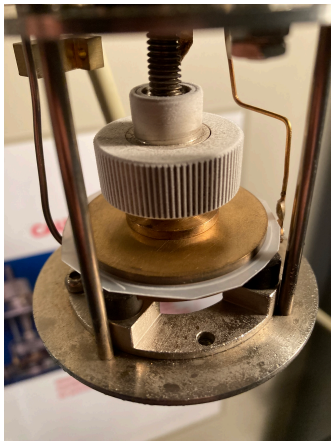

(b) Sample sandwiched between electrodes in the sample cell.

Figure 3.5: Novocontrol Alpha setup

water bath at 80 °C for 4 h. The relative permittivity of both samples can be seen in Figure 3.6a. The permittivity is in the expected range. When it came to the $\tan\delta$ measurement, the samples made by cross-linking in warm water showed a higher loss factor when compared to the samples from the manufacturer. A peak can be observed around 1 to 100 Hz for the water cross-linked sample, which is due to interfacial polarisation [47].

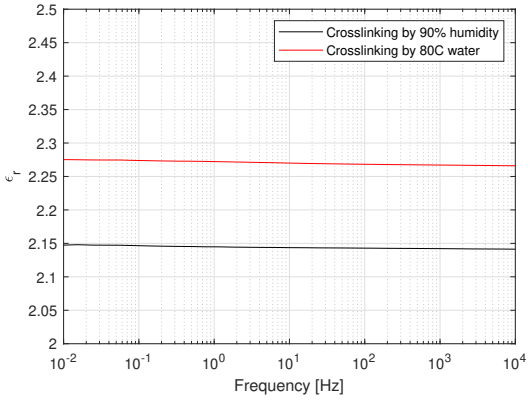

(a) Relative permittivity ε_r

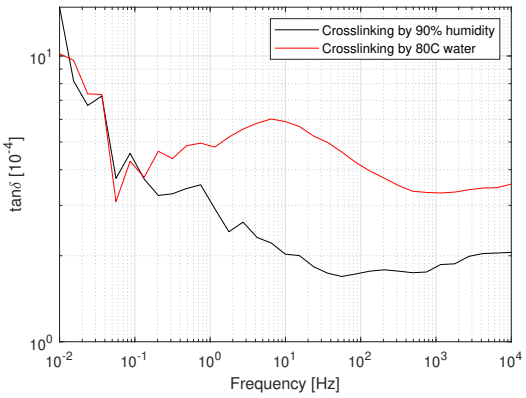

(b) Loss tangent $\tan\delta$

Figure 3.6: Comparison of dielectric spectra of moisture and humidity cross-linked XLPE.

Figure 3.7 shows the dielectric spectrum of the silane cross-linked samples over temperature. The dielectric constant decreases with temperature due to a decrease in crystallinity. The $\tan\delta$ spectrum exhibits a high-frequency peak around 1 to 10 kHz, which may be attributed to interfacial polarisation between the amorphous and crystalline phases, similar to the measurement described above. Another potential explanation for this peak is the presence of polarisable impurities, cross-linking byproducts, and polar side chains in the amorphous regions [48]. At high temperatures, a low-frequency peak also becomes apparent due to the increased motion of polymer chains.

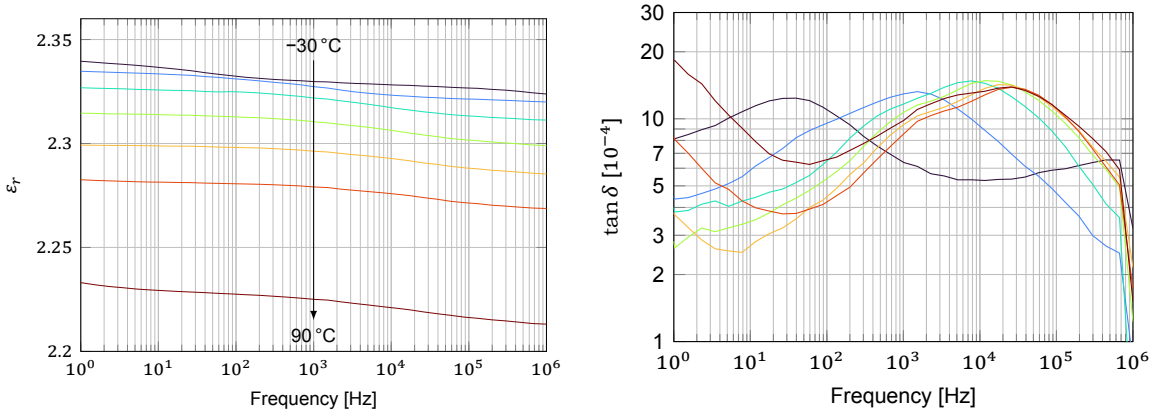

(a) Relative permittivity ε_r

(b) Loss tangent $\tan\delta$

Figure 3.7: Dielectric spectrum of XLPE versus temperature. Colors indicate the temperature of the measurement: −30 °C (dark blue) to 90 °C (dark red) in 20 °C steps.

3.2.3. Polypropylene

The dielectric constant of (isotactic) polypropylene shows a decreasing trend with increasing temperature. This is because iPP is a semi-crystalline polymer, and increasing the temperature results in decreased ordering (and hence density and ε_r) of the crystalline regions [49].

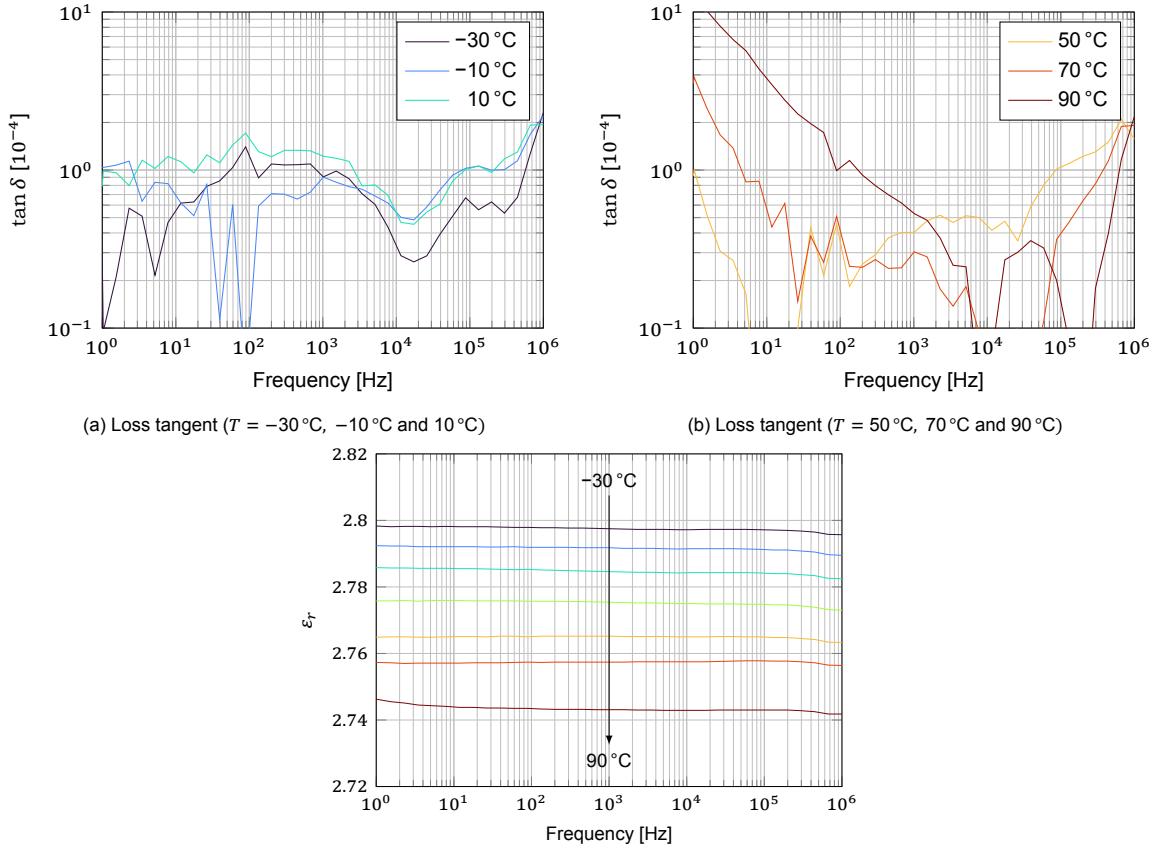

(a) Loss tangent (T = −30 °C, −10 °C and 10 °C)

(b) Loss tangent (T = 50 °C, 70 °C and 90 °C)

(c) Relative permittivity ε_r

Figure 3.8: Dielectric spectrum of polypropylene.

In Figure 3.8b, the $\tan\delta$ at low frequencies increases with temperature. There are two possible explanations for this phenomenon. First, the conductivity of the insulation increases with temperature,

resulting in a slope of −1 (since $\tan\delta$ is defined as $\frac{1}{\omega RC}$). Second, the polymer chains become mobile and contribute to polarisation at low frequencies. Therefore ε_r increases at low frequency as seen in the 90 °C curve in Figure 3.8c. This indicates that the dielectric performance of polypropylene will deteriorate at temperatures close to the maximum conductor temperature of 90 °C. This may be because this polypropylene variant is not explicitly intended for high-voltage use.

3.2.4. HDPE

Like for XLPE and PP, the ε_r of HDPE drops slightly with increasing temperature due to the decreasing crystallinity of the material. In addition, the $\tan\delta$ and ε_r do not vary much with frequency over the measured temperature range, indicating good temperature stability. Usually, HDPE is stable up to 110 °C since the crystallinity drops rapidly above this temperature [50].

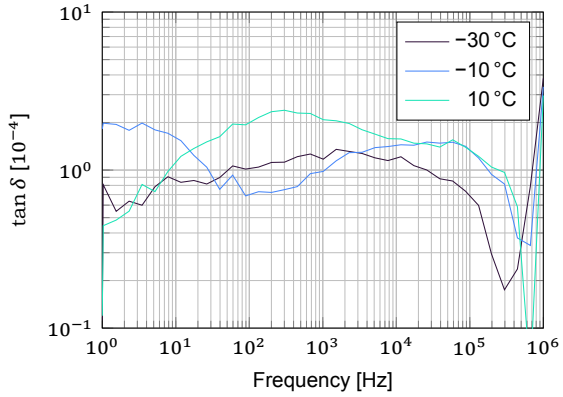

(a) Loss tangent (T = −30 °C, −10 °C and 10 °C)

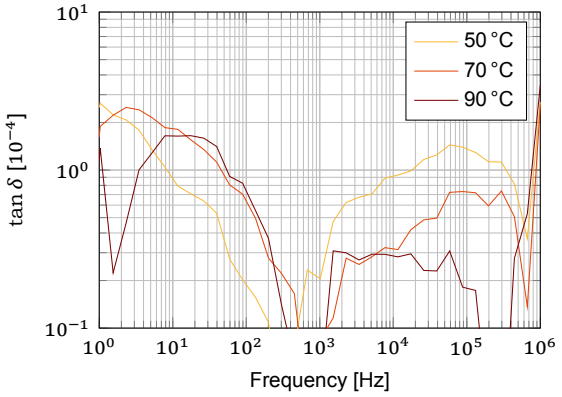

(b) Loss tangent (T = 50 °C, 70 °C and 90 °C)

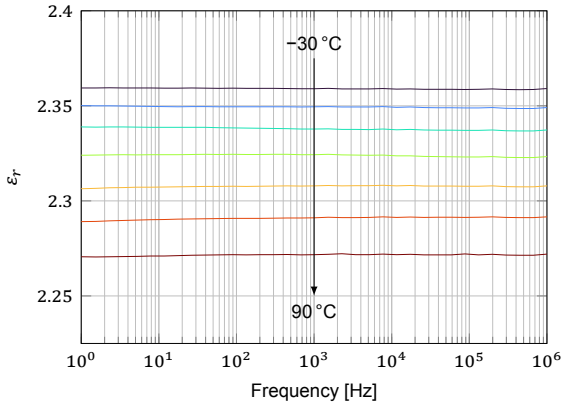

(c) Relative permittivity ε_r

Figure 3.9: Dielectric spectrum of HDPE.

3.3. Conclusion

The chapter dealt with material studies of XLPE, polypropylene, and HDPE using the dielectric spectroscopy technique. Thin material samples were produced using a stainless steel mould and a temperature-controlled mechanical press. The dielectric spectrum of the material samples was measured as a function of temperature. XLPE and HDPE were stable up to the maximum conductor temperature of 90 °C. The crystallinity of polypropylene started decreasing above 50 °C, which indicates that the current polypropylene material must be studied in more detail before DeRegt can use it at higher voltages. The addition of elastomer fillers can improve the electromechanical properties of polypropylene.

4

Single Conductor Testing

In this chapter, the main aim is to find the relationship between electrical and mechanical (bending) ageing. Methods for mechanical ageing and electrical testing of the single conductors are presented. Electrical breakdown tests are performed using step-voltage stress, and the results show that mechanical ageing influences the dielectric strength. Partial discharge analysis was done on these conductors to study the mechanical effect in detail.

4.1. Samples

In this chapter, electrical tests are performed on polymer-insulated cables produced using a conventional extruder. The insulation materials of these cables are XLPE and polypropylene. Both cables have the design with the parameters shown in Table 4.1. Further, these cables are combined into triples (three conductors), with a shared metallic sheath which is grounded and an outer jacket.

Table 4.1: Parameters of the cable used for testing.

Parameter	Value
Conductor area	8.39 mm^2
Insulation thickness	0.88 mm
Line to line voltage	4.5 kV

4.2. Mechanical Ageing Setup

A cyclic bend-over-sheave (CBoS) test is performed on the single conductors. The test setup, built by DeRegt Cables, is shown in Figure 4.1. The piston creates a repetitive linear motion of the cable, which causes it to bend over the sheave wheel at a certain velocity profile. The cable can be divided into three zones:

- The no-bending zone in white does not reach the sheave wheel and hence is not aged. This part of the cable is, therefore, not tested.
- The single bending zone in yellow, which goes over the sheave wheel once.
- The double bending zone (DBZ) in red goes over the sheave wheel twice during each cycle.

The sheave wheel diameter to conductor diameter ratio D/d determines the acceleration factor of the CBoS test. A ratio of 29 is chosen, giving $D_{sheave} = 160$ mm such that it respects the minimum bending radius (MBR) of the cable. The tensile load is applied by putting a mass m_L on the end of the cable.

$$m_L = \frac{kA\sigma_{UTS}}{g} = 28.5\,\text{kg} \tag{4.1}$$

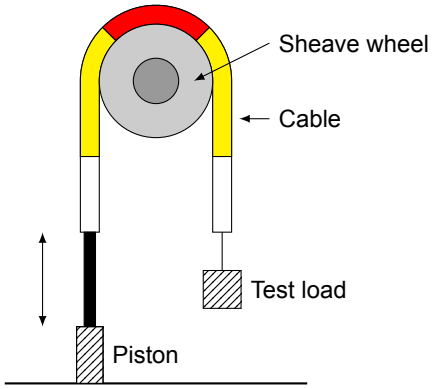

(a) Schematic of CBoS setup. The yellow and red colours of the cable indicate the single and double bending zone, respectively. The white part is not subjected to bending stress.

(b) Mechanical setup for bending.

Figure 4.1: CBoS for single insulated conductors.

where $A = 8.39\,\text{mm}^2$ is the conductor area, $\sigma_{UTS} = 200\,\text{MPa}$ is the ultimate tensile strength, and $g = 9.81\,\text{m/s}^2$ is the gravitational acceleration. The constant $k = 1/6$ is used to ensure that the applied load is at least six times lower than the tensile strength of the conductor. The used CBoS parameters are presented in Table 4.2.

Table 4.2: CBoS parameters for mechanical ageing.

Parameter	Value	Note
Cycle time	10 s	
Sheave wheel diameter	160 mm	MBR =100 mm
Load	28.5 kg	
Number of cycles	5000; 10,000	

Pre-study A pre-study was performed in the initial months of this research to answer some questions like whether this kind of bending stress would affect the degradation of the dielectric, whether these samples could be electrically broken, and how a setup can be created for electrical breakdown and mechanical testing. The results of this pre-study can be found in Appendix B.2.

4.3. Electrical Test Setup

The electrical breakdown setup consists of several components: a high voltage source (transformer), variac, current limiting resistor, capacitive divider, and test vessel with the sample. Everything is placed inside a grounded metal cage enclosure with an interlock system. The setup is shown in Figure 4.2.

Water Tank The high voltage and ground must be supplied to the cable. Because the cables under investigation do not have a metallic sheath, water provides a ground electrode for the cable. This

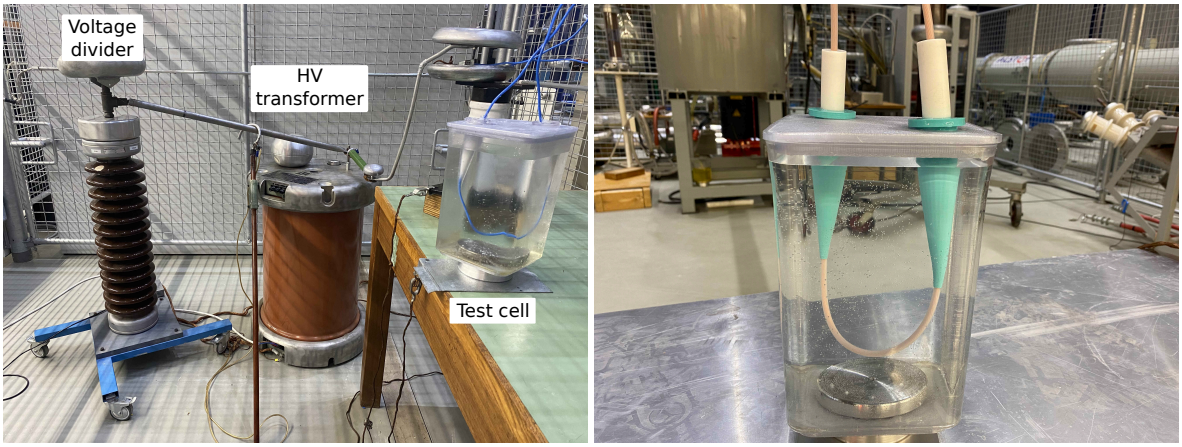

(a) Breakdown setup for single conductors.

(b) Close-up of the test cell.

Figure 4.2: Photographs of the electrical test setup.

ensures an almost perfect interface between the insulation and the “electrode.” The effect of salt water on short breakdown tests is irrelevant. It was shown that in full-scale testing, the effect of salinity on breakdown strength was insignificant [51]. The conductivity of tap water used for this experiment was found to be approx. 460 µS/cm using an LF 330 conductivity meter.

Test Cell Excessive partial discharges were observed at the triple point formed by the water (functioning as the ground electrode), cable insulation, and air. A bushing was designed to reduce the field strength at this location. This lowered the electric field strength and eliminated the discharges in the desired test voltage range. After several iterations, the final design is presented in Section 4.3.2.

4.3.1. Test Procedure

First, the breakdown voltage was found by increasing the voltage linearly with a slope of 500 V/s. After knowing the ramp breakdown voltage, the remaining tests are performed with step voltage stress. Starting from 0 V, steps of 5 kV were taken every 30 s until 60 % of the ramp breakdown was reached. Afterwards, steps of 1 kV for every 30 s until breakdown. This method is used for mechanically aged and unaged insulation. Using this procedure, the time to breakdown is usually in the range of 5 to 10 min.

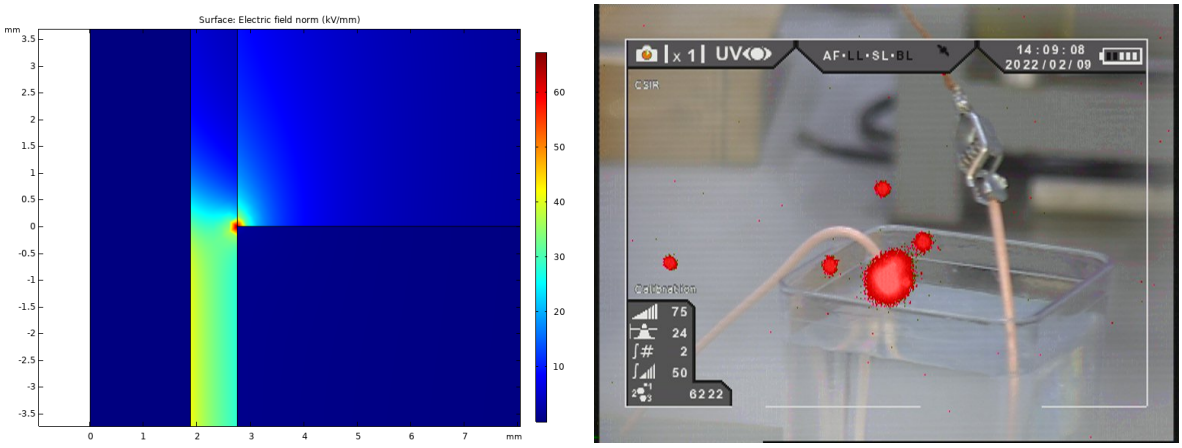

(a) Triple point due to air, water and insulation.

(b) Corona camera picture showing discharges at the triple point.

Figure 4.3: Field enhancement at the triple point.

4.3.2. Challenges

A triple point is formed at the interface of the water (conductor), air and cable insulation. Field enhancement occurs at this point because the ground electrode is terminated abruptly. Flashover occurred at a relatively low voltage, which disrupted the testing. The field distribution is simulated using COMSOL and shown in Figure 4.3. The partial discharges at the triple point were captured with the CoroCam. Several bushing iterations were designed to control the field strength at the triple point and increase the flashover voltage.

Bushing 1 – PVC Pipe For the first bushing, a PVC pipe was filled with grease to increase the overall diameter of the construction, thereby decreasing the stress at the triple point. The pipe was terminated using watertight caps. However, during experiments, it was noticed that the cable broke only at the tip of the watertight caps under water. Further simulations showed that the field is also enhanced at the tip inside the water, as shown in Figure 4.4a. Thus the design needed to be modified.

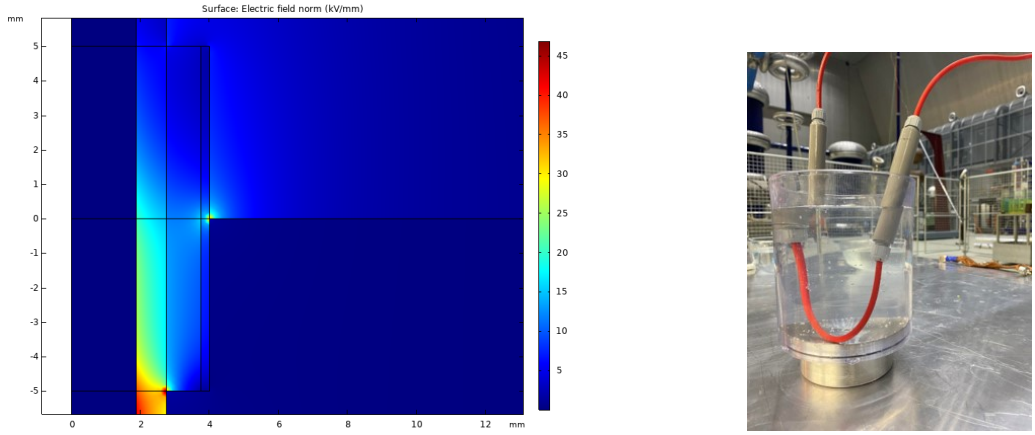

(a) Bushing design 1 in COMSOL.

(b) Bushing made with PVC pipe.

Figure 4.4: Triple point when cable under water.

Bushing 2 – Teflon Tube The second bushing was made from a Teflon tube with a shaped tip. The ends of the cone were designed using electrode grading so that electric field lines make a smooth transition from the insulation through the bushing to the ground electrode. This can be seen in Figure 4.5b. When testing with this Teflon bushing, the cable broke again at the tip as it did not provide a watertight seal due to its inflexibility. As a result, the effect of the cone was counteracted, and this design was unsuitable for testing.

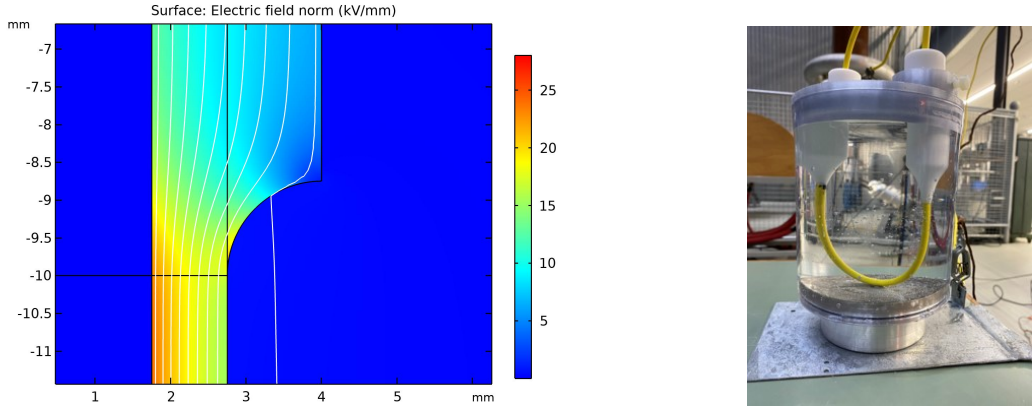

(a) Bushing design 2 in COMSOL.

(b) Bushing with Teflon.

Figure 4.5: Modified design to eliminate the triple point.

Bushing 3 – Cones To resolve the issues of the previous iteration, the tip of a glue gun was used: it provides the desired conical shape and a watertight seal around the cable. After this proof of concept, the final cone design was 3D printed (FDM technology) using thermoplastic polyurethane (TPU), shown in Figure 4.8a. The flexible nature of TPU made it possible to make the ends watertight.

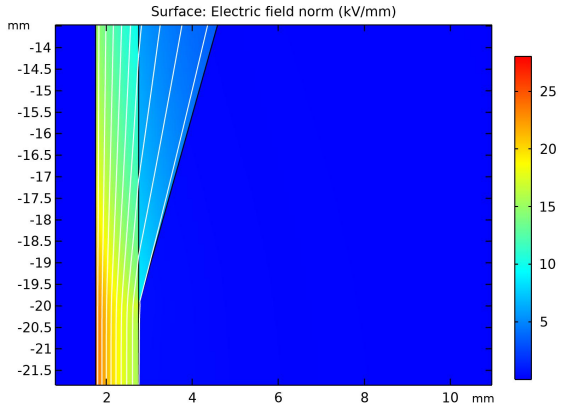

(a) Bushing design 3 in COMSOL.

(b) CoroCAM photograph with the bushing, which eliminates the triple point discharges. Discharges have moved to the upper part of the cone.

Figure 4.6: Elimination of field enhancement and triple point with cone bushing.

TPU has high moisture absorption, which may lead to the failure of the cones. Experimental observation of water absorption of TPU cones immersed in water at room temperature of 21 °C is shown in Figure 4.7. During experiments, it is advisable to put the TPU cones in the oven at 45 °C at regular intervals to avoid water seeping through the cones. Another approach for producing cones is using SLA 3D printing technology and materials with low water absorption properties. Flexible resin is an example of such a material. Cones printed using this resin (shown in Figure 4.8b) showed no significant water absorption.

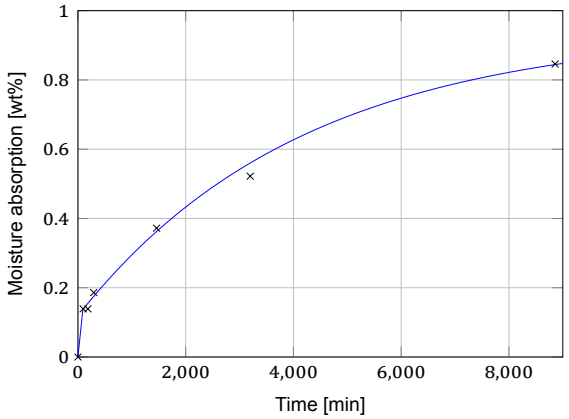

Figure 4.7: Moisture Absorption curve of TPU cones over a time span of 8000 min. The black crosses ($\times$) are measurement points, and the blue line is an exponential curve fit through the measurements ($\tau = 4.2 \times 10^3$ s).

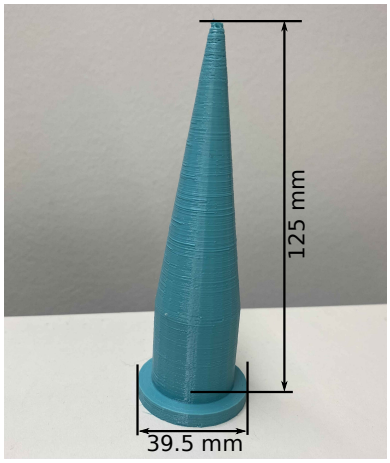

(a) TPU cones

(b) Flexible resin cones

Figure 4.8: Final cone designs. TPU cones were used for prototyping and the initial testing phase. For later tests, flexible resin cones were used.

4.4. Breakdown Results

In the following paragraphs, the results of short breakdown tests on XLPE and polypropylene cable segments (20 cm) are analysed. The cable segments were mechanically aged using the CBoS setup according to the procedure.

4.4.1. Weibull Statistics

Weibull distribution is the most widely used distribution for reliability analysis [52]. It is recommended by IEEE 1407/IEC 62539 [53] for reliability and lifetime data analysis. The scale parameter α and shape parameter β are extracted using the two-parameter Weibull distribution. The scale parameter gives the 63.2 % of the failure rate of samples, and the shape parameter β is the slope of the distribution curve and indicates the spread of the research.

$$F(t) = 1 - \exp\left(-\left(\frac{t}{\alpha}\right)^{\beta}\right) \tag{4.2}$$

Two methods are commonly used to estimate the parameters of the Weibull distribution: Rank Regression (RR) and Maximum Likelihood Estimation (MLE). The maximum likelihood estimation method is more effective than rank regression in situations with significant censoring, such as when there are many suspensions [52]. Therefore, MLE was chosen to process the results of this project.

4.4.2. Effect of CBoS Ageing

From the literature review, it was clear that mechanical stress affects the cable's dielectric properties as described in Section 2.5. To further explore this, AC breakdown tests were performed on unaged samples and samples that had undergone CBoS ageing.

XLPE The breakdown results for XLPE are presented in Figure 4.9, along with the fit to the Weibull distribution. It is clear from the data shown in Table 4.3 that mechanical ageing on the sheave wheel has affected the dielectric breakdown strength. The scale parameter is somewhat reduced, but the β is also reduced, indicating a change in the ageing mechanism.

Further analysis (Table 4.4) showed that the data could be split into two sub-populations: a set of points degraded by the mechanical ageing and another set that showed almost no degradation. The cable was degraded locally, resulting in varying results on short cable samples. The log-likelihood $-2\mathcal{L}$ of the split datasets are lower, indicating a better fit than the single population analysis. Cables under bending fatigue do not degrade everywhere but instead undergo local degradation.

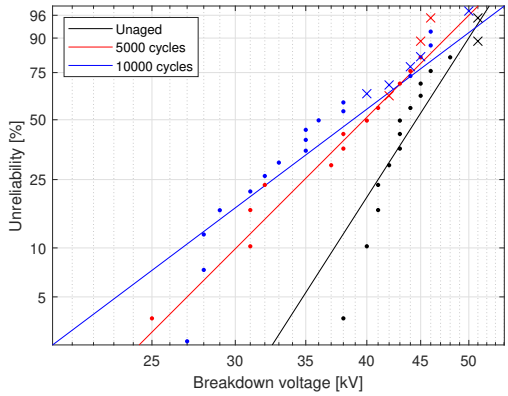

(a) Effect of mechanical ageing.

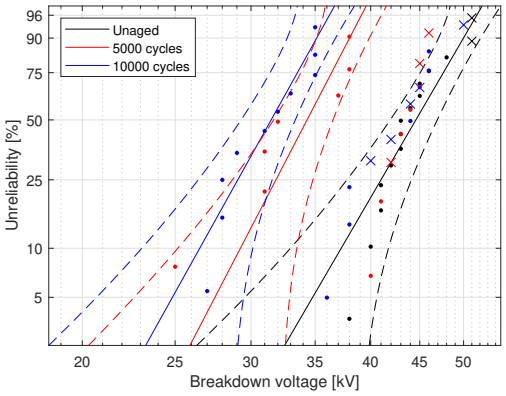

(b) Using data splitting for aged samples.

Figure 4.9: Weibull probability plot of XLPE. Dots (·) indicate the breakdown voltage, while crosses (×) indicate censored observations.

Table 4.3: Effect of mechanical ageing on breakdown voltage.

Number of cycles	α	β	$-2\mathcal{L}$
0	46.2 ± 4.6 kV	10.5	82.5
5000	42.0 ± 2.9 kV	6.7	87.0
10,000	41.7 ± 3.4 kV	5.0	123.9

Table 4.4: Data splitting for aged samples.

Number of cycles		α	β	$-2\mathcal{L}$
0		46.2 ± 4.6 kV	10.5	82.5
5000	low	35.4 ± 2.0 kV	11.8	71.5
	high	45.5 ± 2.9 kV		
10,000	low	32.6 ± 1.6 kV	11.0	95.7
	high	46.9 ± 2.9 kV		

Polypropylene When it came to mechanically aged samples of 5000 and 10,000 cycles, neither could be broken even at 54 kV. The experiments were repeated several times with consistent results. The insulation showed significant whitening after bending, as shown in Figure 4.6, possibly due to strain crystallisation [54]. For further investigation, PD measurements were subsequently conducted to determine the underlying cause of this phenomenon.

Table 4.5: Effect of mechanical ageing on breakdown voltage.

Number of cycles	α	β
0	44.8 ± 1.6 kV	26.9

Table 4.6: Whitening of polypropylene insulation due to bending.

4.5. Partial Discharge Analysis

Phase-resolved partial discharge (PRPD) patterns of the cable samples were recorded using the classical detection circuit and a Hipotronics DDX9101 partial discharge detector to explain the effect of mechanical ageing. The setup consisting of cable, aquarium, calibrator, coupling capacitor and coupling device can be seen in Figure 4.10a. Calibration was performed before each sample measurement. Each PRPD pattern was obtained by recording PD for 120 s.

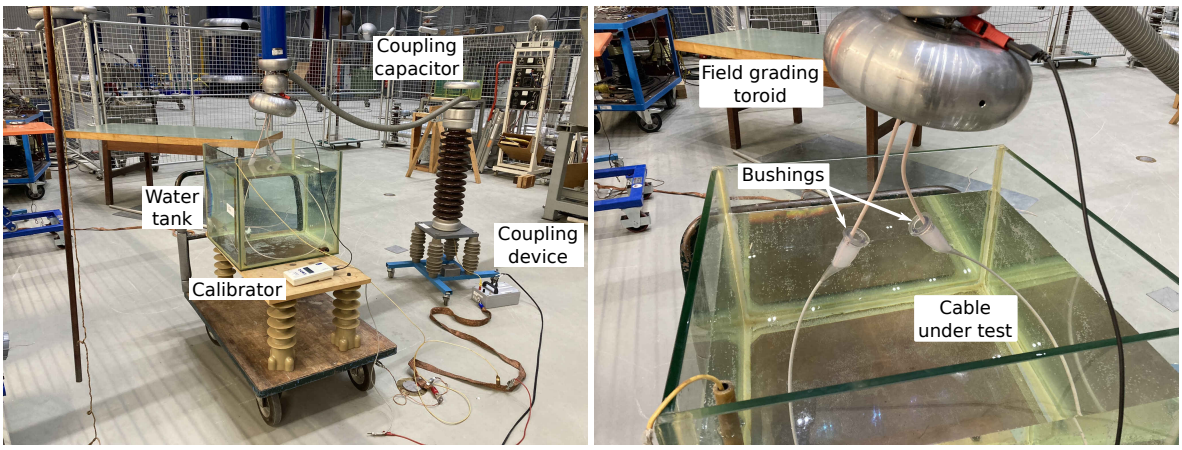

(a) PD setup with coupling capacitor

(b) Close-up of cable in water

Figure 4.10: Photographs of partial discharge setup

The inception (PDIV) and extinction (PDEV) voltages are presented in Table 4.7. The PRPD patterns are recorded at a voltage approximately 20 % higher than the PDIV. Figures 4.11 and 4.13 shows the PRPD patterns obtained for the six cable samples.

Table 4.7: PD inception and extinction voltages.

Insulation material	Number of cycles	PDIV	PDEV	Testing voltage
XLPE	0	6.1 kV	5.8 kV	7.2 kV
	5000	2.9 kV	2.9 kV	3.6 kV
	10,000	2.6 kV	2.6 kV	3.1 kV
XLPE (thermal)	10,000	3.0 kV	2.9 kV	3.6 kV
PP	0	6.1 kV	6.0 kV	7.1 kV
	5000	4.1 kV	4.0 kV	4.9 kV
	10,000	3.8 kV	3.4 kV	4.6 kV
PP (thermal)	5000	3.5 kV	3.2 kV	4.2 kV
	10,000	3.5 kV	3.0 kV	4.2 kV

Both materials show highly unsymmetrical PRPD patterns, concentrated on the negative half-cycle. This indicates that the cavities are bounded by the HV electrode. A symmetrical pattern, on the other hand, means that the cavity is surrounded by the dielectric.

4.5.1. XLPE

The patterns of aged and unaged XLPE show that the PD magnitude increased with mechanical ageing. The patterns are quite unsymmetrical, leaning heavily toward the negative half-cycle. For the 10000-cycle XLPE, a rabbit-ear pattern becomes apparent, commonly observed due to cavities formed by ageing (here due to the bending fatigue). The increased PD magnitude and reduced PDIV indicate that the cavities become larger when XLPE cables undergo bending fatigue. From observations over 1800 s, the rabbit ear disappears, and the pattern becomes more symmetrical, as shown in Appendix C.1. This may be because the by-products of PD activity are increasing the surface conductivity

of the cavity surface, which can lower the effective voltage across the cavity and hence decrease PD activity [55].

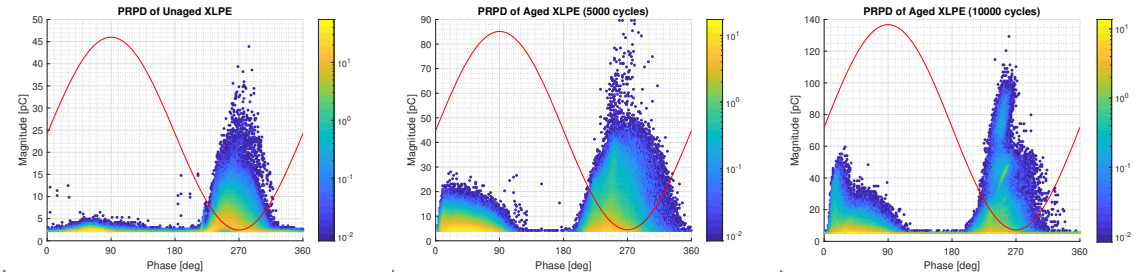

(a) Unaged (b) Aged for 5000 cycles (c) Aged for 10,000 cycles

Figure 4.11: Effect of mechanical ageing on the partial discharge characteristics of XLPE.

Thermal Ageing To see if thermal relaxation of the cables can reverse the mechanical ageing effect, several samples were heated to 90 °C for the same amount of time as it took for mechanical ageing (10 s/cycle). PRPD patterns were taken after thermal ageing of XLPE (10000 cycles) and PP (5000 and 10000 cycles).

For XLPE samples, the thermal ageing helps relax the effect of bending fatigue, as shown in Figure 4.12b. The XLPE showed a decrease in the magnitude of PD after a few minutes of voltage application which could indicate that thermal ageing helped relax some of the mechanical stress, which was expected from the literature [26].

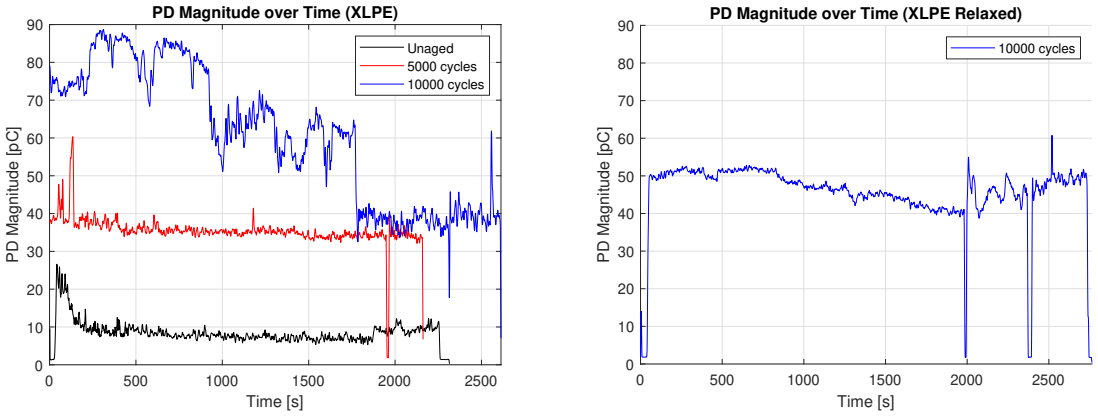

(a) Mechanically aged. (b) Thermally relaxed.

Figure 4.12: Discharge magnitude of XLPE over time.

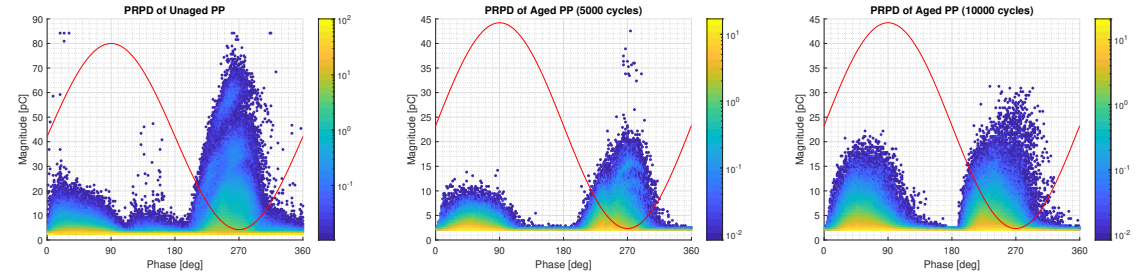

(a) Unaged (b) Aged for 5000 cycles (c) Aged for 10,000 cycles

Figure 4.13: Effect of mechanical ageing on the partial discharge characteristics of polypropylene.

4.5.2. Polypropylene

The PRPD pattern for polypropylene becomes more symmetrical after mechanical ageing, and the PD magnitude and repetition rate become much lower. This may indicate the growth of tiny cavities, e.g., due to the strain crystallization process. As the number of ageing cycles increases beyond 5000, the PD magnitude increases slightly, which could indicate enlargement of the small cavities.

Thermal ageing The mechanical effects can be relaxed for the 5000 cycle-aged polypropylene. Its PD magnitude becomes similar to the unaged pieces after a few minutes. However, the results in Figure 4.14 showed that the mechanical effects could not be reversed after a certain number of cycles (for 10,000 cycles).

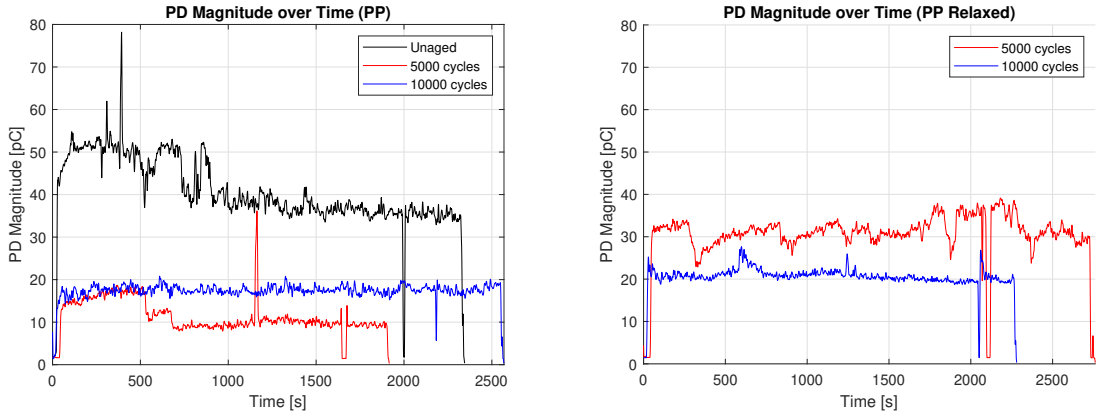

(a) Mechanically aged

(b) Thermally relaxed

Figure 4.14: Discharge magnitude of polypropylene over time.

4.6. Conclusion

In this chapter, the effect of bending fatigue on single conductors and triples is studied. Mechanical ageing of single conductor cables directly on the sheave wheel was performed. A bushing was designed to electrically test cable samples using water as the ground electrode.

Unaged XLPE and PP cables showed similar breakdown voltages. As expected, ageing the XLPE caused the breakdown voltage to reduce. After ageing 5000 cycles, a 20 % decrease was observed, and 10,000 cycles showed a 30 % decrease with respect to the unaged cables. It can also be noted that the relationship between the degradation and the number of cycles is not linear. The degradation of XLPE is further confirmed by PD analysis, which shows a rise in the magnitude of PD with increasing ageing cycles. Polypropylene, on the other hand, could not be broken after ageing. PD analysis showed a decrease in the PD magnitude. This could indicate the formation of small cavities.

5

Triple Cable Testing

This chapter examined a cable comprising three conductors (called a triple) in a helix structure by subjecting it to mechanical ageing. The triples also have a jacket made of a thermoplastic elastomer. The aim is to observe any differences compared to the direct ageing of single conductors on a wheel. Two diagnostic tests are conducted on these cables to analyse any disparities in degradation: namely partial discharge analysis and dielectric frequency response measurements. Cross-sections are made of cable samples to find voids and cavities in their structure.

5.1. Mechanical Ageing Setup

The effect of accelerated bending fatigue directly on the cable has been studied in detail in the previous chapter. The next step is testing triples (consisting of three conductors with a shared copper tape sheath and jacket) using the mechanical ageing setup in Figure 5.1a. The goal is to evaluate the effect of the helical structure of the conductors on their resistance to bending fatigue.

(a) CBoS setup for cable triples with jacket.

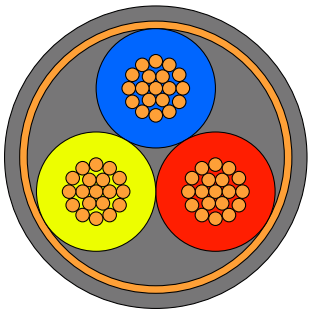

(b) Cable sample with three conductors and a jacket.

Figure 5.1: Testing of cable triples

The bending procedure described in Section 4.2 remains unchanged, but the loading mass is tripled. Instead of a single conductor, a triple consisting of three conductors and a jacket is subjected to cyclic

bending with three times the load used for the single conductors. The parameters of the CBoS test are shown in Table 5.1.

Table 5.1: CBoS parameters for mechanical ageing of triples.

Parameter	Value
Cycle time	10 s
Sheave wheel diameter	240 mm
Load	85.5 kg
Number of cycles	5000; 10,000; 20,000

5.2. Partial Discharge Analysis

PD analysis was performed on the conductors of XLPE and polypropylene triples to study the effect of mechanical bending fatigue on the triple. The method of analysis is the same as described before in Section 4.5. The inception (PDIV) and extinction (PDEV) voltages are presented in Table 5.2. The PRPD patterns are recorded at a voltage of approx. 20 % higher than the PDIV.

5.2.1. XLPE

The PDIV and PDEV of XLPE are presented in Table 5.2. The data shows a minimal difference in the PDIV for aged XLPE samples subjected to 10,000 and 20,000 cycles, which suggests that after a certain number of cycles, the sole effect of bending may not cause significant additional degradation in the dielectric properties.

Table 5.2: PD inception and extinction voltages of XLPE.

Insulation material	Number of cycles	PDIV	PDEV	Testing voltage
XLPE	0	4.8 kV 4.5 kV 3.5 kV	4.0 kV 4.1 kV 3.3 kV	5.4 kV 4.8 kV 4.2 kV
XLPE	10,000	3.0 kV 3.2 kV 2.8 kV	2.8 kV 3.2 kV 2.5 kV	3.6 kV 3.8 kV 3.4 kV
XLPE	10,000	2.8 kV 3.3 kV 3.5 kV	2.2 kV 3.0 kV 3.1 kV	3.4 kV 4.0 kV 4.2 kV
XLPE	20,000	3.2 kV 3.1 kV 2.8 kV	3.1 kV 2.8 kV 2.8 kV	3.8 kV 3.7 kV 3.4 kV

It was anticipated that the ageing might have the same effect as the single conductors due to the addition of a jacket. However, based on the analysis of the partial discharge (PD) magnitude over time, as depicted in Figure 5.2, it is observed that the magnitude of PD differs among the individual conductors within the same triple, even after undergoing identical mechanical cycles. This observation has led to the hypothesis that the individual conductors may degrade at varying rates when a cable with multiple cores is subjected to the same bending cycles.

Although the degradation rates differ, the decreased inception voltage indicates that bending fatigue degrades the insulation compared to the unaged cable. Again, the unsymmetrical PD patterns (see Figure 5.3) indicate growing electrode-bounded cavities (delaminations) when XLPE undergoes bending fatigue.

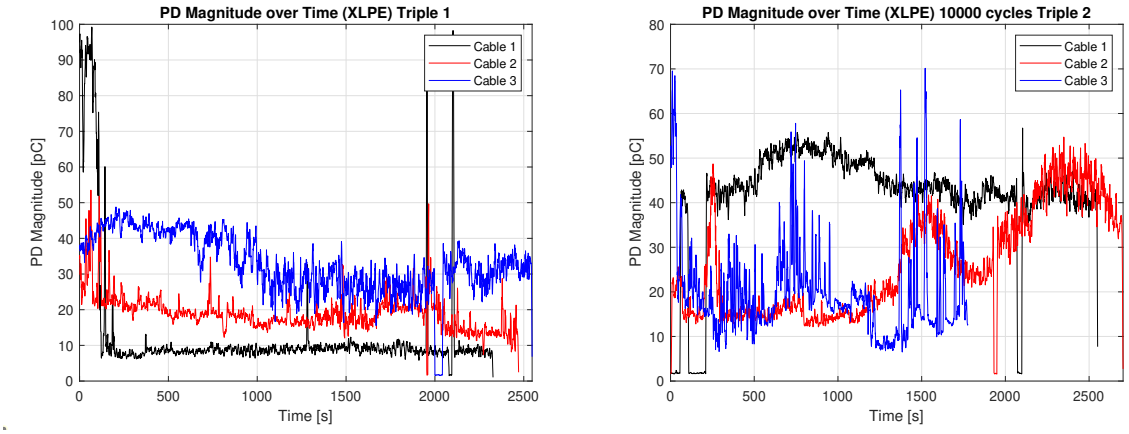

(a) Triple 1 (b) Triple 2

Figure 5.2: Discharge magnitude of XLPE triples over time.

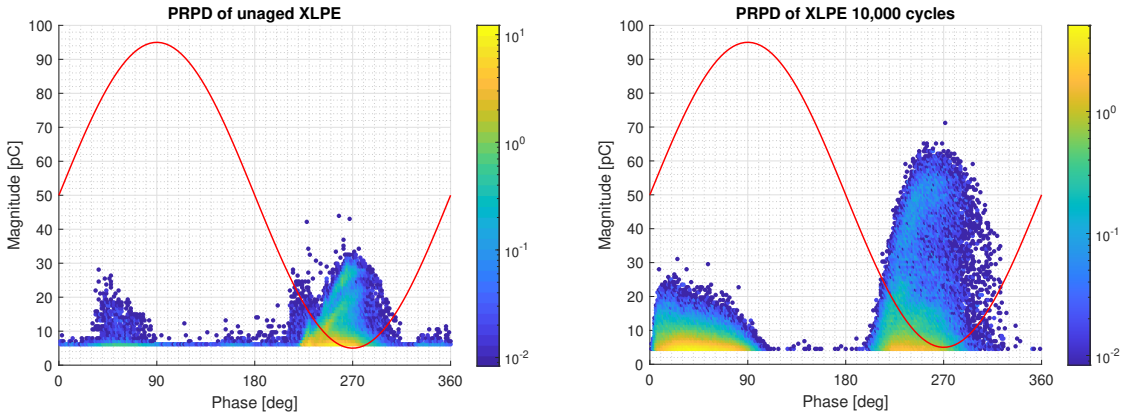

(a) Unaged (b) Aged for 10,000 cycles

Figure 5.3: Effect of mechanical ageing on the partial discharge characteristics of XLPE.

5.2.2. Polypropylene

The PDIV and PDEV of polypropylene are presented in Table 5.3. The PDIV has decreased with the increase in bending cycles, which differs from the single conductors of polypropylene. This could be because the insulation gets damaged during cabling, as seen from the whitening in Figure 5.4.

Table 5.3: PD inception and extinction voltages of PP.

Insulation material	Number of cycles	PDIV	PDEV	Testing voltage
PP	0	4.4 kV 3.9 kV 4.3 kV	4.1 kV 3.6 kV 3.9 kV	5.3 kV 4.7 kV 5.2 kV
PP	10,000	3.3 kV 3.7 kV 3.0 kV	3.2 kV 3.5 kV 2.9 kV	4.0 kV 4.4 kV 3.6 kV
PP	20,000	3.3 kV 2.8 kV 2.6 kV	3.0 kV 2.6 kV 2.4 kV	4.0 kV 3.4 kV 3.1 kV

Figure 5.5 shows that the cabling degrades the insulation, just like for XLPE. The PD magnitude in-

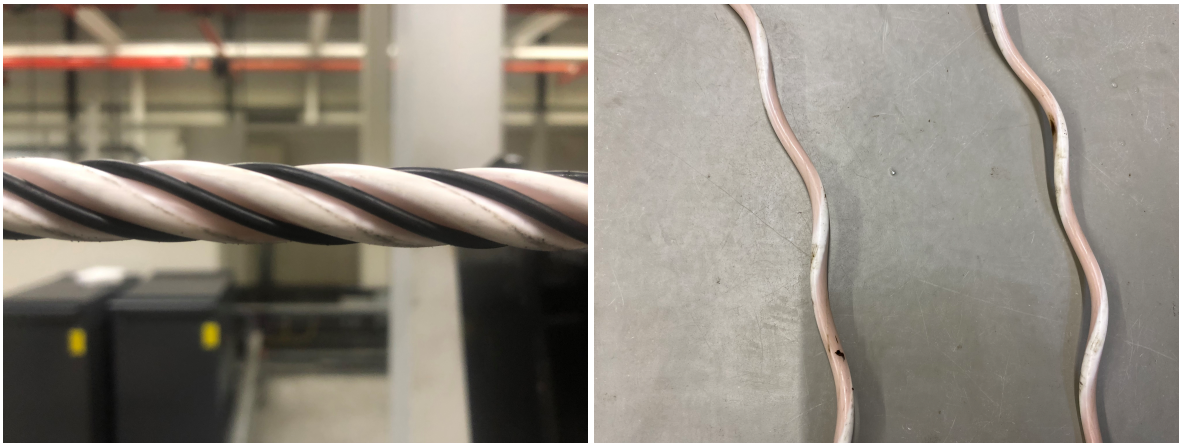

(a) Whitening of insulation during cabling

(b) After dissection of triples of PP

Figure 5.4: Damage to PP when it undergoes cabling

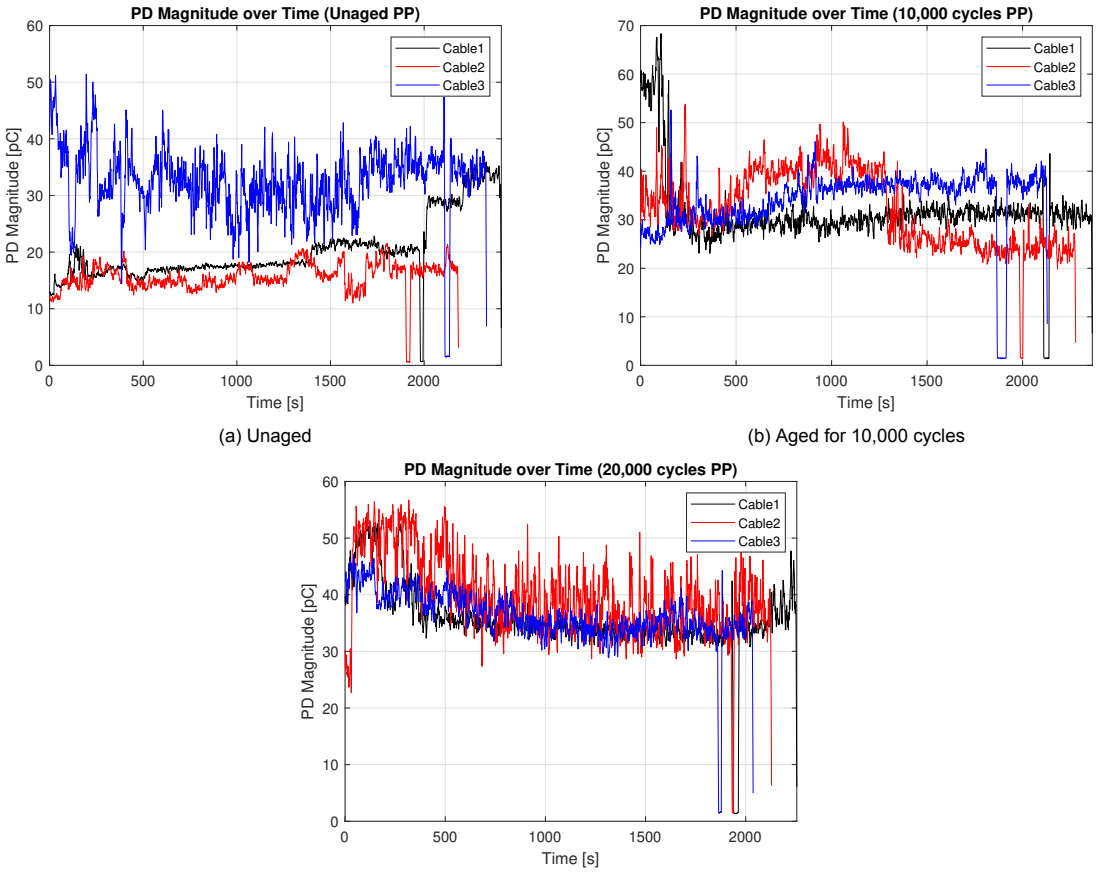

(a) Unaged

(b) Aged for 10,000 cycles

(c) Aged for 20,000 cycles

Figure 5.5: Effect of mechanical ageing on the partial discharge characteristics of polypropylene.

creases with the number of bending cycles, which differs from the single conductor results of polypropylene, where the magnitude decreases. The patterns shown in Figure 5.6 are mostly symmetric for all ageing states, indicating discharges in dielectric-bounded cavities. The PD magnitude grows, and the PDIV drops with the number of bending cycles, which means the cavities are growing. It can be concluded that there are no delaminations, unlike XLPE.

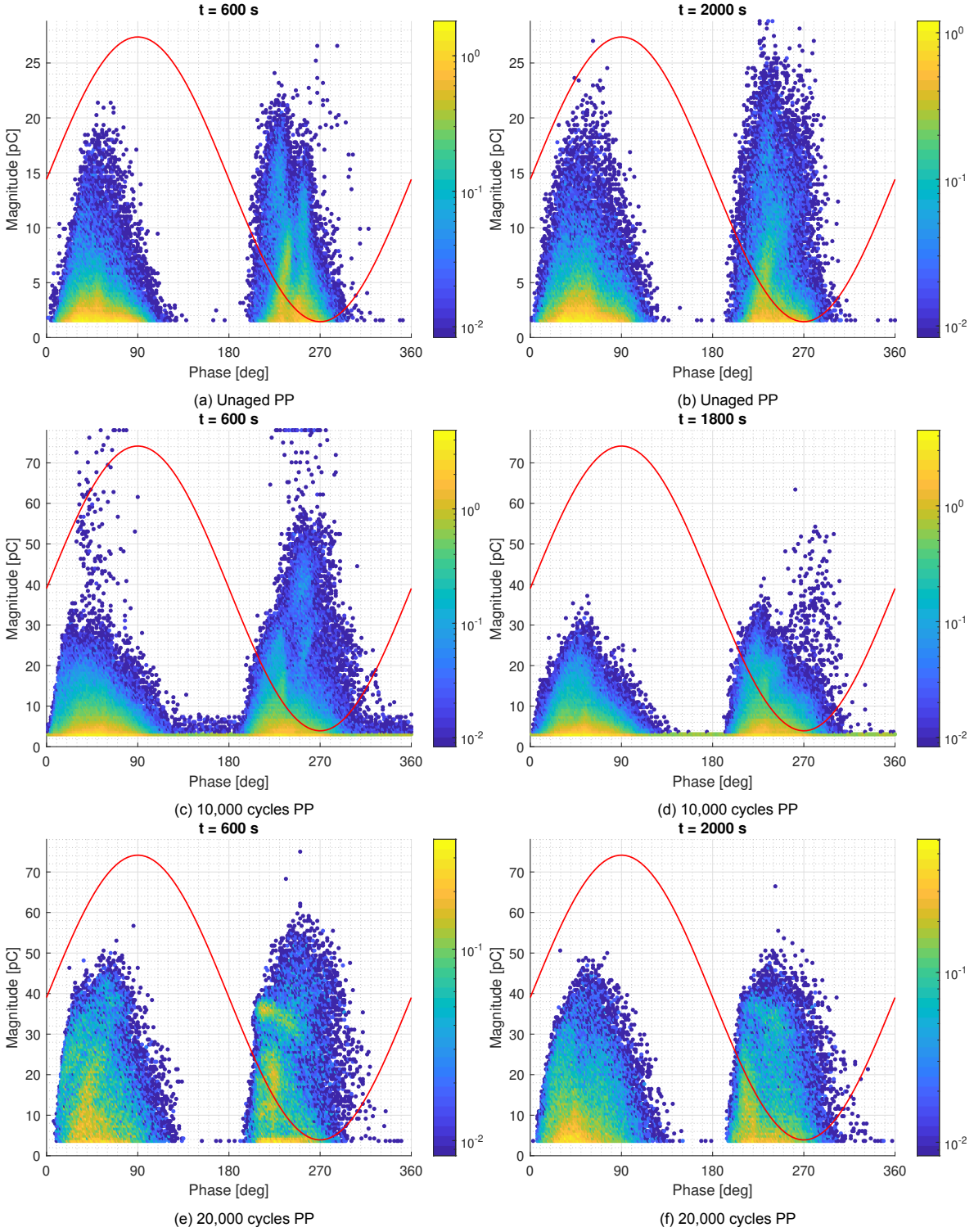

Figure 5.6: PRPD patterns of PP with different bending cycles over time

5.2.3. Modified Paschen Curve

The Paschen curve shows the breakdown voltage of gases at low pressure as a function of pressure and distance (cavity size). These graphs can be modified to show cavity breakdown strength as a function of cavity size. The modified Paschen curve of air is shown in Figure 5.7

The field strength inside the cavity E_{cav} can be derived from the field strength in the insulation E_{ins}.

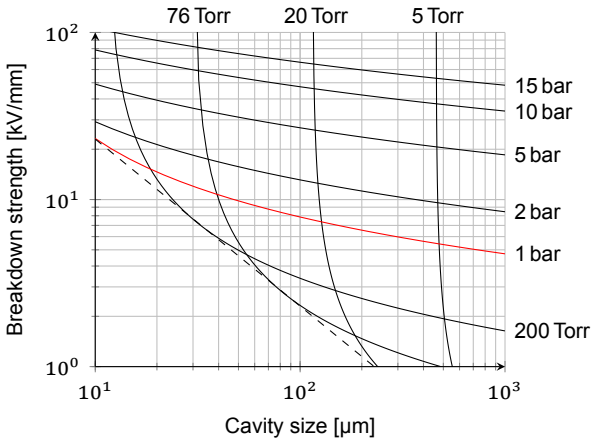

Figure 5.7: Modified Paschen curve (adapted from Kreuger [56]).

The maximum field is of interest, so the field at $r = a$ is taken.

$$E_{ins}(r) = k\frac{U}{r\ln(b/a)}, \tag{5.1}$$

$$E_{cav}^{max} = \varepsilon_r E_{ins}(r = a), \tag{5.2}$$

where k is the field-enhancement factor due to stranding (here taken to be $k = 1.3$ based on COMSOL simulations [57]), a and b are the inner and outer radius, U is the peak voltage, and ε_r is the dielectric constant of the insulation.

Taking the inception voltages shown in Table 5.2, approximate cavity sizes can be calculated based on the Paschen curve, as explained above. For the unaged XLPE (PDIV $= 6.1$ kV), cavity sizes are on the order of 10 to 15 µm. For the mechanically aged pieces, the cavities are expected to be in the order of 50 to 150 µm by taking the highest and lowest recorded inception voltages.

5.3. Breakdown Results

The PD magnitudes showed some variations between conductors of the same triple. To investigate this further, short breakdown tests are performed on 20 cm samples of conductors from two triples, which were subjected to 10,000 cycles. The results, presented in Figure 5.8, are compared to the results of the unaged conductors. It seems conductor 1 in Figure 5.8a and conductor 3 in Figure 5.8b have similar breakdown strength to the unaged conductors. This seems to support the hypothesis that the conductors from a triple age at varying rates.

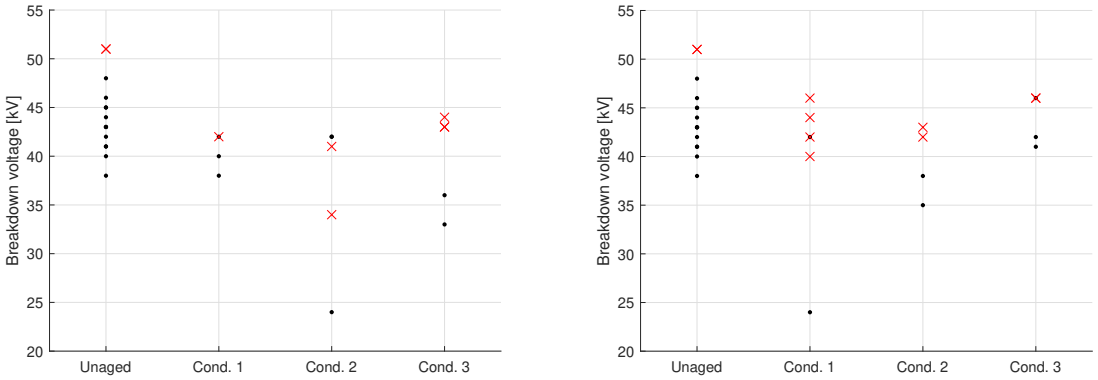

(a) Triple 1

(b) Triple 2

Figure 5.8: Breakdown results for 10,000 cycle-aged XLPE triples compared against unaged XLPE. Dots (·) indicate breakdown voltages and crosses (×) indicate censored observations.

5.4. Capacitance and Loss Measurements

Capacitance and loss measurements were performed on each of the conductors of a triple using the IDAX 300. To goal of this measurement is to identify any changes due to the bending fatigue that could indicate degradation of the insulation. The capacitance and loss measurements were performed on unaged and aged cable pieces (5000, 10,000 and 20,000 cycles). The measurements were done inside a Faraday cage to suppress any noise or interference.

XLPE The measurements for XLPE are presented in Figure 5.9. There is no trend in the dissipation factor $\tan\delta$ with electrical ageing. Any differences can be attributed to differences in the measurement

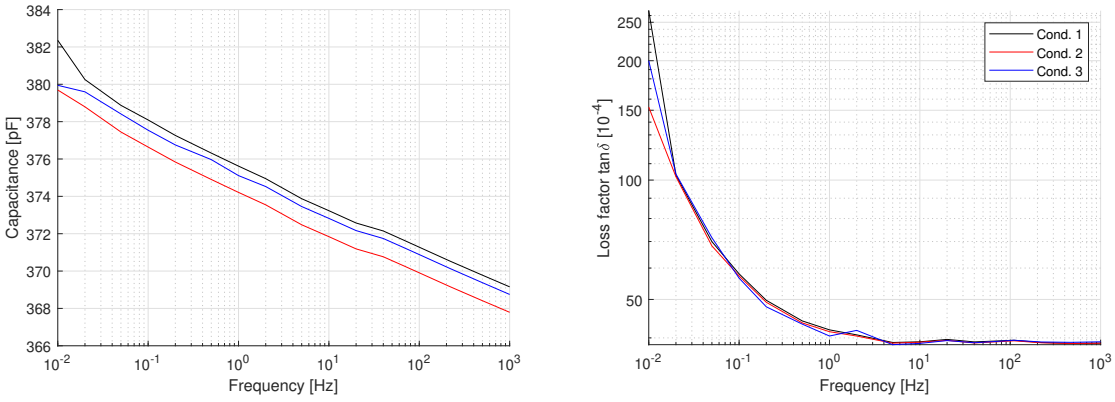

(a) Capacitance (unaged)

(b) Loss tangent (unaged)

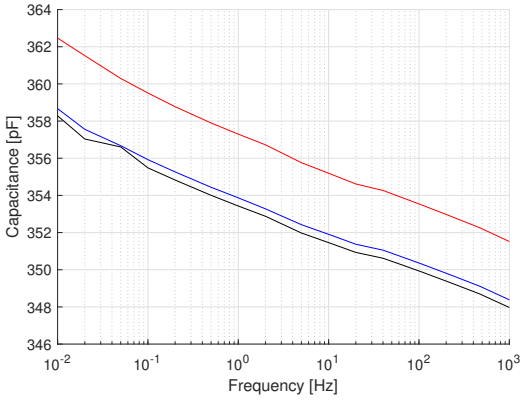

(c) Capacitance (5000 cycles)

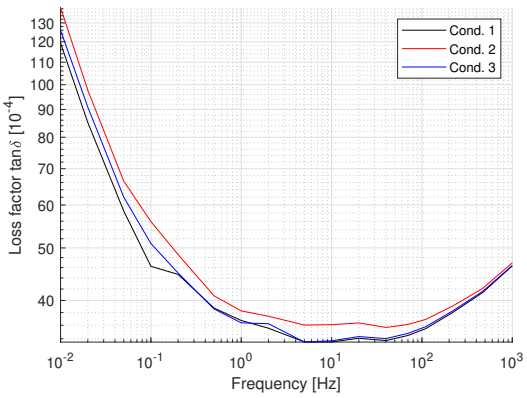

(d) Loss tangent (5000 cycles)

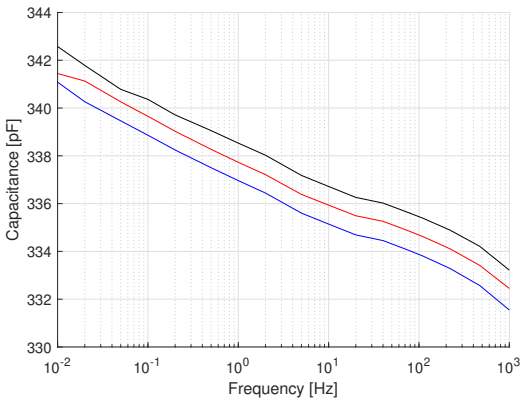

(e) Capacitance (10,000 cycles)

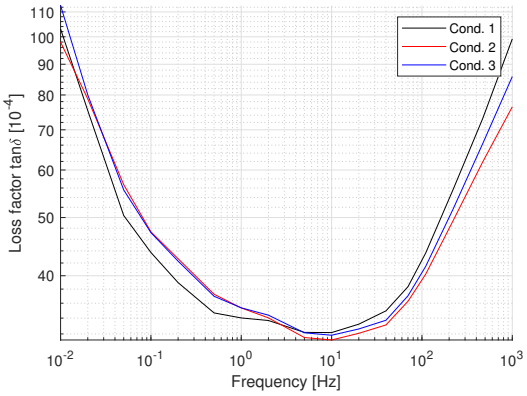

(f) Loss tangent (10,000 cycles)

Figure 5.9: Capacitance and loss measurements on XLPE triples.

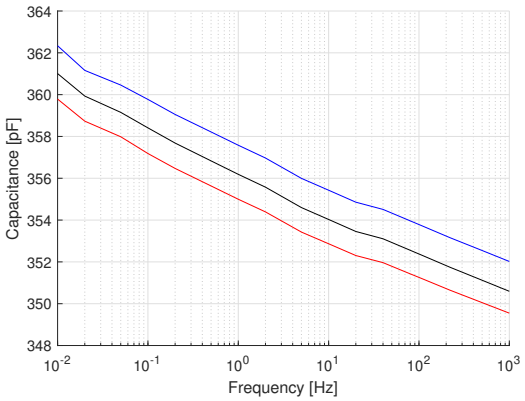

(g) Capacitance (20,000 cycles)

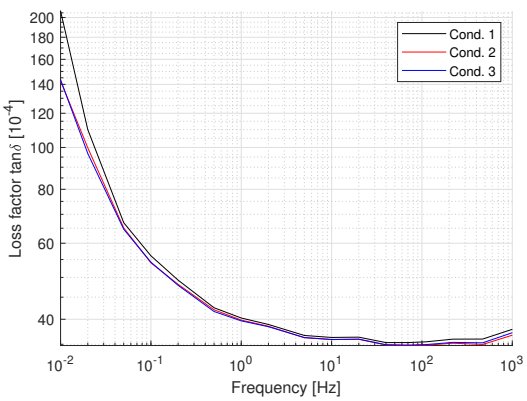

(h) Loss tangent (20,000 cycles)

Figure 5.9 (*Continued.*): Capacitance and loss measurements on XLPE triples.

setup between cables.

As for the capacitance, there is little variation between the three conductors in a triple. Minor variations are possible because of the tolerance on the insulation thickness and filling compound. Between triples (with different ageing states), there are significant differences in capacitance, up to several tens of pF. Although the capacitance decreases with bending cycles (which may be expected based on the formation of large air-filled cavities), the capacitance measurement is not a good indicator due to its sensitivity to other parameters.

Polypropylene The measurements for PP are presented in Figure 5.10. On average, the capacitance for polypropylene exhibits a decreasing trend, which could be attributed to the growth of cavities in the dielectric with the increase in bending cycles. There is no trend in the dissipation factor $\tan\delta$ with electrical ageing.

Summary Although the capacitance seems to follow some trend with mechanical ageing cycles, there is a large spread in results between conductors in a triple. Additionally, many other factors could influence the capacitance and loss factor, such as variations in the insulation thickness and filling compound. Therefore, capacitance and $\tan\delta$ measurement is not a good method to determine the mechanical ageing state of mechanically aged cables.

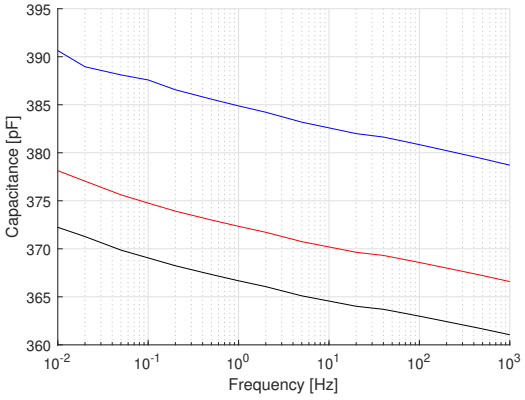

(a) Capacitance (unaged)

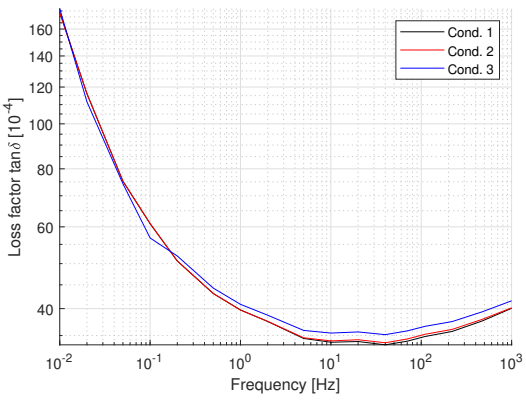

(b) Loss tangent (unaged)

Figure 5.10: Capacitance and loss measurements on PP triples.

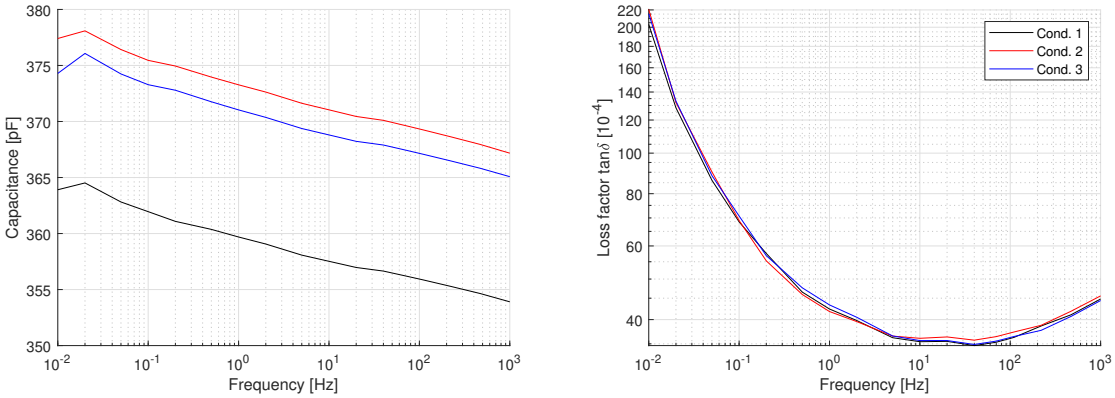

(c) Capacitance (5000 cycles)

(d) Loss tangent (5000 cycles)

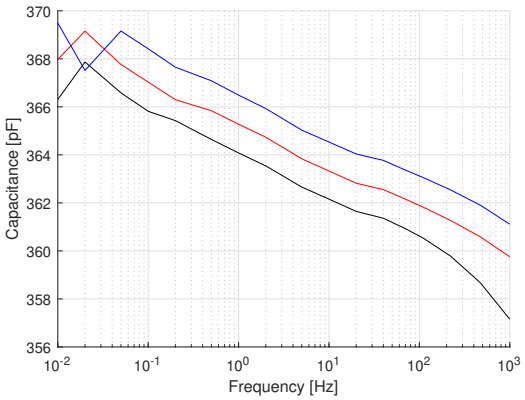

(e) Capacitance (10,000 cycles)

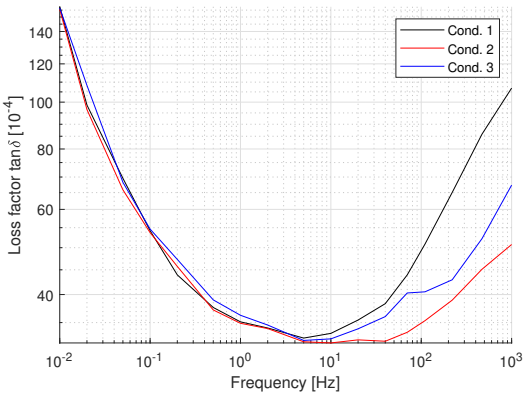

(f) Loss tangent (10,000 cycles)

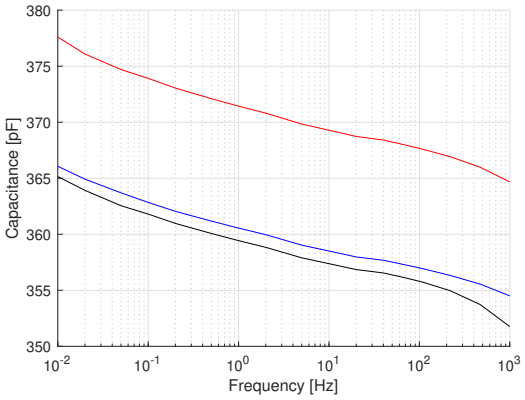

(g) Capacitance (20,000 cycles)

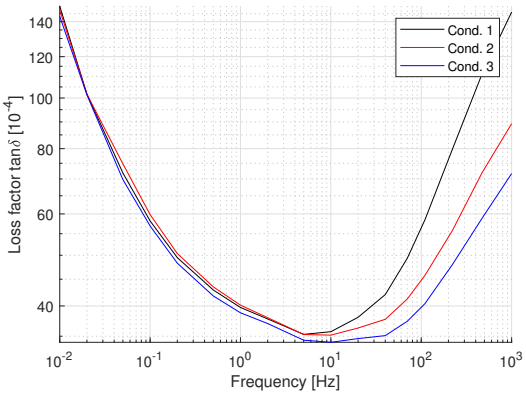

(h) Loss tangent (20,000 cycles)

Figure 5.10 (*Continued.*): Capacitance and loss measurements on PP triples.

5.5. Cable Cross-Section Analysis

Cross-sections were made for XLPE and PP aged at different cycles to prove that delaminations occurred due to bending stress. Cable samples were cast in epoxy in a vacuum oven at 60 °C. The vacuum caused the epoxy to move up the cable, preserving the delaminations during cutting and polishing.

XLPE Before cabling, there is no significant delamination between the conductor and insulation. The voids are challenging to see with the microscope and are at most 10 µm in size, which confirms the calculations based on the modified Paschen curve. After cabling, delaminations of 20 to 70 µm can be

seen in a few locations, as shown in Figure 5.11b. It can be concluded that bending the cable undergoes during the cabling process causes a lot of damage to the cable, which may reduce the usable voltage and lifetime.

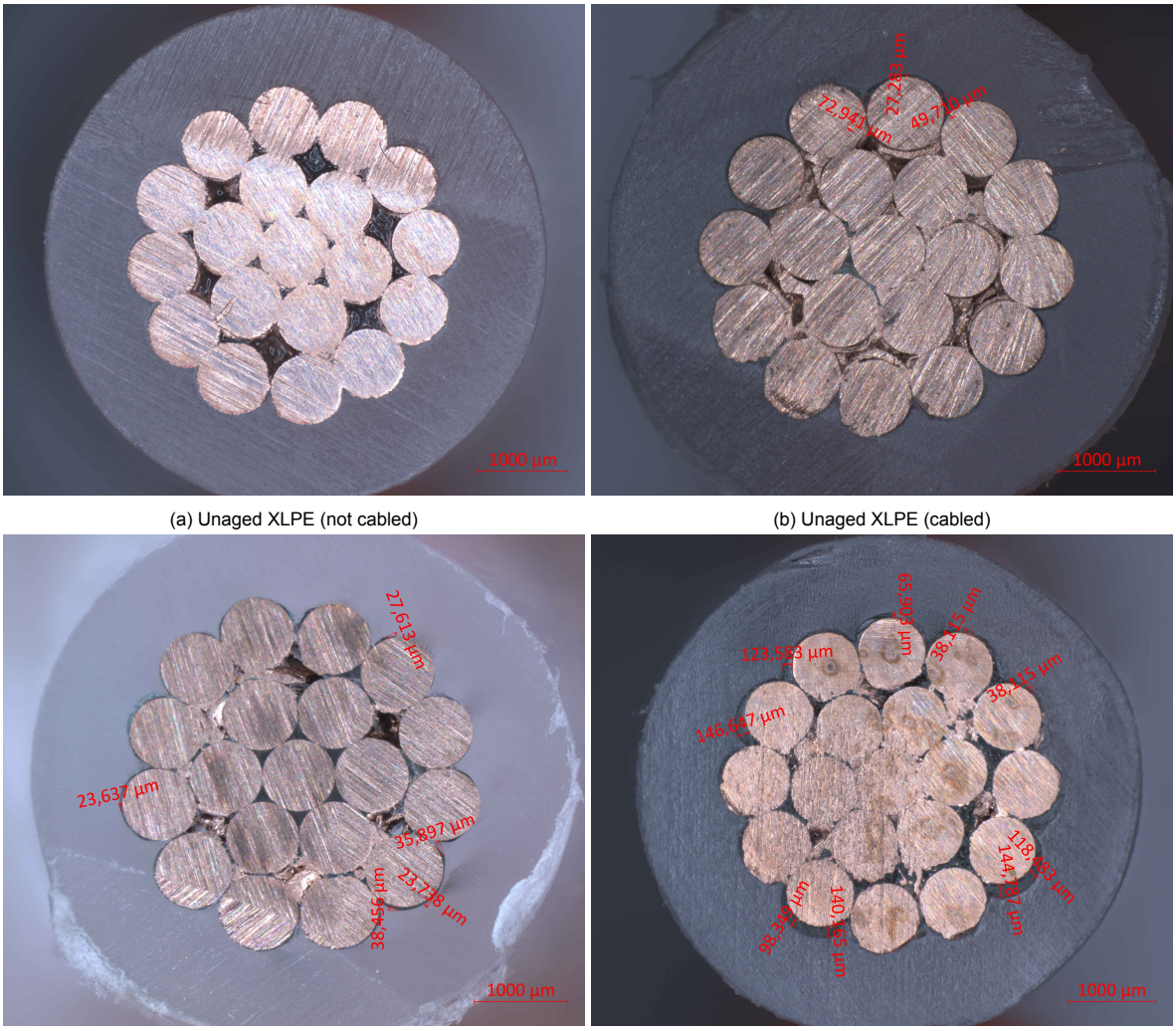

(a) Unaged XLPE (not cabled)

(b) Unaged XLPE (cabled)

(c) 10,000 cycles XLPE (cabled)

(d) 20,000 cycles XLPE (cabled)

Figure 5.11: Cross-section of XLPE conductors in various states of mechanical ageing. Delamination sizes are indicated in red.

As the cables are mechanically aged (see Figures 5.11c and 5.11d), more and larger delamination sites are created. The largest voids can be found at the sides of the conductor strands due to the twisting of the strands. With increased bending cycles, delaminations also occur on top of the strands, and their size grows larger. After 20,000 cycles, the cavity sizes range from 40 to 150 µm. The size of the cavities is roughly in the range derived from the modified Paschen curve. However, any deviations can be explained by the fact that only two cross-sections of each cable segment were made. Any variations over the cable length (known to exist because of the variation in breakdown voltage between segments) are thus not taken into account.

Polypropylene For polypropylene, the cross-sections (in Figure 5.12) showed no significant delamination even after ageing it for 20,000 cycles. This verifies the PD measurements in Figure 5.6, which show mostly symmetrical patterns corresponding to dielectric-bounded cavities. The whitening of polypropylene insulation due to cabling and mechanical ageing is also visible in the top right of Figure 5.12a and bottom right of Figure 5.12b.

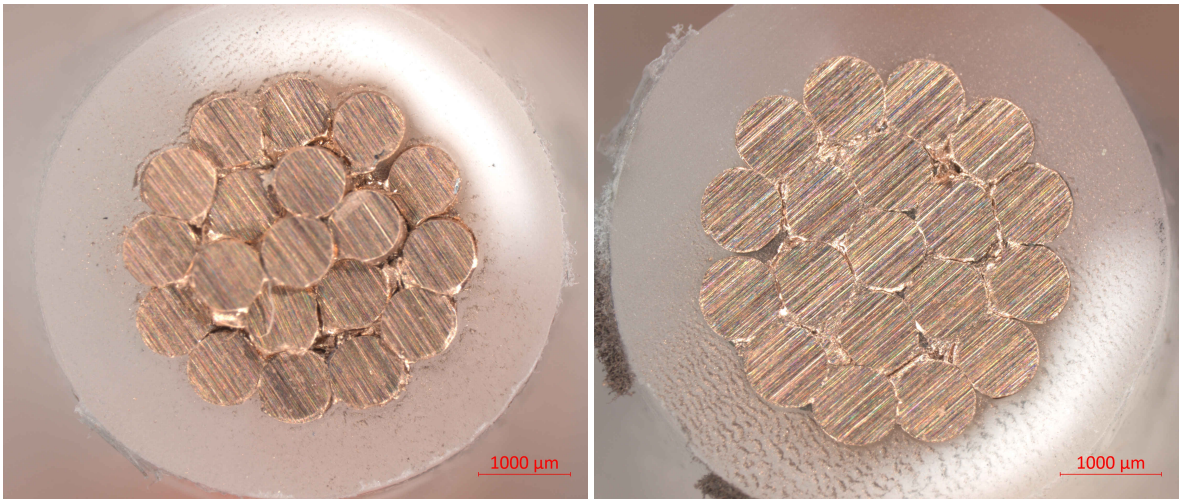

(a) Unaged polypropylene (cabled) (b) 20,000 cycles polypropylene (cabled)

Figure 5.12: Cross-section of polypropylene conductors in various states of mechanical ageing.

5.6. Conclusion

In this chapter, triples in a helix structure with a jacket were subjected to cyclic bending fatigue, and various analyses were conducted to assess the impact on the cables. PD analysis revealed that the magnitude of PD differed among the individual conductors within the same cable triple, even after undergoing identical bending cycles. This suggests that the conductors may degrade at varying rates under bending fatigue.

For XLPE, it was found that cyclic bending causes the delamination of the conductor-insulation interface, resulting in a highly asymmetric PD pattern. Cross-section examinations confirmed the presence of delaminations with sizes 40 to 150 µm in the aged samples, which coincides with the sizes calculated from the inception voltages. Unaged cables already had very small delaminations, on the order of 10 µm.

In polypropylene, on the other hand, no delamination was observed even at 20,000 cycles. This is confirmed by the symmetrical PD patterns, which indicate dielectric-bounded cavities instead. These cavities could be formed through the strain crystallisation process.

6

Full Scale Testing

In this chapter, HDPE cable with armour is aged using a real CBoS test, which combines bending and tensile stress. After subjecting the cable to a total of 20,000 cycles, the cables are subjected to electrical tests and dissected to examine any changes that may have occurred in the insulation material. An important goal in this chapter is to derive the slope of the lifetime curve before and after CBoS ageing.

6.1. Mechanical Ageing Setup

Dynamic cables undergo a lot of mechanical stress, which is the main cause of failure in most cases, as discussed in Chapter 1. The method of ageing is similar to the CBoS in Section 4.2. The major difference is the cable armour which takes most of the load instead of pulling on the conductors. During CBoS fatigue ageing, the cables are exposed to both bending and tensile loads [58]. Research performed by Cárdenas et al. [44] showed that the cyclic loading, the seawater, and the ultraviolet radiation (UV) accelerated the degradation process of HDPE used as an outer sheath in umbilical cables. The paper also concludes that most of the degradation of HDPE was caused by cyclic loading. In this study, the effect of seawater and UV radiation are not considered, but the bend-over-sheave test is a type of cyclic loading.

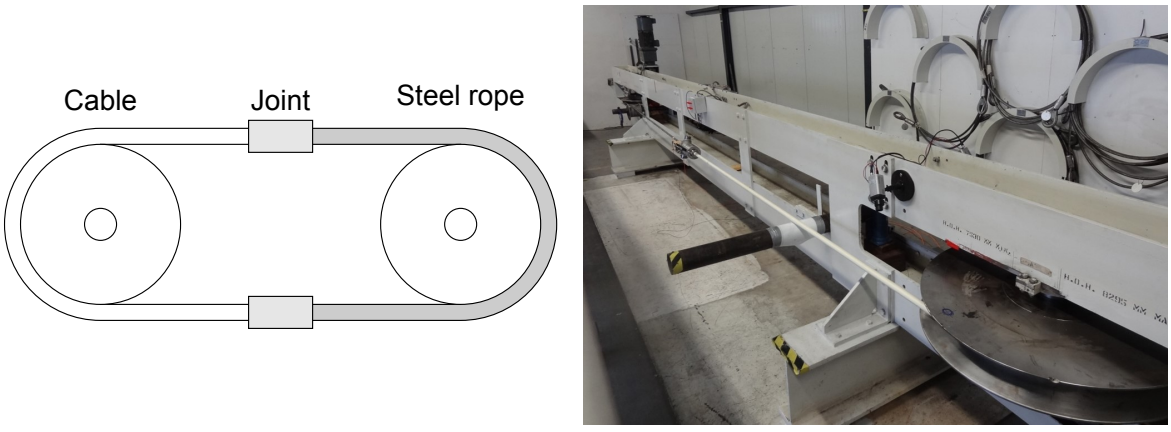

(a) Schematic

(b) CBoS Machine used for Ageing Cables with Armour

Figure 6.1: Loaded CBoS Setup

Tests were performed on an ROV cable made of HDPE with steel armour, which underwent 20,000 cycles on the test machine as shown in Figure 6.1. The stroke length of the test was 2 m, which is also shown in the distance profile, along with the velocity profile seen in Figure 6.2. The other parameters for CBoS are shown in Table 6.1.

Table 6.1: CBoS Parameters for Mechanical Ageing of HDPE Cable

Parameter	Value
Cycle Time	13.7 s
Sheave wheel diameter	1.2 m
Test Load	78 kN
Number of cycles	20,000

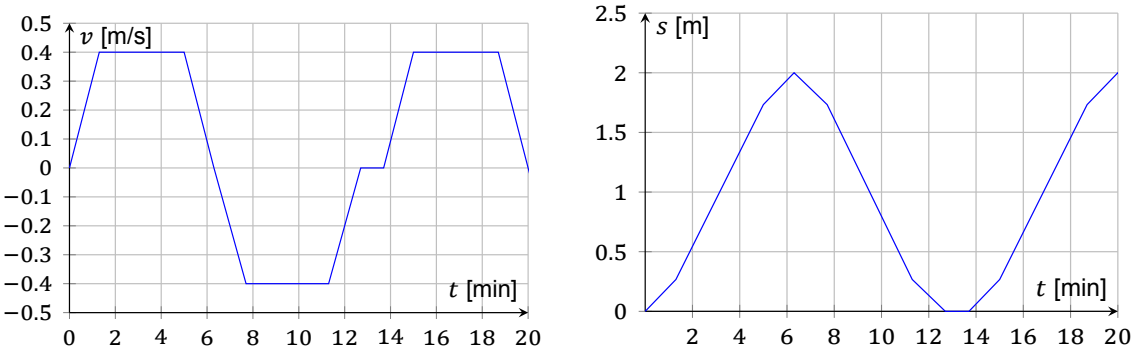

(a) Velocity Profile

(b) Displacement Profile

Figure 6.2: Loaded CBoS Process Profiles

6.2. Pre-Conditioning with Water

The general method for moisture saturation of insulation is to put the extruded cable into a water tank in direct contact with the outer semicon [59]. However, an outer semicon is not available in the samples under study. The preconditioning should be done for enough time so that water can absorb into the insulation and screen before the start of wet ageing [51]. The conditioning time t_c at a temperature of 55 ± 5 °C can be calculated using the equation

$$t_c = 100 + 46t, \tag{6.1}$$

where t is the insulation thickness [51, 59]. However, this equation is valid for insulation thickness greater than 8.8 mm. Thinner insulation has a fixed conditioning time of 500 h [59].

From the literature, it was found that after wet ageing at different frequencies, beyond the conditioning time t_c, the moisture content in XLPE insulation does not change much, indicating that the insulation is fully saturated with water. The wet-aged samples observed under the microscope had bow-tie trees with lengths less than 100 µm. Another interesting observation is that bow-tie tree growth does not significantly change after the saturation/conditioning time. So most of the growth was seen only during the initial phase, after which the rate did not show any drastic change even after a long time. This was also confirmed using modelling [51].

6.2.1. Moisture Saturation of HDPE

To implement the concept in Section 6.2, the preconditioning criteria of CIGRE TB 722 [59] are chosen. The conductors are kept in a water bath at 55 °C for 500 h (since the insulation thickness is <8.8 mm), after which breakdown tests are performed following the procedure in Section 4.3.1. $\mathrm{Tan}\,\delta$ measurements are performed at different intervals using the setup shown in Figure 6.3 to monitor the water saturation of the HDPE insulation.

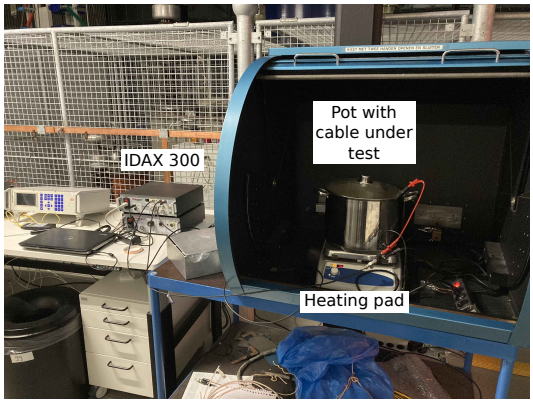

(a) Moisture saturation setup with shielding box. The IDAX 300 is connected to the pot and HDPE-insulated conductor.

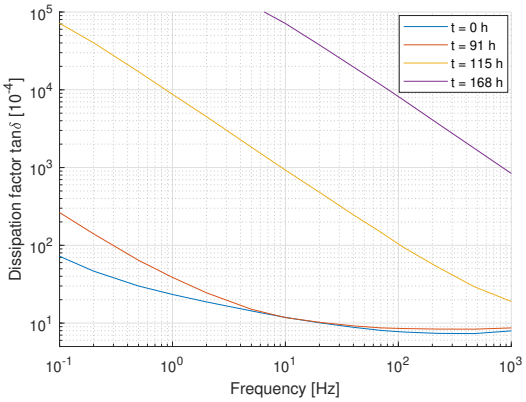

(b) Moisture saturation of HDPE monitored over 150 h using $\tan\delta$ measurement. The increasing $\tan\delta$ indicates a reducing insulation resistance and hence the absorption of moisture.

Figure 6.3: HDPE conductor moisture saturation

6.3. Visual Inspection

XLPE and HDPE cables with armour were dissected to inspect visually. Several interesting observations from these cables and their effect on cable performance are covered in this section.

6.3.1. Scratches due to Cabling

Indentations were observed on the outside of the XLPE insulation (Figure 6.4a). The indentations were aligned with the edges of the copper tape placed around the cable. Mechanical damage (such as the observed surface scratches) can initiate treeing [25].

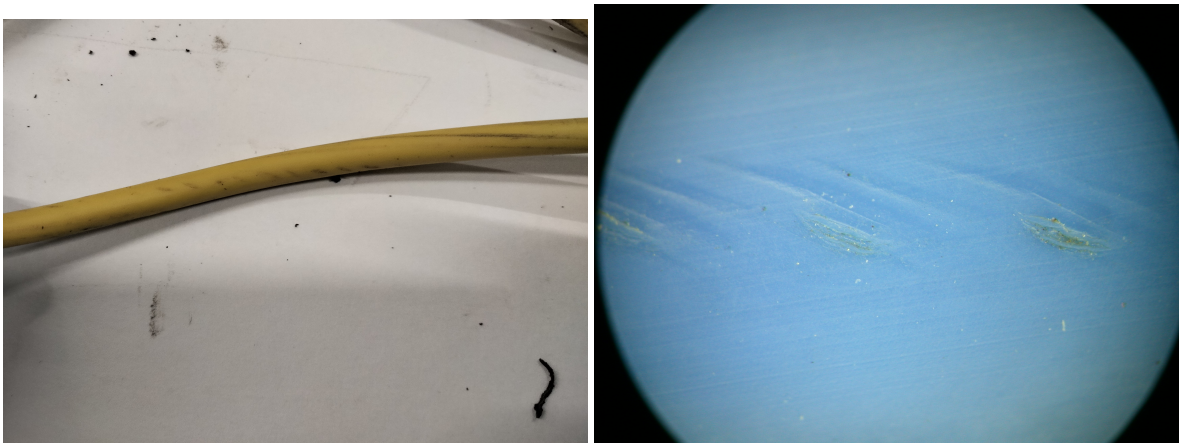

(a) Single conductor from a failed cable on field

(b) New cable from production

Figure 6.4: Indentations on cables

Similar indentations are observed on newly produced cables, see Figure 6.4b, indicating that they are not formed due to prolonged dynamic mechanical stress (but may be worsened). Instead, the production process should be improved (for example, by folding the copper tape) to prevent such indentations.

6.3.2. Voids in Filling Compound

The filling compound (depolymerised rubber, DPR) does not evenly fill the space between the conductors, forming voids between the conductors as shown in Figure 6.5a. These can lead to failures in the cable when applying high voltage since there may be a significant electric field in the filling compound due to the lack of individual sheaths.

(a) Voids in the DPR filling compound.

(b) CBoS aged cable with embedded copper tape particles.

Figure 6.5: Defects in a dissected cable.

6.3.3. Copper Particles after Ageing

After bending fatigue tests, these indentations were found to get deeper, and some slivers of copper tape became embedded into the damaged parts, as shown in Figure 6.5b. Therefore, the scratches from production lead to deeper cuts during cyclic bending ageing of the insulation. The copper particles could initiate the breakdown of the insulation.

6.4. Breakdown Results

The same method used in Chapter 4 for the single conductor is used again for testing the HDPE cable samples. The electrical parameters of the HDPE cable used are shown in Table 6.2.

Table 6.2: Electrical Parameters of HDPE Cable

Parameter	Value
Conductor area	3.02 mm^2
Insulation thickness	0.76 mm
Line to line voltage	2.0 kV

6.4.1. Mechanical Ageing

The behaviour observed in the short breakdown results is similar to the ageing of single conductors. This proves that the dielectric degradation due to bending occurs even in cables with armour and no direct loading of the conductors. This finding supports the results presented in Chapter 4. Again, two datasets were observed where only some parts of the cable have aged, while others perform as well as the unaged samples. Hence, the theory of local degradation is valid even in the case of a full cable.

Table 6.3: Mechanically Unaged vs Aged vs Moisture saturated Results

Number of cycles	α	β
0	35.5 ± 1.2 kV	12.9
20,000	25.6 ± 1.8 kV	9.5
20,000 (with moisture)	19.6 ± 1.1 kV	7.0

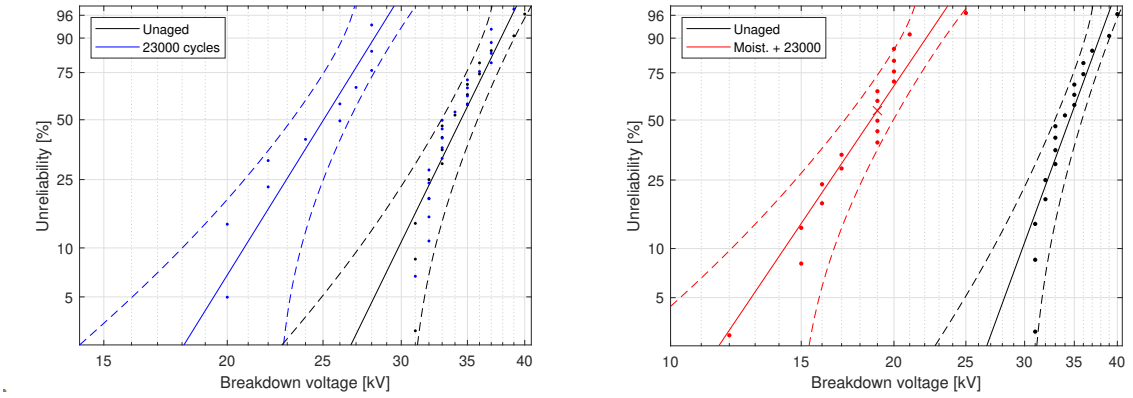

(a) HDPE unaged vs mechanically aged

(b) HDPE unaged vs moisture saturated mechanically aged

Figure 6.6: Effect of ageing and moisture degradation on insulation

6.4.2. Mechanical Ageing and Moisture

The absence of two distinct data sets in the breakdown results of the moisture-saturated insulation suggests that the unaged insulation has also undergone degradation as a result of moisture exposure shown in Figure 6.6b.

6.5. Lifetime Results

Researchers have implemented accelerated ageing techniques because insulating materials would take significant time to age naturally under normal operating conditions. Obtaining aged samples from the field for the necessary testing and assessment is inconvenient, which has led to the implementation of these techniques [60]. The main goal is to derive the slope of the lifetime curve, which is described by a power law (6.2) with exponent n.

$$L(U) = L_0 \left(\frac{U}{U_0} \right)^{-n} \tag{6.2}$$

Obtaining lifetime results for the unaged samples was straightforward. Voltage levels were chosen with the α derived from the short breakdown tests shown in Table 6.6. The voltage levels were chosen so the samples could be broken within a realistic time (approx. 1 h). These tests were also done on 20 cm pieces, which resulted in $n = 18$.

However, the real challenge was testing for the aged pieces. As described above, the aged samples

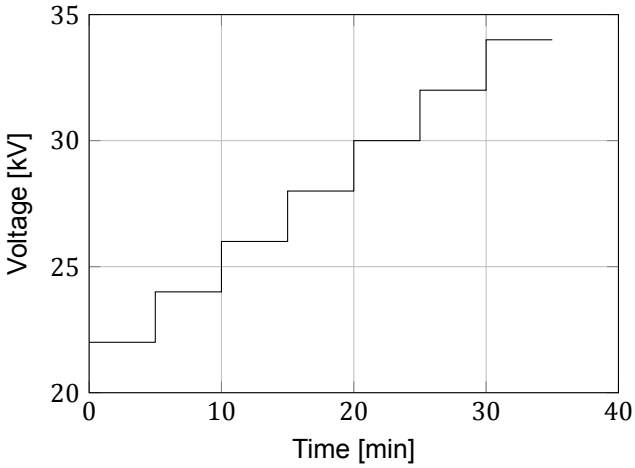

Figure 6.7: Step-level stress profile starting at 22 kV for aged HDPE lifetime tests.

comprise two subpopulations with different breakdown voltages. Therefore, performing tests at fixed voltage levels may result in many samples not failing. A step-stress testing approach is chosen to resolve this problem: by increasing the voltage according to a stress profile (as shown in Figure 6.7), the breakdown of the sample is guaranteed.

6.5.1. Cumulative Stress Model

The main benefit of the step-stress testing approach is that it guarantees a reasonable number of failures when increasing the applied stress. This helps reduce the test duration and the variability of failure times. However, it is important to note that a step-stress test does not accurately replicate actual conditions, where most insulation operates under constant stress. The step-stress test aims to evaluate the insulation lifetime under consistent operating conditions, considering the cumulative effect of successive stress exposures. As a result, the model used for this assessment becomes more sophisticated and complex compared to the case of constant stress [61].

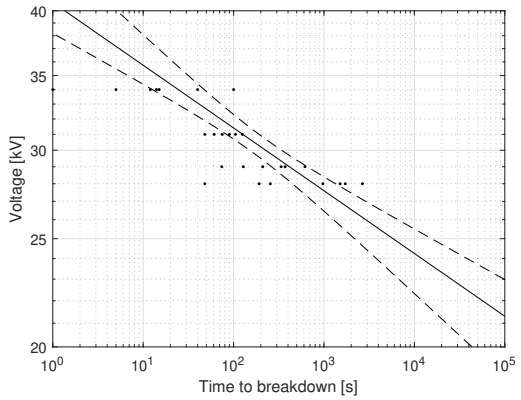

(a) Unaged ($n = 18$, $\beta = 1.06$).

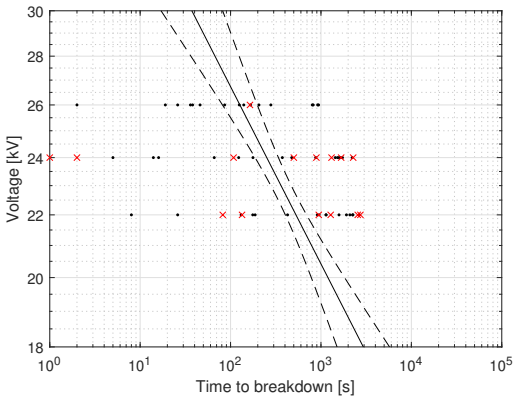

(b) Aged for 20,000 cycles ($n = 9$, $\beta = 1.03$).

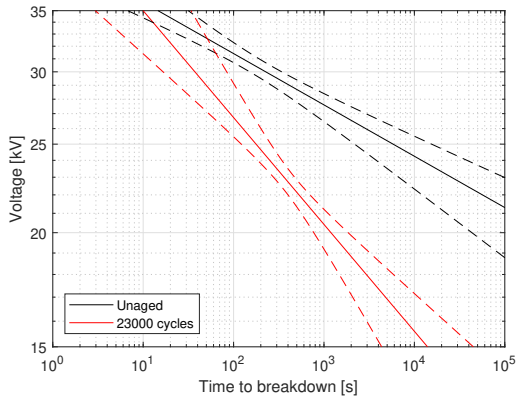

(c) Comparison between unaged and aged lifetime curves.

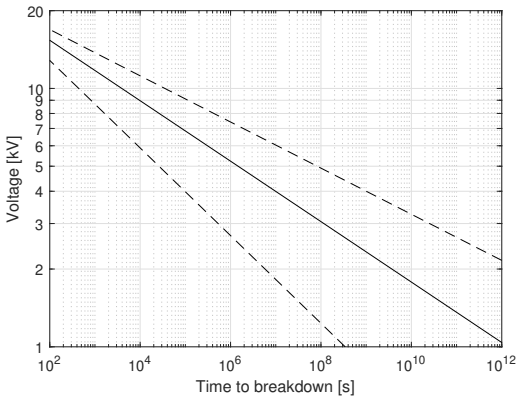

(d) Extrapolated B1 life in the voltage range of interest.

Figure 6.8: Lifetime test results of HDPE cable.

6.5.2. Test Results

Three stress profiles were chosen for lifetime testing of the aged cables. One starting from 22 kV and increasing 2 kV for every 5 min. Subsequently, the second profile started from 24 kV and the third from 26 kV. These profiles were chosen after observing that otherwise, a long time is required for breakdown, making it difficult to obtain a significant set of breakdown times to determine the effect of CBoS on cable lifetime. After completion of lifetime testing, it was found that:

- The power law exponent n changed from 18 to 9 for samples subjected to combined bending and tension loading as seen in Figure 6.8c.

- Cables in the same layer of an umbilical cable experience different degradation rates, as seen in the triples in Chapter 4.
- The part on the sheave wheel, which underwent bending and tensional stress, still maintained the local ageing phenomenon as expected.
- Some parts that underwent purely tensional forces showed much more degradation than the part on the sheave wheel. This may be partly due to the masterbatch, which could negatively affect the tensional strength of polymer [62]. Masterbatches in HDPE can also cause differences in crystallinity and spherulite size [63].

The lifetime curves in Figure 6.8 were obtained under highly accelerated conditions. The test voltage is over 10 times the rated line-to-ground voltage. This means that the extrapolated lifetime curve may not give a realistic indication of cable lifetime. The high acceleration can result in failure modes which might not occur at the operating voltages. However, it does give a lower limit on the lifetime that may be expected.

6.5.3. Length Effect

The tests in this research were performed on 20 cm segments of single conductors. These results could be translated to more realistic cable lengths using the length effect described by (6.3). The scale parameter can be either breakdown voltage or time to breakdown. The shape parameter β remains the same.

$$\frac{\alpha(\ell)}{\alpha_1} = \left(\frac{\ell}{\ell_1}\right)^{-1/\beta}, \tag{6.3}$$

where α_1 is the scale parameter at length ℓ_1 and ℓ is the desired cable length. As an example, the breakdown voltage and lifetime of the HDPE cable (at its nominal line-to-earth voltage 2.0 kV/$\sqrt{3}$ = 1.2 kV) are extrapolated from $\ell_1 = 20$ cm to $\ell = 3$ km, which is a normal length for ROV umbilicals.

$$U_{bd} = U_{bd,1}\left(\frac{\ell}{\ell_1}\right)^{-1/\beta} = 25.6\,\text{kV} \cdot \left(\frac{3\,\text{km}}{20\,\text{cm}}\right)^{-1/9.5} = 9.3\,\text{kV} \tag{6.4}$$

$$L_{B1} = L_{B1,1}\left(\frac{\ell}{\ell_1}\right)^{-1/\beta} = 1.13 \times 10^8\,\text{h} \cdot \left(\frac{3\,\text{km}}{20\,\text{cm}}\right)^{-1/1.03} = 9.9 \times 10^3\,\text{h} \tag{6.5}$$

The B1 life is less than the intended 10,000 h of operational lifetime (limited by the mechanical life of the armour). However, the extrapolation factor and confidence intervals are considerable. It should be expected that the lifetime increases significantly below the PD inception voltage, for example.

If these calculations are to be used for future engineering purposes, several things must be considered. First, the main aim of the measurements was not to derive a lifetime but to evaluate the effect of bending on the general shape of the lifetime curve and the power law exponent n. Tests were performed on single conductors, which do not represent the entire cable system. Second, since the tests were performed on very short samples, a large extrapolation factor is required, reducing the accuracy of the estimate.

6.6. Partial Discharge Analysis

Partial discharges of aged and unaged HDPE cable samples were analysed to see the effect of ageing on the full cable. The inception (PDIV) and extinction (PDEV) voltages are presented in Table 6.4. The PDIV of the yellow conductors shows almost no degradation. This matches the lifetime test results, where the yellow conductor had a much longer lifetime than the brown conductor, showing a significant PDIV reduction.

Table 6.4: PD inception and extinction voltages.

Number of cycles	Colour	PDIV	PDEV	Testing voltage
0	Blue	5.8 kV	5.5 kV	7.2 kV
	Brown	6.1 kV	5.8 kV	7.3 kV
	Yellow	6.2 kV	5.9 kV	7.4 kV
20,000	Blue	5.2 kV	3.7 kV	6.2 kV
	Brown	3.9 kV	3.3 kV	4.7 kV
	Yellow	6.4 kV	6.2 kV	7.7 kV

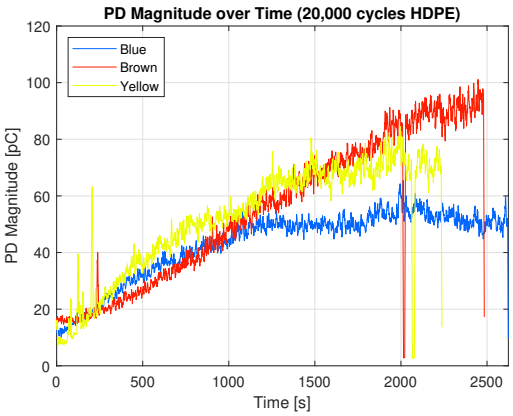

Figure 6.9: PD magnitude over time of 20,000 cycle HDPE.

Unsymmetrical patterns are observed for the unaged and aged HDPE samples (see Figure 6.6a). In this case, the origin of the partial discharges is the delamination of the conductor-insulator interface, as shown for XLPE in the previous chapter. PRPD patterns of the different coloured cables over time show that the discharges in the negative cycle are growing. It could be that the magnitude becomes more stable after a longer period of ageing, like for the blue conductor.

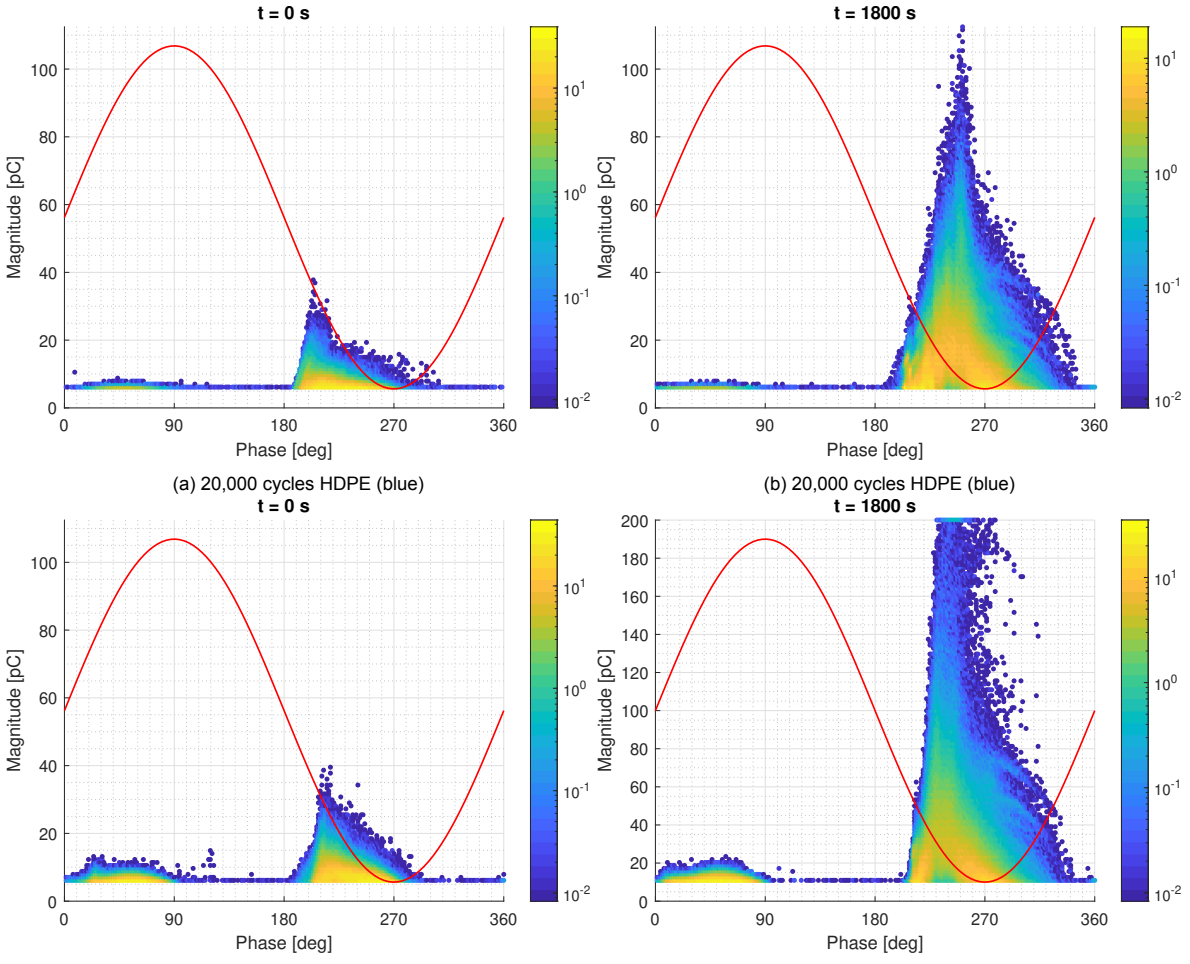

(a) 20,000 cycles HDPE (blue)

(b) 20,000 cycles HDPE (blue)

(c) 20,000 cycles HDPE (brown)

(d) 20,000 cycles HDPE (brown)

Figure 6.10: PRPD patterns of 20,000 cycle HDPE over time

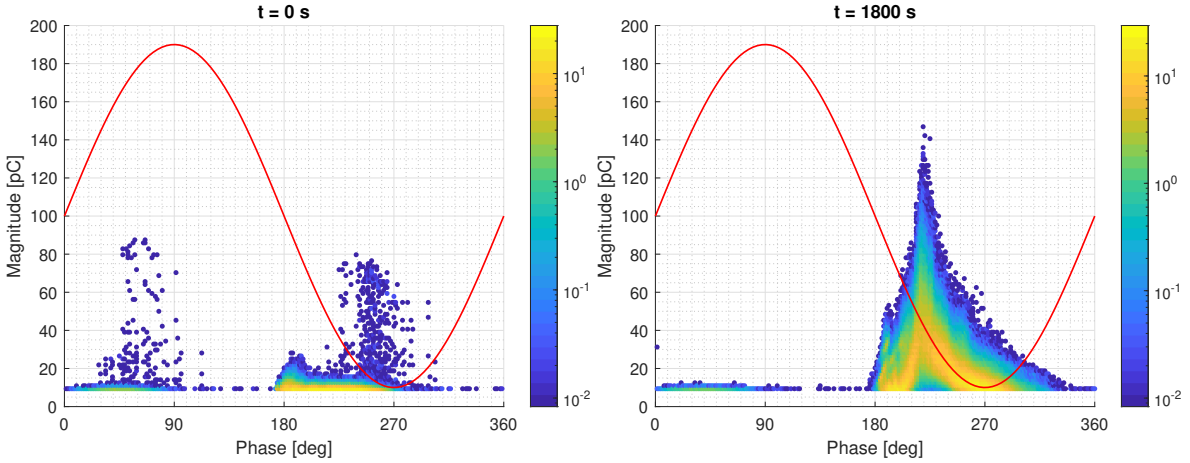

(e) 20,000 cycles HDPE (yellow)

(f) 20,000 cycles HDPE (yellow)

Figure 6.10 (*Continued.*): PRPD patterns of 20,000 cycle HDPE over time

6.7. Conclusion

In conclusion, this chapter presented the results of ageing HDPE cables with armour subjected to 20,000 cycles using the Cyclic Bending over Sheave (CBoS) test. The mechanical ageing setup applied bending and tensile stress to the cables, simulating the dynamic mechanical stress experienced in real applications. This was followed by electrical testing on single power conductors.

The breakdown results showed that the insulation degradation due to bending occurs even in cables with armour and no direct loading on the conductors. Again, the degradation was localised in the insulation due to delaminations at the conductor-insulation interface. One of the main objectives of this chapter was to determine the slope of the lifetime curve before and after CBoS ageing. There was a significant decrease in the power law exponent n from 18 to 9. The degradation rates of cables in the same layer of the full cable differed when subjected to the CBoS ageing.

7

Conclusion and Recommendations

This chapter aims to summarise the main outcomes of the research on the ageing and lifetime of ROV umbilical cables. By revisiting the research questions, a comprehensive understanding of the findings is made. Additionally, any limitations encountered during the study are addressed, and suggestions for potential future research topics are given.

7.1. Conclusion

In this research, ROV umbilical cables were studied to identify the limitations of the current processes when taking the cable designs to a higher voltage. The main focus was on the effect of bending stress on the insulation properties of XLPE, HDPE, and polypropylene insulating materials. This thesis goal has been achieved, and the main findings and conclusions are summarised based on the research questions.

What are the factors influencing the ageing and lifetime of umbilical cables? Little research is available on the ageing and lifetime of umbilical cables. However, much of the knowledge of the phenomena in power cables can be utilized. In dynamic power cables, the focus is usually on water treeing. However, since water treeing takes a long time to develop, it is not directly of interest for the current application: short-lifetime umbilical cables.

The major causes of electrical breakdown in umbilical cables could originate from non-electrical causes: mechanical stress (e.g., bending or tensile stress) or thermal stress. Therefore, this thesis focused on cyclic bending stress, which is representative of the motion that the cable undergoes on the winch during the launching and recovery of the ROV.

How can the cyclic bending fatigue be accurately replicated in cable tests? As noted, ROV umbilical cables undergo a combination of mechanical stresses during operation. The part of the cable on the winch undergoes cyclic bending in combination with tensile stress since the entire weight of the ROV is supported by the umbilical cable. This type of mechanical stress is replicated in three ways using a cyclic bend-over-sheave setup:

- Single conductor ageing: Single conductors of XLPE and PP were directly aged for 5000 and 10,000 cycles on a sheave wheel with an appropriate diameter. This setup represented a worst case of cyclic bending on the dielectric.
- Triple conductor ageing: Cables with three conductors (three-phase system, called a triple) made of XLPE and PP, arranged in a helix structure with a jacket, were subjected to ageing on a sheave wheel for 5000, 10,000 and 20,000 cycles. Using this setup, the effect of helix structure on ageing could be studied.
- Cable with armour: An entire ROV cable with armour is subjected to combined bending and tension forces (23,000 cycles) during ageing. The last method is the most representative of the real conditions that the cable has to undergo.

What methods can be used to electrically test the single conductors of a cable without the grounded sheath? Since a high-voltage and ground electrode are necessary for HV testing, the ground must be provided to the conductor. Tap water (measured conductivity 470 µS/cm) is used as a ground electrode. This ensured an almost perfect interface between the outer insulation. However, it is worth noting that when using small testing lengths of approximately 20 cm, there is a risk of discharges occurring at the triple point where the cable enters the water. Bushings were designed to reduce the field strength and eliminate discharges at this triple point.

A test setup using tap water as a ground electrode and specially designed bushings capable of testing up to 50 kV over a length of approximately 20 cm has been developed to prevent discharges along the conductor surface during testing Therefore, the design effectively addresses the issues associated with testing at high voltage, providing a solution that eliminates potential problems and ensures reliable testing conditions.

How does cyclic ending stress affect the dielectric properties of the cable? After different types of cycling bending tests on the dielectric, the following conclusions were drawn about the effect of bending stress. For the single conductors:

- The XLPE insulation demonstrated clear degradation with increasing bending cycles. Notably, this degradation was localized within the bending zone. The breakdown strength does not decrease linearly with bending cycles. Additionally, the analysis of partial discharge (PD) patterns provided further evidence of degradation, showing that the electrode-bounded cavities (due to delamination) were formed.
- When comparing unaged samples, the PP insulation exhibited similar breakdown strength to XLPE. However, the aged PP samples had a breakdown strength above what could be tested. The analysis of partial discharge (PD) indicated a decreased magnitude of PD in the aged samples compared to the unaged ones. This phenomenon could be attributed to strain crystallization, which also explains the observed whitening of the insulation in the bending zone.

The influence of the helix structure on bending was investigated for the triple cables.

- For XLPE, the impact of bending on the triple cables was less pronounced than that of the single conductors. Nevertheless, varying degrees of degradation were observed among the different cables within the helix structure. PD analysis was performed on these samples, and based on the inception voltage, the size of the cavities was estimated to be in the range of 40 to 150 µm. The patterns were again mainly asymmetrical, indicating delamination. Samples were cast in epoxy to make cross-sections to validate this hypothesis. The cross-sections showed a growing number and size of delaminations with increasing mechanical ageing cycles.
- For PP, it was observed that the cabling process had damaged the dielectric, leaving whitening marks on the insulation. When further aged using the CBoS setup, the partial discharge magnitude increased. Unlike XLPE, the PRPD patterns were symmetric, indicating the growth of dielectric-bound cavities. Cross-sections of aged and unaged cable samples confirmed this observation: no significant delaminations could be seen.

Lifetime tests on the full cable showed significant degradation in lifetime slope n from 18 to 9 due to the combined effect of bending and tension. Similar to XLPE, HDPE also showed delamination.

7.2. Recommendations for Future Work

This section presents an outline of the potential areas for further investigation and improvements based on the findings and limitations of the current study.

- **Combined thermo-mechanical ageing**: The cable undergoes combined thermal and mechanical stresses on the winch. Due to safety concerns, this type of ageing could not be carried out in this project. Nevertheless, the effects of thermal ageing and bending were investigated separately. The cable should undergo thermal cycles (e.g., through induced current heating) during CBoS testing to obtain the most representative conditions.

- **Evaluation of Mechanical Ageing Setup**: Assessing if the rollers in the CBoS ageing setup impact the ageing process and determining the effectiveness of using a fixed stroke length for combined ageing.
- **Polypropylene**: Currently, isotactic polypropylene is used in production. However, literature has found that this type of polypropylene does not have the best mechanical and thermal properties. Therefore, a better polypropylene blend that is more suitable for this application should be found. Preferably, it should have a lower glass temperature to prevent brittleness at low temperatures and achieve better thermal stability of the crystalline phase.
- **Twin and triple extrusion**: One of the main conclusions presented in this thesis is that cyclic bending stress can cause delamination of the conductor–insulator interface. This is partly due to the conventional extrusion process used for producing the cables. If a layer of semicon is introduced at the interface (through a twin or triple extrusion process), this may improve the performance of the cable under bending stress. However, it has to be evaluated and validated through further testing.
- **Cabling Process**: The cabling process seems to cause physical damage to the cables. This includes indentation of the surface of the cable and small delaminations of the conductor–insulation interface. It will be essential to monitor the cabling process to avoid such damage to the virgin cables, which may otherwise lead to early failure in the field.
- **Masterbatch**: The effect of masterbatch pigments on the properties of the insulation cannot be ignored, especially when it comes to mechanical properties. For example, the brown-coloured conductors of the HDPE cables showed more degradation than the yellow and blue conductors. Therefore, a study should be performed into the types of masterbatch pigments and their effect on the electromechanical properties of the insulation.

A

Definitions and Abbreviations

A.1. List of Symbols

Symbol	Units	Description
A	[m^2]	Area
C	[F]	Capacitance
E	[V/m]	Electric field strength
f	[Hz]	Frequency
F	[-]	Cumulative distribution function; unreliability
g	[m/s^2]	Gravitational acceleration
L	[h]	Lifetime
$\mathcal{L}$	[-]	Log-likelihood
m	[kg]	Mass
n	[-]	Lifetime power law exponent
p	[Pa]	Pressure
R	[Ω]	Resistance
t	[s]	Time
	[m]	Insulation thickness
$\tan\delta$	[-]	Dissipation factor
T	[°C]	Temperature
T_g	[°C]	Glass transition temperature
U	[V]	Voltage
α	[-]	Weibull scale parameter
β	[-]	Weibull shape parameter
ϵ_0	[F/m]	Vacuum permittivity
ϵ_r	[-]	Relative permittivity, dielectric constant
ϵ'	[F/m]	Real permittivity
ϵ''	[F/m]	Imaginary permittivity
ρ	[Ω m]	Electrical resistivity
σ	[S/m]	Electrical conductivity
σ_{UTS}	[Pa]	Ultimate tensile strength
ω	[rad/s]	Angular frequency

A.2. List of Abbreviations

Abbreviation	Description
AC	Alternating current
CBoS	Cyclic bend-over-sheave
DBZ	Double bending zone

Abbreviation	Description
DPR	Depolymerized rubber
DS	Dielectric spectroscopy
FEM	Finite element method
HDPE	High-density polyethylene
HV	High voltage
LV	Low voltage
MBR	Minimum bending radius
MLE	Maximum likelihood estimation
MV	Medium voltage
PD	Partial discharge
PDIV	Partial discharge inception voltage
PDEV	Partial discharge extinction voltage
PP	Polypropylene
PRPD	Phase-resolved partial discharge
PVC	Polyvinyl chloride
ROV	Remotely operated vehicle
SIED	Stress-induced electrochemical degradation
TMS	Tether management system
TPU	Thermoplastic polyurethane
XLPE	Cross-linked polyethylene

B

Prestudy Results

B.1. Thin Samples

When creating thin samples, allowing them to cool down from elevated temperatures is essential to prevent deformation. Employing a Teflon sheet under high pressure is unsuitable as it tends to deform. Initially, the Teflon sheet was used to prevent the samples from sticking to the mould. However, with a stainless steel mould, this issue was resolved by applying release agents before usage. These challenges are shown in Figure B.1.

(a) Deformation due to sudden cooling of XLPE

(b) Deformation of Teflon under pressure

Figure B.1: Challeges of making flat samples

B.2. Effect of CBoS Ageing on XLPE

A small prestudy was performed on XLPE cable samples to validate the hypothesis that bending fatigue causes insulation degradation before producing the samples used in this thesis. The cables were aged for 4000 and 8000 cycles using the CBoS procedure described in the main text.

Electrical tests on unaged and 4000 cycle-aged samples were performed on large samples of 50 to 70 cm. These tests show an evident degradation in breakdown voltage, but test results have a similar β as expected from theory. On the other hand, short samples (20 cm) of 8000 cycle cables were tested. These suddenly showed a large spread in results (lower β), which is suspicious. It is hypothesised that this is due to variations in the ageing state of the cable over its length. Analysis using two subpopulations (a “high” and “low” dataset) confirms that a part of the 20 cm samples is essentially unaged, and the β of both the high and low set are more in the range of the original β, as expected. The results of the two analyses are presented in Tables B.1 and B.2.

This analysis is further validated by the fact that the ageing state of the cable varies over its length, which is confirmed by the cross-sections made of the cable in Chapter 5. The parts with no delamination

have a high breakdown voltage, whereas those with delaminations are in the dataset with the low breakdown voltage.

Table B.1: Weibull Parameters

Number of cycles	α	β	$-2\mathcal{L}$
0	31.4 ± 5.5 kV	8.0	65.2
4000	25.6 ± 4.0 kV	9.6	54.4
8000	24.8 ± 6.0 kV	4.1	84.1

Table B.2: Weibull Parameters for Split Data

Number of cycles		α	β	$-2\mathcal{L}$
0		31.4 ± 5.5 kV	8.0	65.2
4000		25.6 ± 4.0 kV	9.6	54.4
8000	low	19.9 ± 4.8 kV	5.7	68.9
	high	30.3 ± 4.3 kV	10.4	

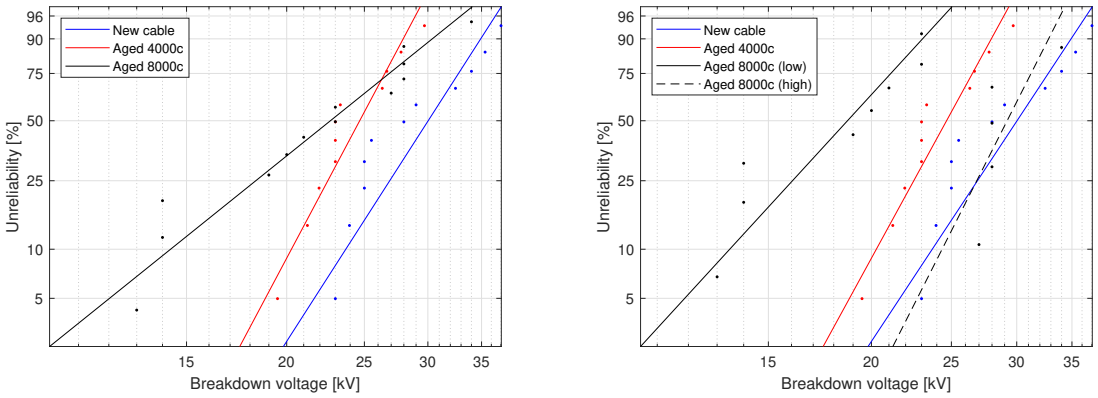

(a) Breakdown Voltages of Aged XLPE

(b) Split 8000 Cycle Data

Figure B.2: Weibull Plot of XLPE Breakdown Tests

B.3. Bushing Trials

Several bushing trials had to be designed and tested to obtain a reliable design. All iterations are shown in Figure B.3.

Figure B.3: Bushing trials made of different materials done starting from the left (a) PVC pipe with water-tight cap, (b) modified glue cap, (c) Teflon cone, (d) PET cone, and (e) TPU cone.

C

PD Results

C.1. Single Conductors XLPE

The PRPD pattern over time for increasing number of ageing cycles is shown in Figure C.1. In general, the magnitude of the PD increases with mechanical ageing, and decreases over time. A rabbit ear pattern, associated with cavities in the dielectric, appears after mechanical ageing (see for example Figure C.1e). After 30 min of PD measurement at 3.1 kV the rabbit ear has disappeared.

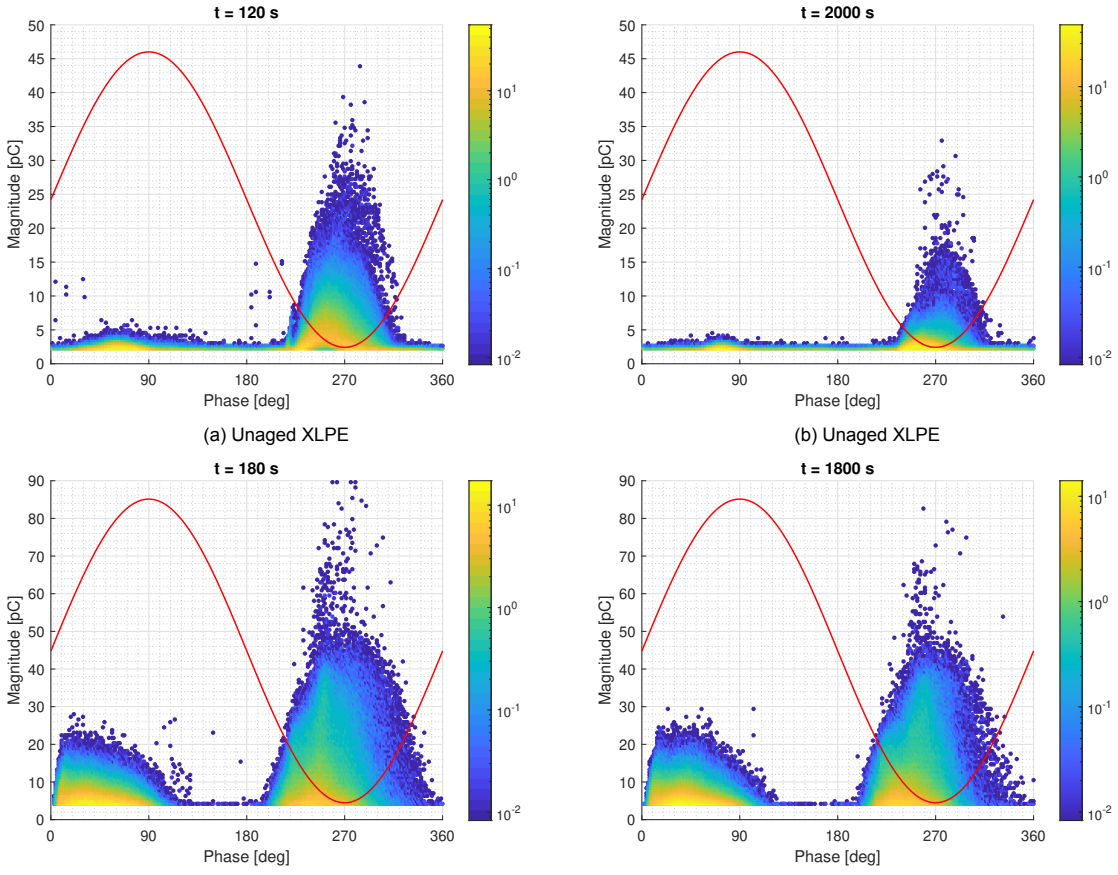

(a) Unaged XLPE

(b) Unaged XLPE

(c) 5000 cycles XLPE

(d) 5000 cycles XLPE

Figure C.1: PRPD patterns of XLPE with different bending cycles over time.

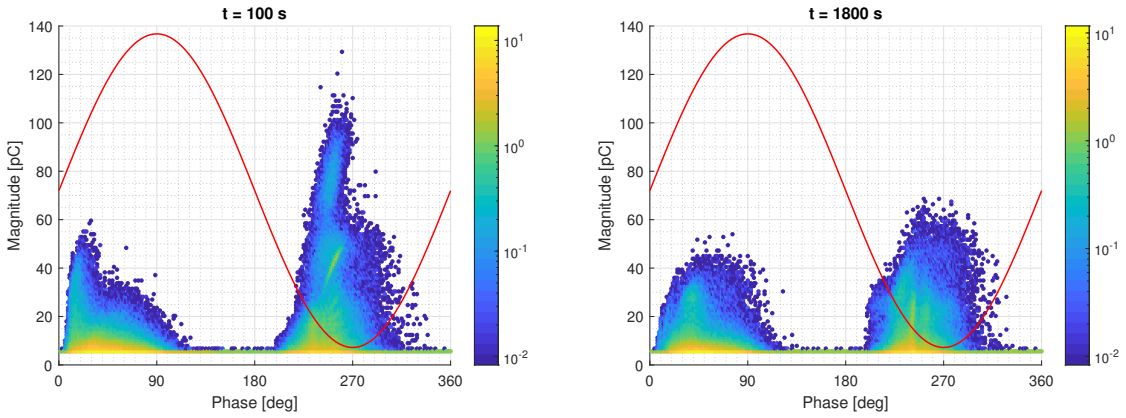

(e) 10,000 cycles XLPE

(f) 10,000 cycles XLPE

Figure C.1 (*Continued.*): PRPD patterns of XLPE with different bending cycles over time.

C.2. Single Conductor Polypropylene

As explained in Chapter 4 polypropylene shows a more symmetric pattern with the increase in the number of bending cycles as shown in PRPRD patterns in Figure C.2. The small cavities seems to

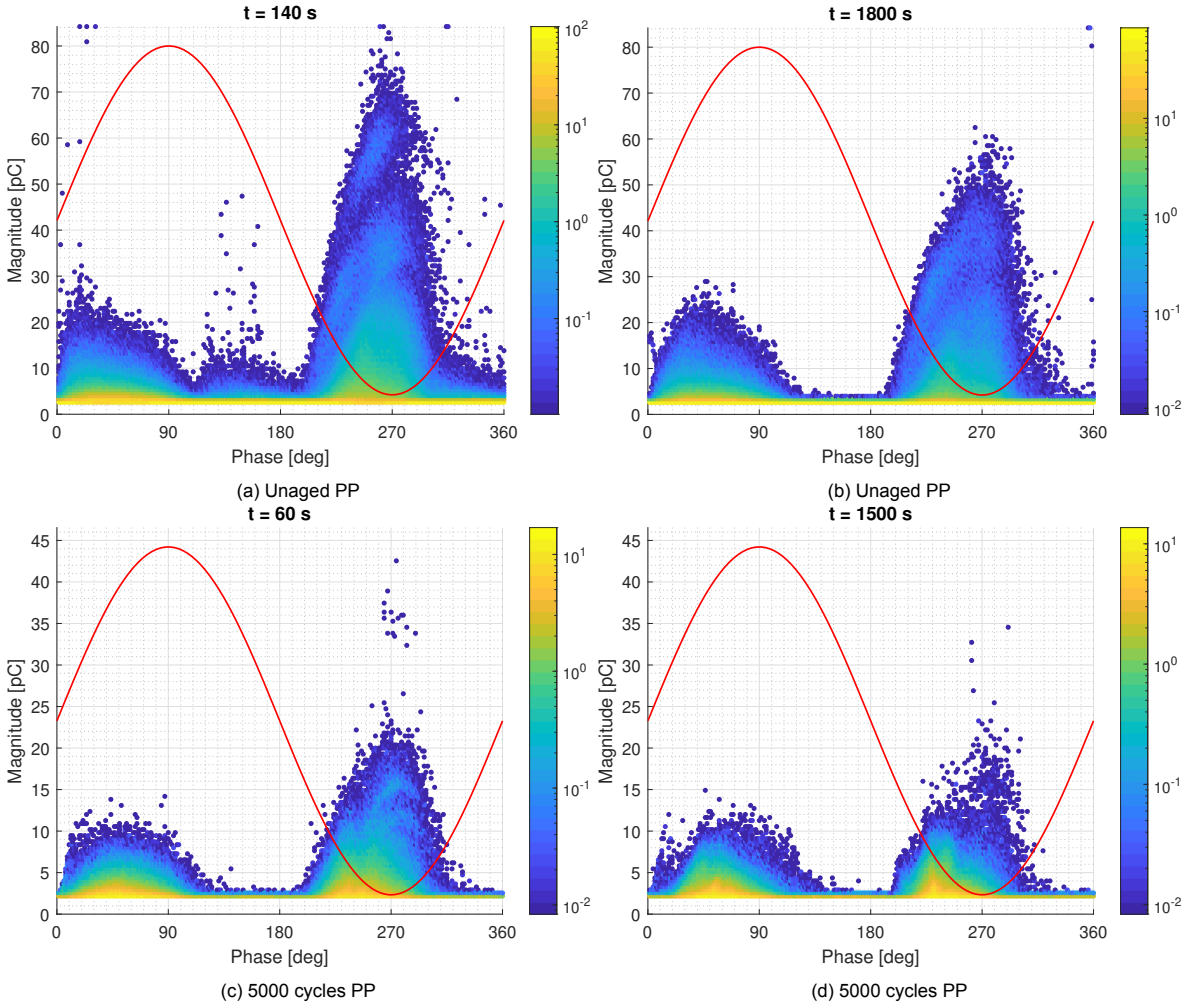

(a) Unaged PP

(b) Unaged PP

(c) 5000 cycles PP

(d) 5000 cycles PP

Figure C.2: PRPD patterns of PP with different bending cycles over time.

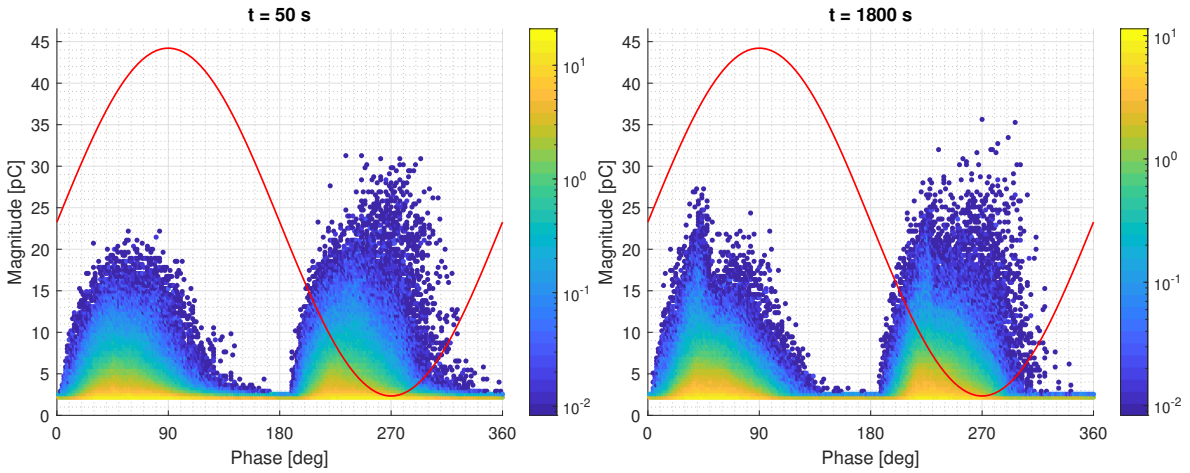

(e) 10,000 cycles PP (f) 10,000 cycles PP

Figure C.2 (*Continued.*): PRPD patterns of PP with different bending cycles over time.

form during initial bending at 5000 cycles following which it grows during the subsequent ageing.

C.3. Triple XLPE

In Figure C.3 the individual conductors of 10,000 cycles aged triple is presented. Here the different ageing rates for the conductors of the same triple could be seen.

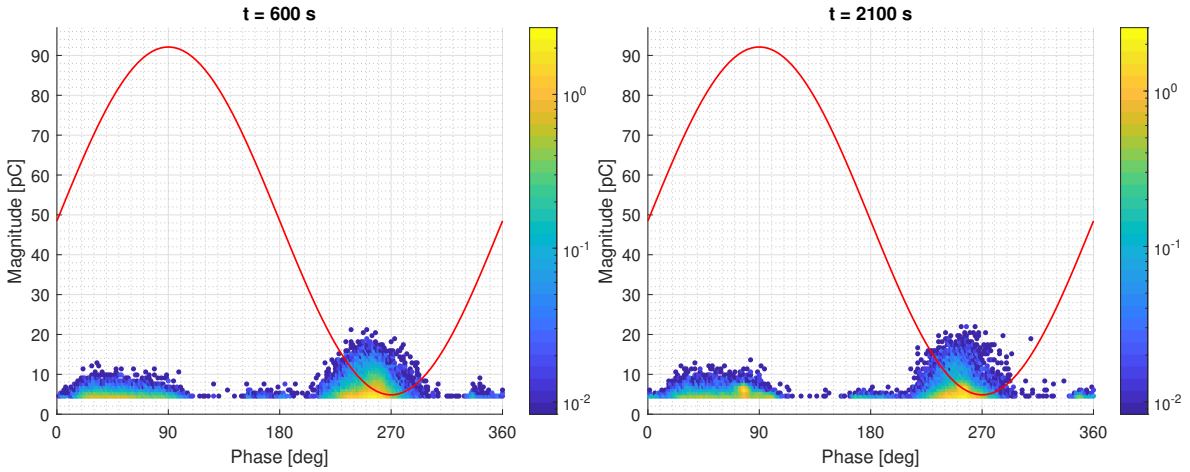

(a) Conductor 1 from triple (b) Conductor 1 from triple

Figure C.3: PRPD patterns of XLPE with 10,000 bending cycles over time.

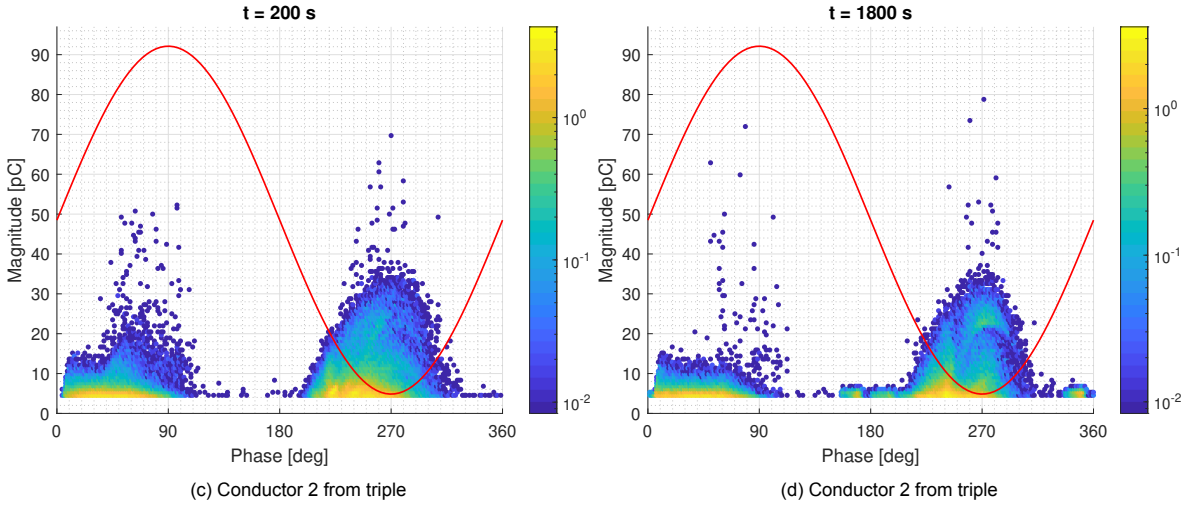

(c) Conductor 2 from triple

(d) Conductor 2 from triple

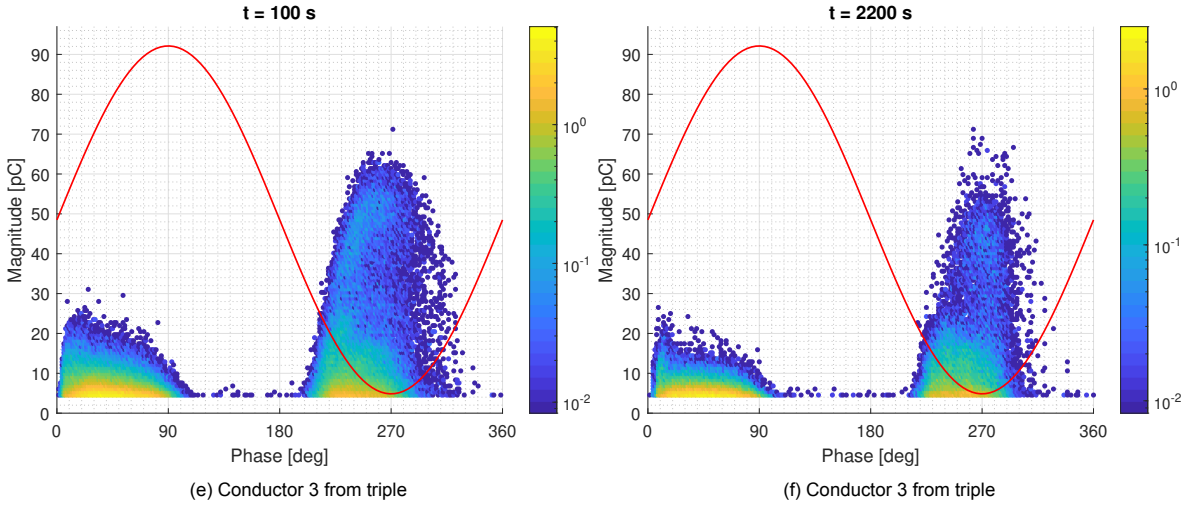

(e) Conductor 3 from triple

(f) Conductor 3 from triple

Figure C.3 (*Continued.*): PRPD patterns of XLPE with 10,000 bending cycles over time.

Bibliography

[1] S. Shah and M. G. Niasar, "The Effect of Bending Fatigue on the Breakdown Strength of Polymer-Insulated Conductors," in *Jicable'23 – 11th International Conference on Insulated Power Cables*, Lyon, Jun. 2023.

[2] O. A. N. Eidsvik and I. Schjølberg, "Finite element cable-model for Remotely Operated Vehicles (ROVs) by application of beam theory," *Ocean Engineering*, vol. 163, pp. 322–336, 2018, doi:https://doi.org/10.1016/j.oceaneng.2018.06.012.

[3] P. Chen, Y. Liu, S. Yang, J. Chen, Q. Zhang, and Y. Tang, "Dynamic characteristics of deep-sea ROV umbilical cables under complex sea conditions," *Ocean Engineering*, vol. 239, p. 109854, 2021, doi:https://doi.org/10.1016/j.oceaneng.2021.109854.

[4] R. D. Christ and R. L. Wernli, "Chapter 8 – Cables and Connectors," in *The ROV Manual (Second Edition)*, 2nd ed. Oxford: Butterworth-Heinemann, 2014, pp. 163–220, doi:10.1016/B978-0-08-098288-5.00008-7.

[5] E. Ildstad and H. Faremo, "Effect of dynamic mechanical load on water treeing of XLPE cables," in *2012 International Conference on High Voltage Engineering and Application*, 2012, pp. 55–58, doi:10.1109/ICHVE.2012.6357057.

[6] M. P. Spencer and L. S. Fifield, "Effect of Mechanical Deformation on the Dielectric Electric Field in Dynamic Umbilical Cables," in *2021 IEEE Conference on Electrical Insulation and Dielectric Phenomena (CEIDP)*, 2021, pp. 651–654, doi:10.1109/CEIDP50766.2021.9705442.

[7] W. Quan and Q. Chang, "Variable-Length Cable Dynamics of Payout and Reel-in With a Vertically Tethered Underwater Drill Rig," *IEEE Access*, vol. 8, pp. 66 625–66 637, Apr. 2020, doi:10.1109/ACCESS.2020.2984752.

[8] J. Morshedian and P. M. Hosseinpour, "Polyethylene Cross-linking by Two-step Silane Method: A Review," *Iranian Polymer Journal*, vol. 18, pp. 103–128, 02 2009.

[9] S. Balafutas, *Power Cable Theory and Manufacturing Process*, 2007.

[10] C. Meola, G. Carlomagno, and G. Giorleo, "Cross-Linked Polyethylene," in *Encyclopedia of Chemical Processing*. Taylor & Francis, Jan. 2005, vol. 1, pp. 577–588.

[11] H. Ahmad and D. Rodrigue, "Crosslinked polyethylene: A review on the crosslinking techniques, manufacturing methods, applications, and recycling," *Polymer Engineering & Science*, vol. 62, no. 8, pp. 2376–2401, 2022, doi:10.1002/pen.26049.

[12] S. Hellesø, J. T. Benjaminsen, M. Selsjord, and S. Hvidsten, "Water tree initiation and growth in XLPE cables under static and dynamic mechanical stress," in *2012 IEEE International Symposium on Electrical Insulation*, 2012, pp. 623–627, doi:10.1109/ELINSL.2012.6251546.

[13] E. David, J.-L. Parpal, and J.-P. Crine, "Influence of internal mechanical stress and strain on electrical performance of polyethylene electrical treeing resistance," *IEEE Transactions on Dielectrics and Electrical Insulation*, vol. 3, no. 2, pp. 248–257, 1996, doi:10.1109/94.486777.

[14] D. Wald, F. O. Igbinovia, and P. Raikisto, "Thermoplastic Insulation System for Power Cables," in *2020 IEEE PES/IAS PowerAfrica*, 2020, pp. 1–5, doi:10.1109/PowerAfrica49420.2020.9219839.

[15] S. Belli, G. Perego, A. Bareggi, L. Caimi, F. Donazzi, and E. Zaccone, "P-Laser: Breakthrough in power cable systems," in *2010 IEEE International Symposium on Electrical Insulation*, 2010, pp. 1–5, doi:10.1109/ELINSL.2010.5549826.

[16] Rehau AG, “RAUKANTEX PP Technical information,” Sep. 2018. [Online]. Available: https://www.rehau.com/downloads/406436/raukantex-pp.pdf

[17] A. S. Vaughan, C. D. Green, I. L. Hosier, G. C. Stevens, A. Pye, J. L. Thomas, S. J. Sutton, and T. Geussens, “Thermoplastic high performance cable insulation systems for flexible system operation,” in *2015 IEEE Electrical Insulation Conference (EIC)*, 2015, pp. 543–546, doi:10.1109/ICACACT.2014.7223570.

[18] Borealis AG, “Polyethylene HE3366 Product Datasheet,” Oct. 2016, ed. 5. [Online]. Available: https://www.borealisgroup.com/products/catalogue/product-name-he3366

[19] J.-H. Kwon, M.-H. Park, K.-J. Lim, and H.-K. Lee, “Investigation on electrical characteristics of HDPE mixed with EVA applied for recycleable power cable insulation,” in *2012 IEEE International Conference on Condition Monitoring and Diagnosis*, 2012, pp. 1039–1042, doi:10.1109/CMD.2012.6416334.

[20] Padanaplast, “Polidan® EC/MD XLPE Technical Information,” Sep. 2022, v1.1. [Online]. Available: https://www.padanaplast.com/pp/images/TDS/TDS_Polidan_EC_MD_v_11__September_2022.pdf

[21] J. Ullah, E. Harkin-Jones, A. Mcilhagger, C. Magee, D. Tormey, F. Dave, R. Sherlock, and D. Dixon, “The effect of masterbatch pigments on the crystallisation, morphology, and shrinkage behaviour of isotactic polypropylene,” *Journal of Polymer Research*, vol. 29, 05 2022, doi:10.1007/s10965-022-03028-z.

[22] J. Bacalhau, T. Cunha, and C. Afonso, “Effect of Ni content on the Hardenability of a Bainitic Steel for Plastics Processing,” in *COBEM 2017 (24th ABCM International Congress of Mechanical Engineering)*, Dec. 2017, doi:10.26678/ABCM.COBEM2017.COB17-1174.

[23] N. Hampton, R. A. Hartlein, H. Lennartsson, H. Orton, and R. Ramachandran, “Long-life XLPE insulated power cable,” *JICABLE’07 – International Conference on Power Insulated Cables*, 2007. [Online]. Available: https://www.jicable.org/2007/Actes/Session_C51/JIC07_C515.pdf

[24] M. Narkis, A. Tzur, A. Vaxman, and H. G. Fritz, “Some properties of silane-grafted moisture-crosslinked polyethylene,” *Polymer Engineering & Science*, vol. 25, no. 13, pp. 857–862, Sep. 1985, doi:https://doi.org/10.1002/pen.760251311.

[25] E. Steennis, “Water treeing: The behaviour of water trees in extruded cable insulation,” Ph.D. dissertation, Delft University of Technology, Jun. 1989. [Online]. Available: http://resolver.tudelft.nl/uuid:6891382c-9dfb-4460-9968-355c33192d62

[26] E. David, J.-L. Parpal, and J.-P. Crine, “Influence of internal stress and strain on electrical treeing in XLPE,” in *Proceedings of IEEE Conference on Electrical Insulation and Dielectric Phenomena*, 1994, pp. 575–581, doi:10.1109/CEIDP.1994.592032.

[27] A. Bulinski, S. Bamji, and J. Densley, “The effects of moisture content, frequency and temperature on the life of miniature XLPE cables,” in *1982 IEEE International Conference on Electrical Insulation*, 1982, pp. 283–286, doi:10.1109/EIC.1982.7464490.

[28] R. N. Fard, O.-A. Eidsvik, E. Tedeschi, and I. Schølberg, “Cable Selection Considerations for Subsea Vehicles,” in *2018 OCEANS - MTS/IEEE Kobe Techno-Oceans (OTO)*, 2018, pp. 1–8, doi:10.1109/OCEANSKOBE.2018.8559225.

[29] G. Skeie, N. Sodahl, and O. Steinkjer, “Efficient Fatigue Analysis of Helix Elements in Umbilicals and Flexible Risers: Theory and Applications,” *Journal of Applied Mathematics*, vol. 2012, Special Issue, Jun. 2012, doi:10.1155/2012/246812.

[30] M. Komperød, “Novel Simulations of Subsea Cables and Umbilicals with Bitumen-Coated Armor Wires using UFLEX2D,” in *International Ocean and Polar Engineering Conference*, vol. All Days, Jun. 2016.

[31] M. Choudhary, M. Shafiq, I. Kiitam, A. Hussain, I. Palu, and P. Taklaja, “A Review of Aging Models for Electrical Insulation in Power Cables,” *Energies*, vol. 15, no. 9, 2022, doi:10.3390/en15093408.

[32] J. Densley, “Ageing Mechanisms and Diagnostics for Power Cables – An Overview,” *IEEE Electrical Insulation Magazine*, vol. 17, no. 1, pp. 14–22, 2001, doi:10.1109/57.901613.

[33] K. Uchida, Y. Kato, M. Nakade, D. Inoue, H. Sakakibara, and H. Tanaka, “Estimating the Remaining Life of Water-Treed XLPE Cable by VLF Voltage Withstand Tests,” *Furukawa Review*, vol. 20, Apr. 2001.

[34] A. Ponniran and M. S. Kamarudin, “Study on the performance of underground XLPE cables in service based on tan delta and capacitance measurements,” in *2008 IEEE 2nd International Power and Energy Conference*, 2008, pp. 39–43, doi:10.1109/PECON.2008.4762442.

[35] TC 20 – Electric Cables, “IEC 60502-2:2005 – Power cables with extruded insulation and their accessories for rated voltages from 1 kV (U_m = 1.2 kV) up to 30 kV (U_m = 36 kV) - Part 2: Cables for rated voltages from 6 kV (U_m = 7.2 kV) up to 30 kV (U_m = 36 kV),” 2005. [Online]. Available: https://webstore.iec.ch/publication/2272

[36] A. Abideen, F. Mauseth, Ø. Hestad, and H. Faremo, “Review of Water Treeing in Polymeric Insulated Cables,” *Proceedings of the Nordic Insulation Symposium*, vol. 27, 07 2022, doi:10.5324/nordis.v27i1.4732.

[37] L. Hui, L. S. Schadler, and J. K. Nelson, “The influence of moisture on the electrical properties of crosslinked polyethylene/silica nanocomposites,” *IEEE Transactions on Dielectrics and Electrical Insulation*, vol. 20, no. 2, pp. 641–653, 2013, doi:10.1109/TDEI.2013.6508768.

[38] E. Mellinger, T. Aabo, A. Bowen, C. Katz, and R. Petitt, “High voltage testing of an ROV electro-optical tether cable,” in *MTS/IEEE Oceans 2001. An Ocean Odyssey. Conference Proceedings (IEEE Cat. No.01CH37295)*, 2001, pp. 1145–1150 vol.2, doi:10.1109/OCEANS.2001.968275.

[39] I. Kyere, J. Walker, and D. Nicolae, “Partial Discharge Analysis in Power Cables using 3D Phase Resolved Patterns,” in *23rd South African Universities Power Engineering Conference*, Jul. 2018.

[40] M. G. Niasar, “Partial discharge signatures of defects in insulation systems consisting of oil and oil-impregnated paper,” Licentiate thesis, KTH Royal Institute of Technology, 2005. [Online]. Available: https://urn.kb.se/resolve?urn=urn%3Anbn%3Ase%3Akth%3Adiva-105785

[41] Z. Yan, H. Yan, W. Li, Y. Tian, C. Zhang, and X. Chen, “Effect of Blending Modification on the Mechanical and Dielectric Properties of Polypropylene for Environment-friendly Cable Insulation,” in *2022 IEEE/IAS Industrial and Commercial Power System Asia (I&CPS Asia)*, 2022, pp. 997–1001, doi:10.1109/ICPSAsia55496.2022.9949721.

[42] E. Ildstad and S. T. Hagen, “Electrical treeing and breakdown of mechanically strained XLPE cable insulation,” in *Conference Record of the 1992 IEEE International Symposium on Electrical Insulation*, Jul. 1992, pp. 135–139, doi:10.1109/ELINSL.1992.247035.

[43] J. Yan, H.-t. Hu, H.-l. Lu, Y.-c. Yin, Y.-f. Bu, and Q.-z. Lu, “Experimental Study on the Influence of Cross-Section Type of Marine Cable Conductors on the Bending Performance,” *China Ocean Engineering*, vol. 36, no. 4, pp. 629–637, Aug. 2022, doi:10.1007/s13344-022-0053-4.

[44] N. O. Cárdenas, I. F. Machado, and E. Gonçalves, “Cyclic loading and marine environment effects on the properties of HDPE umbilical cables,” *Journal of Materials Science*, vol. 42, no. 19, pp. 6935–6941, 2007, doi:10.1007/s10853-006-1313-z.

[45] K. Aljoumaa and Z. Ajji, “Mechanical and electrical properties of gamma-irradiated silane crosslinked polyethylene (Si-XLPE),” *Journal of Radioanalytical and Nuclear Chemistry*, vol. 307, Jun. 2015, doi:10.1007/s10967-015-4236-9.

[46] S. V. Suraci, C. Li, and D. Fabiani, “Dielectric Spectroscopy as a Condition Monitoring Technique for Low-Voltage Cables: Onsite Aging Assessment and Sensitivity Analyses,” *Energies*, vol. 15, no. 4, 2022, doi:10.3390/en15041509.

[47] E. Mustafa, R. Afia, O. Nouini, and Z. A. Tamus, “Implementation of Non-Destructive Electrical Condition Monitoring Techniques on Low-Voltage Nuclear Cables: I. Irradiation Aging of EPR/C-SPE Cables,” *Energies*, vol. 14, p. 5139, Aug. 2021, doi:10.3390/en14165139.

[48] A. Motori, G. Montanari, and S. Gubanski, “Investigation of relaxation processes in thermally-aged xlpe cable models,” in *IEEE Conf. Electr. Insul. Dielectr. Phenom.*, 1993, pp. 751–756, doi:10.1109/CEIDP.1993.378883.

[49] J. Świergiel and J. Jadżyn, “A virtual transition from polypropylene glycol (PPG) to polypropylene oxide (PPO),” *Journal of Molecular Liquids*, vol. 304, p. 112748, 2020, doi:j.molliq.2020.112748.

[50] M. G. Niasar, “ET4625 High Voltage Cable Systems – Lecture 2 – Cable components and manufacturing,” Feb. 2022, lecture slides, accessed 2023-07-04.

[51] J. Featherstone, A. Neumann, J. Wan, and L. Harris, “Full Scale Wet Age Testing of XLPE Insulated Power Cables in Salt Water,” in *JICABLE’19 – 10th International Conference on Power Insulated Cables*, 2019. [Online]. Available: https://www.jicable.org/TOUT_JICABLE/2019/2019-B10-2.pdf

[52] U. Genschel and W. Q. Meeker, “A Comparison of Maximum Likelihood and Median-Rank Regression for Weibull Estimation,” *Qual. Eng.*, vol. 22, no. 4, pp. 236–255, Aug. 2010, doi:10.1080/08982112.2010.503447.

[53] “IEC/IEEE Guide for the Statistical Analysis of Electrical Insulation Breakdown Data (Adoption of IEEE Std 930-2004),” *IEC 62539 First Edition 2007-07 IEEE 930*, pp. 1–53, 2007, doi:10.1109/IEEESTD.2007.4288250.

[54] Y. Lu, Y. Wang, R. Chen, J. Zhao, Z. Jiang, and Y. Men, “Cavitation in isotactic polypropylene at large strains during tensile deformation at elevated temperatures,” *Macromolecules*, vol. 48, pp. 5799–5806, 08 2015, doi:10.1021/acs.macromol.5b00818.

[55] M. G. Niasar, “Mechanisms of Electrical Ageing of Oil-impregnated Paper due to Partial Discharges,” Ph.D. dissertation, KTH Royal Institute of Technology, 2015. [Online]. Available: https://urn.kb.se/resolve?urn=urn%3Anbn%3Ase%3Akth%3Adiva-159670

[56] F. H. Kreuger, *Industrial High Voltage: 1. Fields, 2. Dielectrics, 3. Constructions*. Delft University Press, 1991. [Online]. Available: http://resolver.tudelft.nl/uuid:283636d4-e993-431f-8d15-6a0576a74266

[57] S. Shah, “Medium Voltage Cable Design Considerations for ROV Umbilical Cables,” Sep. 2022, Internship Report, Delft University of Technology.

[58] P. F. Lépore and M. A. B. Martinez, “Cyclic-Bend-Over-Sheave Fatigue Testing of an Umbilical for Oil Production in Ultra-Deep Waters,” in *Materials with Complex Behaviour: Modelling, Simulation, Testing, and Applications*. Springer Berlin Heidelberg, 2010, pp. 47–56, doi:10.1007/978-3-642-12667-3_4.

[59] C. W. B1.55, “Recommendations for Additional Testing For Submarine Cables from 6 kV (U_m = 7.2 kV) Up To 60 kV (U_m = 72.5 kV),” CIGRE 722, 2018. [Online]. Available: https://e-cigre.org/publication/722-recommendations-for-additional-testing-for-submarine-cables-from-6-kv-um72-kv-up-to-60-kv-um--725-kv

[60] A. Alghamdi and R. Desuqi, “A study of expected lifetime of xlpe insulation cables working at elevated temperatures by applying accelerated thermal ageing,” *Heliyon*, vol. 6, p. e03120, 01 2020, doi:10.1016/j.heliyon.2019.e03120.

[61] E. Gouno and N. Balakrishnan, “Ch. 23. Step-stress accelerated life test,” in *Adv. Reliab.*, ser. Handbook of Statistics. Elsevier, 2001, vol. 20, pp. 623–693, doi:https://doi.org/10.1016/S0169-7161(01)20025-X.

[62] F. Byrne, P. Ward, J. Kennedy, N. Imaz, D. Hughes, and D. Dowling, “The effect of masterbatch addition on the mechanical, thermal, optical and surface properties of poly(lactic acid),” *J. Polym. Environ.*, vol. 17, pp. 28–33, 01 2014, doi:10.1007/s10924-009-0119-x.

[63] M. J. Lodeiro, P. E. Tomlins, and A. Pearce, “The Influence of Pigments on the Mechanical Properties of High Density Polyethylene (HDPE),” National Physical Laboratory, Tech. Rep., Apr. 2000, accessed: 2023-06-29. [Online]. Available: https://eprintspublications.npl.co.uk/1596/1/CMMT258.pdf